Hydrogel Wound Dressings for the Bioactive Treatment of Acute and Chronic Wounds

DISSERTATION ZUR ERLANGUNG DES DOKTORGRADES DER NATURWISSENSCHAFTEN (DR. RER. NAT.) DER FAKULTÄT FÜR CHEMIE UND PHARMAZIE DER UNIVERSITÄT REGENSBURG

vorgelegt von **Julia Köhler**

aus Würzburg

Mai 2017

Diese Arbeit entstand in der Zeit von Oktober 2012 bis Mai 2017 am Lehrstuhl für Pharmazeutische Technologie an der Universität Regensburg.

Die Arbeit wurde von Herrn Prof. Dr. Achim Göpferich angeleitet.

Promotionsgesuch eingereicht am: 09. Mai 2017

Datum der mündlich Prüfung: 23. Juni 2017

Prüfungsausschuss: Prof. Dr. Joachim Wegener (Vorsitzender)
Prof. Dr. Achim Göpferich (Erstgutachter)
PD Dr. Stephan Schreml (Zweitgutachter)
Apl. Prof. Dr. Rainer Müller (Drittprüfer)

Your assumptions are your windows on the world.

Scrub them off every once in a while, or the light won't come in.

Isaac Asimov

Table of Contents

Chapter 1

Introduction and Goal of the Thesis

Based on this chapter, a review article was submitted: Koehler J, Brandl FP, and Goepferich AM. Hydrogel wound dressings for a bioactive treatment of acute and chronic wounds. Eur. Polym. J. 2017; Manuscript Number: EUROPOL_2017_1345.

1. Introduction

1.1 Wound Healing

An injury of the skin is a severe intervention to the normal function of the human body, as thermal insulation, body fluid retention, protection from exogenous pathogens, and hosting of different sensing receptors are only some of the many important functionalities of the intact skin barrier.[1] To enable fast recovery, the endogenous healing process starts almost instantly.[2] The blood flow is stopped within minutes by the aggregation of platelets and fibrin clot formation (Figure 1A). Thereby released growth factors (GFs) and cell mediators recruit inflammatory cells like neutrophils and monocytes to the wound site (Figure 1B). The aim of the following inflammatory response is the removal of foreign bodies, bacteria, and damaged endogenous tissue.[3]

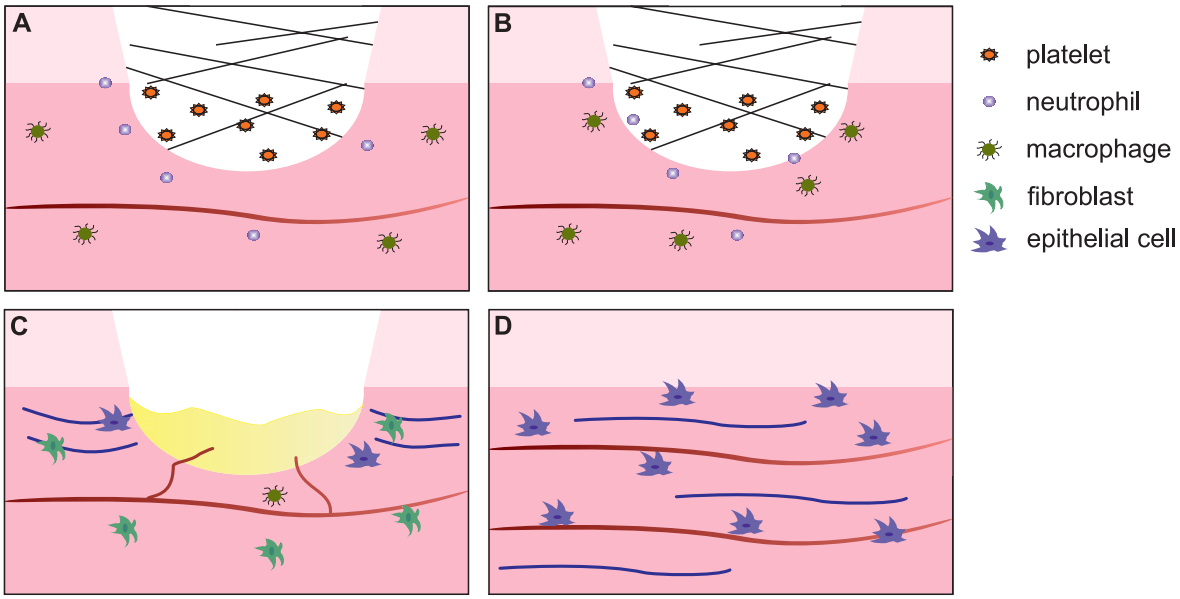

Figure 1. Schematic illustration of the healing process, including the coagulation (A), the inflammation (B), the proliferation (C), and the remodeling (D) phase.[4] The upper light pink layer represents the epidermis; the lower pink layer represents the dermis.

Towards the end of the inflammatory phase, macrophage GFs induce the proliferation and migration of fibroblasts and epithelial cells into the wound (Figure 1C). During the so-called proliferative phase, new blood vessels are formed (in red), the synthesis of strengthening collagen fibers begins (in blue), and granulation tissue (in yellow) is built from epithelial cells, fibroblasts, and keratinocytes. Complete wound healing takes several weeks or month (Figure 1D).[4] The wound finally contracts and the granulation tissue is transformed into the more stable extracellular matrix (ECM).[5] The overall duration of the

healing process depends on the age and the health status of the patient (impairing factors are e.g. diabetes or venous insufficiency), and external factors such as the presence of foreign bodies or infections in the wound. In acute wounds, the healing process follows the above described phases and the wound closure occurs after 8 to 12 weeks.[6] In contrast, chronic wounds mainly remain in the inflammation phase, accompanied by large numbers of wound exudate, heavy infections, pain, and tissue necrosis. Thus, chronic wounds fail to heal over a period of minimum 12 weeks, sometimes it even takes several months or years to full recovery.

1.2 Wound Dressing Requirements

Chronic wounds are a big burden for the patients themselves, facing reduced quality of life, connected to frequent dressing changes, numerous hospital stays, and disabilities in daily life. Furthermore, the economic burden for the health care system is immense.[7] Approximately 20 million patients around the world suffer from chronic wounds and the global wound care market revenue rose to more than 20 billion dollars in 2016.[8,9] Therefore, appropriate wound dressings are required for an unproblematic healing process. Acute wounds should heal in a moist environment for reduced scar formation and facilitated epithelization and cell migration into the wound.[10] Furthermore, the wound dressing should serve as a barrier to external threads like microbes, foreign bodies, or tissue damaging forces. Sufficient mechanical stability (under pressure and tension) is required during the application, the wearing, and the removal of the dressing.[11] Yet, an elastic texture must be maintained, as the dressing should adapt to the specific wound profile and high dressing flexibility is necessary when the patient is moving. The requirements of chronic wound dressings are even more challenging. These dressings additionally have to deal with a high volume of wound exudate; up to 12 $L \cdot m^{-2}$ per day were described for example for venous leg ulcers.[12] Moreover, low adherence to the underlying wound is necessary to protect newly formed tissue from destruction during frequent dressing changes. Especially for the treatment of chronic wounds, but also for the treatment of more complex acute wounds, an active intervention in the healing process is also required.[6] The active wound healing capacity of dressing materials can be based on different components, such as released drugs, the dressing material itself, or incorporated cells. A detailed description of important approaches to bioactive wound dressings can be found below. In any case, the chosen wound dressing should be as supportive to healing as

possible, but at the same time it must be as cost-effective as possible for adoption in clinics.

1.3 Hydrogel Wound Dressings

There is a wide range of different wound dressing types and material compositions on the market, covering the requirements of various kinds of wounds.[13] Traditional dressings like gauze and tulle mainly have a covering effect while maintaining proper gaseous exchange. However, their strong adherence to the wound site causes pain and further lesions during dressing changes. A modern dressing type that combines numerous advantageous properties in one single material is the hydrogel-based wound dressing. Hydrogels consist of around 90% water and 10% natural or synthetic polymers. Because of the high water content, hydrogel dressings are suitable for dry and necrotic wounds. The created moist environment enhances the healing process.[14] Furthermore, it enables a debridement of necrotic tissue, likewise leading to improved healing. On the other hand, hydrogel dressings are also able to absorb high amounts of liquid in contact with exuding wounds. Dependent on the hydrogel composition, a liquid uptake of up to 1000 gram per gram of dressing is described.[15] The permeable hydrogel structure further enables an undisturbed gaseous exchange of CO_2, O_2, and water vapor. In clinical studies, hydrogel dressings were found to reduce the pain for treated patients, induced by a cooling effect of the material, and by its non-adhering nature. The similarity of the hydrogel structure to the structure of the ECM, which is characterized by a vast (polymer) network in an aqueous environment, allows the establishment of a new and very effective wound healing feature, namely the incorporation of cells and biomolecules into the hydrogel polymer network. Further bioactive wound healing properties such as controlled drug release can easily be achieved by a precise chemical modification of the polymer network. For this purpose, various natural and synthetic precursors can be combined, and hydrogel wound dressings with defined wound healing properties can be developed.

1.3.1 Available Hydrogel Base Materials

A widely used hydrogel component with a biological origin is the polysaccharide alginate (Figure 2). Alginate forms hydrogels by ionic cross-linking via $–COO^-$ or, when structurally modified, by chemical cross-linking between additional side chains.[16]

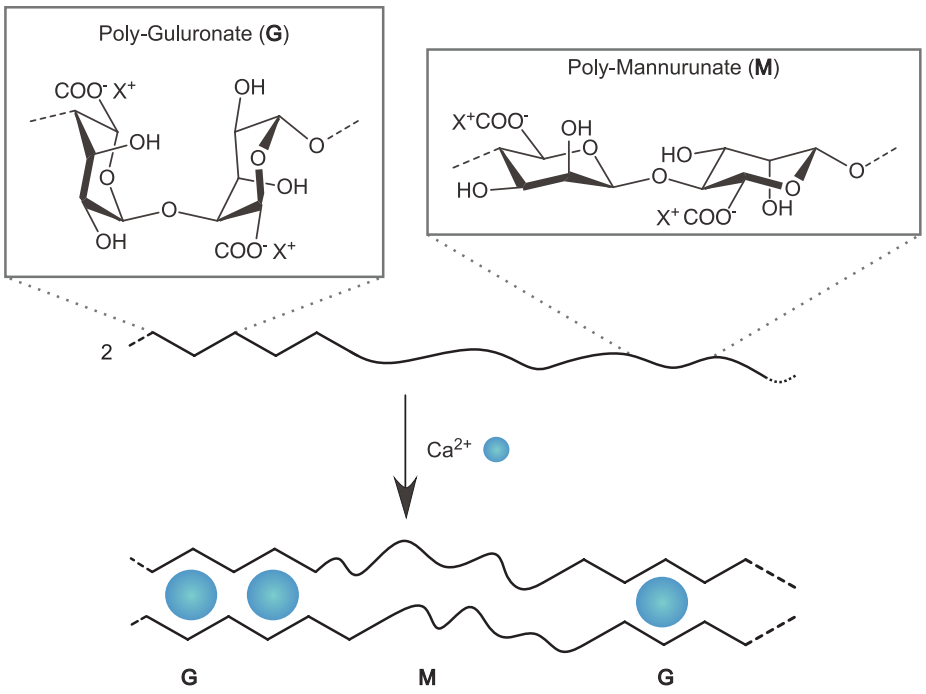

Figure 2. Representative parts of the alginate structure and its ionic cross-linking reaction.

Alginate dressings can absorb high amounts of wound exudate, because of their hydrophilic nature. In contact with bleeding wounds they exhibit a hemostatic effect. But most importantly, they can actively support the wound healing process. Alginate has been proven to enhance cell migration into the wound, to increase the angiogenesis and the production of collagen I, and to reduce the concentration of proinflammatory cytokines in chronic wounds.[17,18] The advantageous material properties of alginate are reflected in the high number of commercially available alginate containing dressings. Alginate dressings are available as various hydrogels (e.g. Nu-Gel® (Systagenix), Tegagel® (3M GmbH)), cryogels (e.g. Algosteril® (4M Medical GmbH), Curasorb® Alginate (Medtronic), Sorbsan® (B. Braun Melsungen AG)), or hydrocolloids (e.g. Comfeel Plus Flexible® (Coloplast AG), Kendall™ Hydrocolloid Dressing (Medtronic)).

Another suitable polysaccharide for medical application is chitosan. Animal studies and clinical trials detected an overall faster healing in chitosan treated wounds.[19–21] Chitosan is hemostatic, bacteriostatic, and fungistatic. Furthermore, it encourages cell proliferation and collagen and hyaluronic acid (HA) formation. However, there are only a few commercial chitosan containing wound dressings, e.g. KytoCel® (MasterCare Medical GmbH), a chitosan cryogel, and Chitoderm® plus (Trusetal Verbandstoffwerk GmbH), a chitosan coated dressing. The big discrepancy between the scientific interest in chitosan dressings and its commercialization might be explained by the animal origin of chitosan; it is a

derivate from chitin, found in shrimp and crab shells. As a natural product, however, it bears a high risk of batch variations, for example concerning the molecular weight.[22] Yet, the biological activity of chitosan is dependent on the molecular weight of the macromolecules.[23–26] Additional drawbacks are the low elasticity of chitosan materials and the difficulty in producing fibrous wound dressings.[1]

The protein collagen is, together with alginate, one of the most frequently used materials in wound coverage. In the human body, collagen occurs inter alia in the ECM, in blood vessels, in bones, and in tendons.[27] The three main forms, Collagen I, II and III, constitute around 75% of dry human skin. Therefore, it is a well-tolerated material that is particularly suitable for wound dressing and tissue engineering applications. For medical use, the main sources are bovine, porcine, and avian derived collagen.[28] Collagen dressings are applied in the form of hydrogels (e.g. CellerateRX® (Wound Care Innovations LLC), Regenecare® Wound Gel (MPM Medical Inc.), Wun'Dres® (Coloplast AG)), fibrous cryogels (e.g. Biobrane® (Smith & Nephew), CollaSorb® (Paul Hartmann AG), Fibracol® (Acelity)), and grounded cryogels (e.g. Medifil® (Human Bio Science, Inc.), Stimulen™ (Southwest Technologies, Inc.)). Collagen is chosen for its high liquid absorbance capacity and its mechanical strength.[29] Furthermore, it plays an active role in wound healing. By recruiting fibroblasts, endothelial cells, and keratinocytes, the vascularization, granulation tissue formation, and collagen deposition is enhanced.[30,31] Moreover, scaring and the rate of bacterial infections is reduced. In current studies, two major issues of collagen are faced; enzymatic degradation of collagen leads to a fast loss of dressing stability and shape, and dependent on the source of the collagen, there is a risk of pathogen transmission.[32–34]

In contrast, wound dressing materials from synthetic precursors are non-infective, they have well defined chemical structures, and their properties can precisely be modified to fulfill the desired material requirements.[13] However, synthetic hydrogels do not actively participate in the wound healing process. Therefore, combinations of natural and synthetic polymers are usually preferred. Examples of available (partially) synthetic wound dressings are the polyacrylamide/polysaccharide-based FlexiGel® (Smith & Nephew), the poly(ethylene glycol) (PEG)/oakin-based Oakin® hydrogel wound dressing (Amerigel), and the polyurethane (PU)-based AquaClear® dressing (Paul Hartmann AG).

1.3.2 Double Network Hydrogels

A general issue of hydrogel materials is their relatively low mechanical stability, which is for example related to structural inhomogeneities in the polymer network and the low

friction between single polymer chains, as hydrogels typically have a polymer content of only 5 to 10%.[35] Yet, this drawback can be avoided by proper selection of the monomers, by chemical modifications of the precursor molecules, and in particular by physical modification of the hydrogel system. A physical hydrogel network modification, particularly aimed at enhancing mechanical resistance, was first described by Gong et al. The group developed hydrogels that consist of two separate polymer networks with internetwork entanglements, so called "double network" (DN) hydrogels (Figure 3).[36]

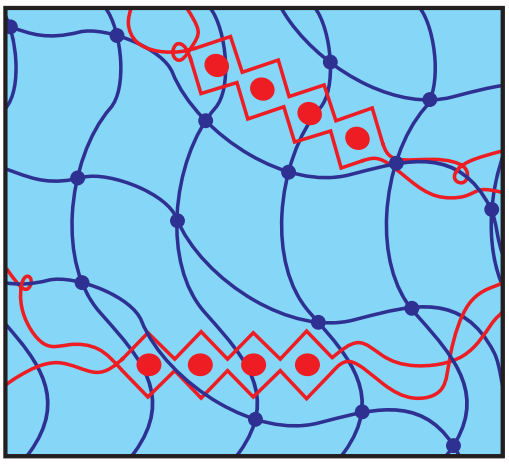

Figure 3. Schematic structure of a double network hydrogel with the covalent network in dark blue and the ionic network in red. Dots represent the cross-linking points.

A DN hydrogel is a special kind of interpenetrating polymer network (IPN) hydrogel, both consisting of two entangled polymer networks. The basic idea behind the use of two polymer networks is the combination of advantageous properties of each single network whilst overcoming their drawbacks. This might be related e.g. to the swelling properties, the biocompatibility, or the chemical stability of the hydrogel.[37,38] DN hydrogels additionally show a disproportional enhancement of the mechanical properties in comparison to the single components.[39] By this means, hydrogels with a maximum tensile stress of up to 10 MPa, a maximum compressive stress of up to 60 MPa, and a maximum strain of up to 2000% under tensile load and up to 95% under compressive load could be developed.[35] The DN hydrogels described by Gong et al. consist of a rigid and densely cross-linked polyelectrolyte as main network (primary network), and a flexible and loosely cross-linked neutral polymer as a far less concentrated secondary network. A typical DN formulation is poly(2-acrylamido-2-methylpropanesulfonic acid) (PAMPS) as primary and polyacrylamide (PAAm) as secondary network.[36] Yet, also "inverse" DN hydrogels with a neutral primary and an ionic secondary network were described to be highly load bearing.

For example, the combination of a neutral PEG network and an ionic poly(acrylic acid) (PAA) network resulted in hydrogels with a maximum tensile stress of up to 12 MPa and a pH-dependent maximum compressive stress of up to 4 MPa.[40,41] Even triple network (TN) hydrogels e.g. consisting of PAMPS/PAAm, oxidized dextran/teleostean/N-carboxyethyl-chitosan, or HA/poly(N,N-dimethylacrylamide) have been described.[42–44] The mechanism behind the stabilizing effect in DN/TN/IPN hydrogels has been intensively investigated. Dependent on the exact nature of the networks (ionic/neutral primary/secondary network, covalently or ionically cross-linked polymers), different concepts have been established. When "classical" DN hydrogels are stretched, first the rigid primary network consumes energy.[35,39] Its covalent bonds break and the network is divided into small clusters. Afterwards, the flexible secondary network can be stretched to a high extent. Hereby, great amounts of energy are dissipated. Additional stabilization comes from the clusters of the primary network, which serve as supplementary cross-links for the secondary network. Another theory points out the importance of voids in the primary network and therefore the high impact of the monomer molecular weight on the mechanical properties.[45] Voids can serve as crack stops. Further energy dissipation takes place because of inter-network entanglements and more importantly, because of intra-network entanglements of the secondary network within the voids. Yet, it must be differentiated between so-called "connected" and "true" DN hydrogels.[46] Nakajima and coworkers found that there might be unreacted functional groups in the primary network which polymerize during the formation of the secondary network. The resulting covalent connections between the two networks can likewise be responsible for the extraordinary stability of these "connected" DN hydrogels. In contrast, a strain hardening process based on the primary network was described for "true" DN hydrogels.[47] At high strain the polymer chains in the irreversibly destroyed primary network get orientated in the direction of the applied load, thus enhancing the mechanical resistance against failure. In "inverse" DN hydrogels, the stabilizing effect comes from physical inter-network interactions, e.g. hydrogen bonding.[39] An important process in the inverse DN hydrogels is therefore strain hardening, which in this case means the enhanced accessibility of hydrogen bond capable sites under high tension, resulting in a stabilization of the respective material.[40] Recently, Sun et al. also investigated IPN hydrogels of ionically cross-linked alginate and covalently cross-linked polyacrylamide with enhanced mechanical stability.[48] Thereby, the group identified two important mechanisms of stabilization, namely the reversible breakage of ionic bonds and meanwhile crack bridging by the covalent network.

1.3.3 Bioactive Hydrogel Wound Dressings

Considering the overall picture of hydrogel properties and in particular the properties of those consisting of two interpenetrating polymer networks, hydrogels are promising materials for wound dressing applications. In terms of liquid handling, the mechanical stability, the patient's compliance, and their chemical versatility, they totally fulfill the wound dressing requirements. However, modern wound dressings should also provide an active intervention in the wound healing process, which can be achieved by the following means.

1.3.3.1 Bioactive Hydrogel Precursors

First, the dressing material itself can participate in the wound healing process. In terms of hydrogel forming materials, especially the biological precursors and their derivates can influence the healing process. Already mentioned examples are alginate, chitosan, and collagen containing hydrogels, which for example enhance cell migration and angiogenesis, or suppress microbial infections.[17,20,31] In recent studies, their usage is proposed for different bioactive wound dressing applications. Straccia et al. reported on ionically cross-linked alginate/Zn^{2+} hydrogel wound dressings.[49] In contrast to ordinary Ca^{2+} cross-linked alginate gels, the zinc containing hydrogels showed improved swelling properties and the release of Zn^{2+} ions resulted in antimicrobial activity against *Escherichia Coli* in vitro. Alginate/HA hydrogel disks gave convincing results in in vitro healing assays with keratinocytes and adipose derived multipotent adult stem cells, as well as in rat wound models.[50] Furthermore, alginate hydrogels treated with non-thermal dielectric-barrier discharge plasma were shown to be suitable candidates for antimicrobial wound dressing applications.[51] Dependent on the plasma treatment time of the alginate gels and the type of bacterial strain, the pathogen load was significantly reduced or even eradicated in a period of seconds to minutes. The Murakami group used a combination of alginate, chitin, chitosan, and fucoidan to create bioactive hydrogel sheets that enhance the formation of granulation tissue and capillaries in wounds with impaired healing.[52] Furthermore, chitosan is frequently used as part of wound dressing materials because of its antimicrobial and hemostatic activity. In recent years, for example chitosan/PEG hydrogels, chitosan/PEG/poly(vinyl pyrrolidone) (PVP) coated cotton fibers, different chitosan/poly(vinyl alcohol) (PVA) sponges and hydrogels, chitosan/PVA/poly(ethylene oxide) (PEO) hydrogels, carboxymethylchitosan/gelatin hydrogels, chitosan/lactic acid cryogels were reported to be suitable wound dressing materials with healing-supportive

properties, regarding the overall healing time, the rate of granulation and epithelization, the formation of collagen and new blood vessels, and the suppression of a prolonged inflammation phase.[53–59] Likewise HA, an ECM derived glycosaminoglycan, can encourage the wound healing process. Different studies described an enhanced collagen deposition, increased re-epithelization, and higher vascularization in wounds because of the treatment with HA containing dressings.[60,61] In detail, HA interacts with endothelial cell receptors, which enhances the respective cell proliferation and thereby the formation of blood vessels.[62] This mechanism can also support the healing of skin grafted wounds, where a high vascularization is crucial for a successful acceptance of the skin graft.[63] Hyalofill®, Hyalosafe® (both Anika Therapeutics), and Hyalo^4 Regen (Fidia Pharma GmbH) are only some examples of commercial HA containing wound dressings.

1.3.3.2 Drug Loaded Hydrogel Wound Dressings

Another strategy of bioactive hydrogel wound dressings is the (controlled) release of drug molecules. The incorporated drug can target numerous fields that are essential for the wound healing process. Analgesics like ibuprofen, morphine, or lidocaine are of special interest in extensive burns, wounds with strong infections, or in palliative medicine.[64–66] Examined hydrogel release matrices are based on PVA, chitosan, and poloxamers. Comparable commercially available products are inter alia the foam dressing Biatain Ibu™ (0.5 $mg \cdot cm^{-1}$ ibuprofen; Coloplast AG) and the alginate/collagen hydrogel Regenecare® Wound Gel (2% lidocaine; MPM Medical, Inc.). For colonized wounds, hydrogel dressings loaded with antimicrobial drugs are the preferred choice. Despite the growing threat of antibiotic resistant bacterial strains, research was conducted for example on ciprofloxacin releasing alginate/chitosan membranes, tetracycline releasing alginate/ cellulose-based hydrogels, gentamycin sulfate releasing chitosan hydrogels, and sodium fusidate releasing PVA/PVP/propylene glycol hydrogels.[67–70] On the other hand, Li et al. focused on the prevention of antibiotic resistances by providing imprinted N-isopropyl-acrylamide (NIPAAm) hydrogel wound dressings which are capable of binding bacterial β-lactamase, the decisive molecule of resistant bacteria.[71] By this means, the antibiotic sensitivity of methicillin-resistant *Staphylococcus Aureus* (MRSA) against Penicillin G was regained successfully. Another strategy to avoid the development of resistant bacterial strains is the use of antimicrobial drugs based for example on bioactive proteins, metals, or natural derived materials. Intensive research has been done on the antimicrobial activity of nanoparticles (NPs) containing silver, titanium dioxide, or zinc oxide. Neibert et al.

developed a competitive antimicrobial dressing material by the incorporation of silver NPs in covalently cross-linked alginate fibers.[72] Moreover, the silver NP fibers enhanced the wound healing process, resulting in containment of the inflammation reaction, decreased healing time, and better quality (e.g. concerning collagen deposition, epidermal thickness, and mechanical stability) of the rebuilt tissue. TiO_2 NPs in combination inter alia with a chitosan/pectin or a chitosan/PVP film exhibit a strong antimicrobial activity and likewise improve the wound healing in animal models.[73,74] To overcome the potential concentration dependent cell toxicity of the mentioned nanoparticles, other researchers focused on the identification of natural antimicrobial agents. This includes essential oil (cinnamon, lavender, tea tree, lemon etc.) encapsulated in an alginate film, lysine dendrimers or its Schiff base with vanillin in burn wound dressings, melatonin released from chitosan/ Pluronic® F127 microspheres, and seaweed extract in PVA/PVP cryogels.[75–79] Widely used antiseptics are octenidine, poly(hexamethylene biguanide) hydrochloride (PHMB), and povidone-iodine.[80,81] PHMB controlled release and antimicrobial activity studies were conducted in combination with HA nanocapsules which are degradable in contact with hyaluronidase, a bacterial enzyme.[82] As part of cellulose dressings, PHMB was superior to povidone-iodine and its activity against *Bacillus Subtilis*, *S. Aureus*, MRSA, *E. Coli*, *Acinetobacter Baumannii*, and *Pseudomonas Aeruginosa* was proven.[83,84] In the clinics, infected wounds can be treated by Iodosorb gel (0.9% w/w iodine; Smith & Nephew), Kerlix® AMD sponge (0.2% PHMB; Covidien), XCell antimicrobial dressing (0.3% PHMB; Xylos), Hydrogel Ag (1% silver sulfadiazine; Gentell), SilvaSorb® sheet (0.13% silver chloride; Medline), Anasept® Antimicrobial Skin & Wound Gel (0.057% sodium hypochlorite; Anacapa Technologies), and many more.

1.3.3.3 Cell and Cell-Derived Protein Loaded Hydrogel Wound Dressings

The most recent class of bioactive hydrogel wound dressings is based on the supportive healing activity of growth factors, cytokines, and (stem) cells. The thorough investigation of the complex wound healing cascade enabled the identification of cell derived proteins that mediate important wound healing processes like cell proliferation and angiogenesis. In this context, the impact of epidermal growth factor (EGF), fibroblast growth factor (FGF), keratinocyte growth factor (KGF), platelet-derived growth factor (PDGF), vascular endothelial growth factor (VEGF), and different forms of platelet-rich plasma (PRP; containing inter alia insulin-like growth factor (IGF-1), PDGF, transforming growth factor-β (TGF-β), and VEGF) have been described.[24,85–88] Human EGF which was

incorporated e.g. in a heparin/PEG or in a IR responsive NIPAAm hydrogel could significantly enhance wound closure in mice, resulting in increased granulation, epithelization, and vascularization.[89,90] Li et al. proposed the combined release of EGF and the antioxidant curcumin from poly(lactic acid) (PLA) NPs in a PLA hydrogel to further enhance the healing process.[91] The group confirmed a positive effect on the formation of collagen, granulation tissue, and new blood vessels. Yet, the transdermal delivery efficiency and the stability of GFs were limited. To overcome this problem, EGF was bound to HA whilst retaining its biological activity.[92] A detailed analysis of the involved wound cytokines revealed a reduction of the inflammatory molecules tumor necrosis factor-α (TNF-α) and interleukin-1 (IL-1), and increased values of the cell proliferation promoting TGF-β and β-defensin-2, because of the EGF-HA treatment. Gelatin gels containing FGF, chitosan hydrogels containing KGF, and chitosan/HA cryogels containing fibrin NPs with VEGF are further examples of recently developed bioactive hydrogel wound dressings.[93–95] Nevertheless, there are indications that the administration of more than one GF might give a better outcome, as the different processes in wound healing include complex interactions between numerous GFs.[85] The application of a GF mixture exceeds the single GF treatment by promoting faster wound healing and a higher rate of epithelization and capillary formation. Relevant approaches are dressing materials with multiple GF loading, such as chitosan/PEO fibers containing PDGF-BB and VEGF, or dressings with (activated) PRP or platelet lysate.[96,97] Appropriate release matrices for PRP derived materials can be chitosan, gelatin, or fibrin.[86,98,99] Spanò et al. even described a bioactive membrane of different blood plasma derived components (PRP, platelet poor plasma, and thrombin) for the treatment of skin ulcers.[100]

A more elegant way to deliver multiple cell-derived proteins to a wound is the direct incorporation of the respective cells into the wound dressing material. This strategy includes fibroblasts, keratinocytes, and stem cells from numerous origins.[88] Differentiated cells (fibroblasts, keratinocytes) are mainly used to produce skin analogues based on degradable, biological matrices like alginate, chitosan, collagen, and gelatin.[101–105] The cellular production of KGF, promoting the epithelization, and VEGF, promoting the vascularization, as well as the direct delivery of the cells to the wound site were found to enhance the wound healing significantly.[103,106] However, the development and application of stem cell containing materials seem to be more promising. Stem cells exhibit a high potential for self-renewal and the ability to differentiate into various cell types, dependent on the surrounding environment. By cell recruitment, the differentiation into dermal cells,

and the secretion of growth factors and cytokines, stem cells can very effectively participate in wound healing.[107] They thereby improve the granulation, the angiogenesis, the epithelization, the production of collagen, and the overall healing time. Prenatal stem cells from the amniotic fluid and neonatal stem cells from the umbilical cord have been successfully integrated in hydrogel wound dressings.[108,109] Even more attention has been paid to adult mesenchymal stem cells (MSCs) and adipose-derived stem cells (ASCs). Chen et al. precisely investigated the impact of bone marrow MSCs containing NIPAAm/ poly(amidoamine) hydrogels on wound healing in diabetic mice.[110] The increased expression of basic FGF is connected to increased angiogenesis and reduced scar formation. A high TGF-β1 level is responsible for enhanced ECM/collagen production, and increased granulation and epithelization, all leading to a better healing of the diabetic wounds. The production of VEGF and PDGF, and therefore the amount of angiogenesis, can be further increased by a hypoxia treatment of the MSCs.[111] Suitable matrices for ASCs may be thermogelling PEG, HA/chitosan, pullan/collagen, or poly(3-hydroxy-butyrate-co-hydroxyvalerate) gels.[112–115] Involved factors in wound healing were identified to be inter alia VEGF and stromal cell derived factor SDF-1 for increased angiogenesis, and matrix metalloproteinase MMP1 and MMP9 for enhanced remodeling of the skin structure. Even ASCs gained from burn wound debridement were able to differentiate into epithelia, dermal and vascular cells, likewise enhancing the healing process.[116,117] Despite the high research interest, the only available GF application to date has been the 0.01% PBGF-BB containing Regranex® Gel (Smith & Nephew). Cell containing wound dressings are limited to skin substitutes with incorporated fibroblasts and keratinocytes. They can be developed from autologous (e.g. PermaDerm™ (Amarantus BioScience Holdings Inc.), clinical phase 2) or allogeneic (neonatal foreskin + bovine collagen; e.g. Apligraft® (Organogenesis Inc.), OrCel® (I-Horus Inc.)) origin.[2] Stem cell wound dressings are still under development. Issues which are responsible for the high discrepancy between the scientific interest and the relevance for clinical applications are the high costs of GFs, the loss of therapeutic activity during prolonged or improper storage, and the risk of cancer which is related to extensive GF and PRP application.[6,97,100] Furthermore, GFs are rapidly degraded by increased MMP concentrations in the chronic wound environment, which leads to the adverse need of frequent dressing changes (e.g. two times a day for Regranex® Gel).[88,118,119] Besides, cell treatment always bears the risk of contamination, related to the donor (transmission of diseases) or the production procedure.[88] Especially concerning stem cells there is no standard procedure for their isolation, processing, and application.[107] This

is furthermore critical, because the microenvironment of stem cells is strongly related to the survival rate and the cell differentiation, both affecting wound healing.

1.4 Concluding Remarks and Future Perspectives

In the field of wound care, there are still many challenges to overcome. The above discussed promising performance of hydrogel wound dressings must be further expanded to correspond to the increasing need for acute and chronic wound treatment options. Especially the development of bioactive dressing materials should be tackled by current research. Yet, big obstacles such as the materials' cost-effectiveness (related to expensive drugs, production procedures, and dressing materials) and reproducibility (related to natural derived products), as well as the patients' safety (related to allogeneic or xenogeneic materials) need to be considered. Hence, alternative concepts including new materials or different modes of action have to come to the fore. One promising approach for the treatment of non-healing wounds might be the readjustment of the wound pH.[120,121] Both, excessive alkaline and acidic pH values were measured in chronic wounds.[122,123] The non-physiological pH milieu has a major impact on numerous processes of the wound healing cascade. In particular, the ability of cells to migrate and proliferate, the biological activity of crucial proteins (GFs, cytokines, MMPs), the supply with oxygen, and the liability to wound infections are all dependent on the wound pH.[123–126] Therefore, the combination of several basic concepts, such as pH-modifying properties, bioactive precursors, and controlled drug release, to one outstanding wound dressing material should be considered in future health care research.

2. Goal of the Thesis

Hydrogel-based wound dressings are one of the most promising materials in wound care, because they fulfill important dressing requirements such as keeping the wound moist whilst absorbing extensive exudate, adhesion-free coverage of the sensitive underlying tissue, pain reduction through a cooling effect, and good biocompatibility. Furthermore, hydrogel wound dressings enable an active intervention in the wound healing process, for example through controlled drug release or cell incorporation. Although hydrogel-based dressings are already on the market, general problems of wound care products still exist. Immense costs of complex technologies, safety concerns regarding drugs or allogeneic/ xenogeneic materials, insufficient technical possibilities for an industrial up-scaling, as

well as special hydrogel-specific issues, such as the lack of mechanical stability, are impeding the clinical implementation of many novel approaches. Yet, new treatment options are urgently requested in view of the current situation in health care. Due to the aging society, clinicians have to face a growing number of severe, acute and chronic wounds in clinical daily life. To meet the clinical needs, the development of new hydrogel wound dressings with enhanced material properties, regarding inter alia the mechanical performance and the fluid handling, is necessary. Further, novel hydrogel dressings should actively promote the wound healing process in an applicable and cost-effective way. For the treatment of acute wounds, antimicrobial dressings are of interest because they can prevent infections that are one of the mayor issues in this field. Chronic wounds are even more complex to handle than acute wounds because crucial cellular processes of the healing cascade are impeded, inter alia caused by a non-physiological pH shift. Therefore, the controlled adaption of the wound pH might be a promising new concept of reviving wound healing by efficient means.

After a general overview of the literature in **Chapter 1**, regarding the current development in the field of bioactive hydrogel-base wound dressings, some of the main drawbacks of hydrogel dressings are addressed within this thesis. In **Chapter 2**, the combination of biocompatible poly(ethylene glycol) diacrylate (PEGDA) and bioactive alginate in one material to exploit the favorable effect of interpenetrating polymer networks (IPNs) is discussed. Especially the impact of an altered network density and different polymerization mechanisms on the mechanical properties of the resulting IPN hydrogels were analyzed. Furthermore, the IPN's suitability for the treatment of acute wounds was evaluated by analyzing its performance as antimicrobial, poly(hexamethylene biguanide) hydrochloride (PHMB) containing dressing.

Further research focused on the development of pH-modifying chronic wound dressings. To address this, the IPN hydrogel system PEGDA/alginate was supplemented with acrylic acid (AA). Different AA containing formulations were assessed for their material and pH-modulating properties. Moreover, cell viability assays and wound healing experiments with alkalosis wound models were conducted to investigate their bioactive properties. The results are presented in **Chapter 3**.

Structural modifications of IPN systems directly influence their material properties, including the mechanical stability and the liquid handling capacity. Hence, the optimization of the PEGDA/AA/alginate hydrogel network structure discussed in **Chapter 4** corresponds to an adaption of its wound healing properties. Particularly the

impact of the PEGDA molecular weight on the material properties was analyzed in detail. Moreover, the decisive structural interactions between the two interpenetrating networks PEGDA/AA and alginate were studied by comparing them to equivalent IPN hydrogel formulations without ionizable functional groups.

Alkaline dressing materials might be an effective tool for the treatment of skin grafted and acidosis chronic wounds. To investigate this assumption, different precursors were screened for their ability to serve as basic, pH-modulating part of PEGDA-based IPN hydrogels in **Chapter 5**. Dependent on the targeted wound type, pH-active molecules with different pK_a values were used and the secondary network (alginate or chitosan) was adapted accordingly. The superficial seeding of human dermal fibroblasts induced additional bioactive properties in terms of a potential cell or cell-derived protein release.

Based on the findings discussed in the previous chapters, a universal approach to pH-modifying chronic wound treatment was conducted and discussed in **Chapter 6**. Mono- and bimolecular buffer systems were chosen as potential pH-active components and combined with the mechanically stabilized IPN hydrogel system PEGDA/alginate. The most promising hydrogel formulation was identified by a bottom-up approach, regarding the wound healing capacity, and further characterized for its overall material performance. An antimicrobial activity by PHMB incorporation and its pH-sensitive release supplemented the bioactive healing properties of the buffering hydrogels.

References

1. Ducheyne P, Healy K, Hutmacher DE, Grainger DW, Kirkpatrick CJ. Comprehensive Biomaterials. Oxford, UK: Elsevier; 2011.
2. Sun BK, Siprashvili Z, Khavari PA. Advances in skin grafting and treatment of cutaneous wounds. Science 2014; 346: 941–945.
3. Ågren M. Wound Healing Biomaterials: Volume 1; Therapies and Regeneration, 1st edn. Swaston, UK: Woodhead Publishing; 2016.
4. Moura LIF, Dias AMA, Carvalho E, Sousa HCd. Recent advances on the development of wound dressings for diabetic foot ulcer treatment-a review. Acta Biomater. 2013; 9: 7093–7114.
5. Morton LM, Phillips TJ. Wound healing and treating wounds. J. Am. Acad. Dermatol. 2016; 74: 589–605.
6. Boateng J, Catanzano O. Advanced therapeutic dressings for effective wound healing--A review. J. Pharm. Sci. 2015; 104: 3653–3680.
7. Fife CE, Carter MJ. Wound care outcomes and associated cost among patients treated in US outpatient wound centers: Data from the US wound registry. Wounds 2012; 24: 10–17.
8. Carlson B, editor. Advanced Wound Care Markets Worldwide. Rockville, MD, USA: Kalorama Information; 2016.
9. The Global Market For Advanced Wound Care Products. London, UK: BMI Research; 2016.
10. Junker JPE, Kamel RA, Caterson EJ, Eriksson E. Clinical impact upon wound healing and inflammation in moist, wet, and dry environments. Adv. Wound Care 2013; 2: 348–356.
11. Boateng JS, Matthews KH, Stevens HNE, Eccleston GM. Wound healing dressings and drug delivery systems: A review. J. Pharm. Sci. 2008; 97: 2892–2923.
12. Cutting KF. Wound exudate: Composition and functions. Brit. J. Community Nurs. 2003; 8: 4–9.
13. Mayet N, Choonara YE, Kumar P, Tomar LK, Tyagi C, Du Toit LC, Pillay V. A comprehensive review of advanced biopolymeric wound healing systems. J. Pharm. Sci. 2014; 103: 2211–2230.

14. Sahiner N, Sagbas S, Sahiner M, Silan C, Aktas N, Turk M. Biocompatible and biodegradable poly(tannic acid) hydrogel with antimicrobial and antioxidant properties. Int. J. Biol. Macromol. 2016; 82: 150–159.
15. Chen Y, Zhang Y, Wang F, Meng W, Yang X, Li P, Jiang J, Tan H, Zheng Y. Preparation of porous carboxymethyl chitosan grafted poly(acrylic acid) superabsorbent by solvent precipitation and its application as a hemostatic wound dressing. Mater. Sci. Eng. C Mater. Biol. Appl. 2016; 63: 18–29.
16. Pawar SN, Edgar KJ. Alginate derivatization: A review of chemistry, properties and applications. Biomaterials 2012; 33: 3279–3305.
17. Lee W-R, Park J-H, Kim K-H, Kim S-J, Park D-H, Chae M-H, Suh S-H, Jeong S-W, Park K-K. The biological effects of topical alginate treatment in an animal model of skin wound healing. Wound Rep. Regen. 2009; 17: 505–510.
18. Wiegand C, Heinze T, Hipler U-C. Comparative in vitro study on cytotoxicity, antimicrobial activity, and binding capacity for pathophysiological factors in chronic wounds of alginate and silver-containing alginate. Wound Repair Regen. 2009; 17: 511–521.
19. Azuma K, Izumi R, Osaki T, Ifuku S, Morimoto M, Saimoto H, Minami S, Okamoto Y. Chitin, chitosan, and its derivatives for wound healing: Old and new materials. J. Funct. Biomater. 2015; 6: 104–142.
20. Jayakumar R, Prabaharan M, Sudheesh Kumar PT, Nair SV, Tamura H. Biomaterials based on chitin and chitosan in wound dressing applications. Biotechnol. Adv. 2011; 29: 322–337.
21. Moura LIF, Dias AMA, Leal EC, Carvalho L, Sousa HC de, Carvalho E. Chitosan-based dressings loaded with neurotensin--An efficient strategy to improve early diabetic wound healing. Acta Biomater. 2014; 10: 843–857.
22. Ng VWL, Chan JMW, Sardon H, Ono RJ, Garcia JM, Yang YY, Hedrick JL. Antimicrobial hydrogels: A new weapon in the arsenal against multidrug-resistant infections. Adv. Drug Deliv. Rev. 2014; 78: 46–62.
23. Phaechamud T, Yodkhum K, Charoenteeraboon J, Tabata Y. Chitosan-aluminum monostearate composite sponge dressing containing asiaticoside for wound healing and angiogenesis promotion in chronic wound. Mater. Sci. Eng. C Mater. Biol. Appl. 2015; 50: 210–225.
24. Patrulea V, Ostafe V, Borchard G, Jordan O. Chitosan as a starting material for wound healing applications. Eur. J. Pharm. Biopharm. 2015; 97: 417–426.

25. Zheng L-Y, Zhu J-F. Study on antimicrobial activity of chitosan with different molecular weights. Carbohydr. Polym. 2003; 54: 527–530.
26. Kean T, Thanou M. Biodegradation, biodistribution and toxicity of chitosan. Adv. Drug Deliv. Rev. 2010; 62: 3–11.
27. Ågren M. Wound Healing Biomaterials: Volume 2; Functional Biomaterials, 1st edn. Swaston, UK: Woodhead Publishing; 2016.
28. Mogosanu GD, Grumezescu AM. Natural and synthetic polymers for wounds and burns dressing. Int. J. Pharm. 2014; 463: 127–136.
29. Malessa R, Kassner A. Degradation-stabilized, biocompatible collagen matrices (US8722854 B2); 2014.
30. Chattopadhyay S, Raines RT. Review collagen-based biomaterials for wound healing. Biopolymers 2014; 101: 821–833.
31. Moura LI, Dias AM, Suesca E, Casadiegos S, Leal EC, Fontanilla MR, Carvalho L, Sousa HCd, Carvalho E. Neurotensin-loaded collagen dressings reduce inflammation and improve wound healing in diabetic mice. Biochim. Biophys. Acta, Mol. Basis Dis. 2014; 1842: 32–43.
32. Helary C, Abed A, Mosser G, Louedec L, Letourneur D, Coradin T, Giraud-Guille MM, Meddahi-Pelle A. Evaluation of dense collagen matrices as medicated wound dressing for the treatment of cutaneous chronic wounds. Biomater. Sci. 2015; 3: 373–382.
33. Willard JJ, Drexler JW, Das A, Roy S, Shilo S, Shoseyov O, Powell HM. Plant-derived human collagen scaffolds for skin tissue engineering. Tissue Eng. Part A 2013; 19: 1507–1518.
34. Natarajan V, Krithica N, Madhan B, Sehgal PK. Preparation and properties of tannic acid cross-linked collagen scaffold and its application in wound healing. J. Biomed. Mater. Res. Part B Appl. Biomater. 2013; 101: 560–567.
35. Gong JP. Why are double network hydrogels so tough? Soft Matter 2010; 6: 2583–2590.
36. Gong JP, Katsuyama Y, Kurokawa T, Osada Y. Double-network hydrogels with extremely high mechanical strength. Adv. Mater. 2003; 15: 1155–1158.
37. Tong X, Yang F. Engineering interpenetrating network hydrogels as biomimetic cell niche with independently tunable biochemical and mechanical properties. Biomaterials 2014; 35: 1807–1815.

38. Li G, Zhang H, Fortin D, Xia H, Zhao Y. Poly(vinyl alcohol)-poly(ethylene glycol) double-network hydrogel: A general approach to shape memory and self-healing functionalities. Langmuir 2015; 31: 11709–11716.
39. Haque MA, Kurokawa T, Gong JP. Super tough double network hydrogels and their application as biomaterials. Polymer 2012; 53: 1805–1822.
40. Myung D, Koh W, Ko J, Hu Y, Carrasco M, Noolandi J, Ta CN, Frank CW. Biomimetic strain hardening in interpenetrating polymer network hydrogels. Polymer 2007; 48: 5376–5387.
41. Waters DJ, Engberg K, Parke-Houben R, Ta CN, Jackson AJ, Toney MF, Frank CW. Structure and mechanism of strength enhancement in interpenetrating polymer network hydrogels. Macromolecules 2011; 44: 5776–5787.
42. Kaneko D, Tada T, Kurokawa T, Gong JP, Osada Y. Mechanically strong hydrogels with ultra-low frictional coefficients. Adv. Mater. 2005; 17: 535–538.
43. Zhang H, Qadeer A, Mynarcik D, Chen W. Delivery of rosiglitazone from an injectable triple interpenetrating network hydrogel composed of naturally derived materials. Biomaterials 2011; 32: 890–898.
44. Tavsanli B, Can V, Okay O. Mechanically strong triple network hydrogels based on hyaluronan and poly(N,N-dimethylacrylamide). Soft Matter 2015; 11: 8517–8524.
45. Tsukeshiba H, Huang M, Na Y-H, Kurokawa T, Kuwabara R, Tanaka Y, Furukawa H, Osada Y, Gong JP. Effect of polymer entanglement on the toughening of double network hydrogels. J. Phys. Chem. B 2005; 109: 16304–16309.
46. Nakajima T, Furukawa H, Tanaka Y, Kurokawa T, Osada Y, Gong JP. True chemical structure of double network hydrogels. Macromolecules 2009; 42: 2184–2189.
47. Nakajima T, Kurokawa T, Ahmed S, Wu W-l, Gong JP. Characterization of internal fracture process of double network hydrogels under uniaxial elongation. Soft Matter 2013; 9: 1955–1966.
48. Sun J-Y, Zhao X, Illeperuma WRK, Chaudhuri O, Oh KH, Mooney DJ, Vlassak JJ, Suo Z. Highly stretchable and tough hydrogels. Nature 2012; 489: 133–136.
49. Straccia MC, d'Ayala GG, Romano I, Laurienzo P. Novel zinc alginate hydrogels prepared by internal setting method with intrinsic antibacterial activity. Carbohydr. Polym. 2015; 125: 103–112.
50. Catanzano O, D'Esposito V, Acierno S, Ambrosio MR, Caro C de, Avagliano C, Russo P, Russo R, Miro A, Ungaro F, Calignano A, Formisano P, Quaglia F. Alginate-

hyaluronan composite hydrogels accelerate wound healing process. Carbohydr. Polym. 2015; 131: 407–414.

51. Poor AE, Ercan UK, Yost A, Brooks AD, Joshi SG. Control of multi-drug-resistant pathogens with non-thermal-plasma-treated alginate wound dressing. Surg. Infect. 2014; 15: 233–243.
52. Murakami K, Aoki H, Nakamura S, Nakamura S-i, Takikawa M, Hanzawa M, Kishimoto S, Hattori H, Tanaka Y, Kiyosawa T, Sato Y, Ishihara M. Hydrogel blends of chitin/chitosan, fucoidan and alginate as healing-impaired wound dressings. Biomaterials 2010; 31: 83–90.
53. Chen C, Liu L, Huang T, Wang Q, Fang Y. Bubble template fabrication of chitosan/ poly(vinyl alcohol) sponges for wound dressing applications. Int. J. Biol. Macromol. 2013; 62: 188–193.
54. Fan L, Yang J, Wu H, Hu Z, Yi J, Tong J, Zhu X. Preparation and characterization of quaternary ammonium chitosan hydrogel with significant antibacterial activity. Int. J. Biol. Macromol. 2015; 79: 830–836.
55. Nacer Khodja A, Mahlous M, Tahtat D, Benamer S, Larbi Youcef S, Chader H, Mouhoub L, Sedgelmaci M, Ammi N, Mansouri MB, Mameri S. Evaluation of healing activity of PVA/chitosan hydrogels on deep second degree burn: Pharmacological and toxicological tests. Burns 2013; 39: 98–104.
56. Anjum S, Arora A, Alam MS, Gupta B. Development of antimicrobial and scar preventive chitosan hydrogel wound dressings. Int. J. Pharm. 2016; 508: 92–101.
57. Chen S-H, Tsao C-T, Chang C-H, Lai Y-T, Wu M-F, Chuang C-N, Chou H-C, Wang C-K, Hsieh K-H. Assessment of reinforced poly(ethylene glycol) chitosan hydrogels as dressings in a mouse skin wound defect model. Mater. Sci. Eng. C Mater. Biol. Appl. 2013; 33: 2584–2594.
58. Huang X, Zhang Y, Zhang X, Xu L, Chen X, Wei S. Influence of radiation crosslinked carboxymethyl-chitosan/gelatin hydrogel on cutaneous wound healing. Mater. Sci. Eng. C Mater. Biol. Appl. 2013; 33: 4816–4824.
59. Baxter RM, Dai T, Kimball J, Wang E, Hamblin MR, Wiesmann WP, McCarthy SJ, Baker SM. Chitosan dressing promotes healing in third degree burns in mice: Gene expression analysis shows biphasic effects for rapid tissue regeneration and decreased fibrotic signaling. J. Biomed. Mater. Res. A 2013; 101: 340–348.
60. Neuman MG, Nanau RM, Oruna-Sanchez L, Coto G. Hyaluronic acid and wound healing. J. Pharm. Pharm. Sci. 2015; 18: 53–60.

61. Anilkumar TV, Muhamed J, Jose A, Jyothi A, Mohanan PV, Krishnan LK. Advantages of hyaluronic acid as a component of fibrin sheet for care of acute wound. Biologicals 2011; 39: 81–88.
62. Silva LPd, Pirraco RP, Santos TC, Novoa-Carballal R, Cerqueira MT, Reis RL, Correlo VM, Marques AP. Neovascularization induced by the hyaluronic acid-based spongy-like hydrogels degradation products. ACS Appl. Mater. Interfaces 2016; 8: 33464–33474.
63. Zhao J-Y, Chai J-K, Song H-F, Zhang J, Xu M-H, Liang Y-D. Influence of hyaluronic acid on wound healing using composite porcine acellular dermal matrix grafts and autologous skin in rabbits. Int. Wound J. 2013; 10: 562–572.
64. Morgado PI, Lisboa PF, Ribeiro MP, Miguel SP, Simões PC, Correia IJ, Aguiar-Ricardo A. Poly(vinyl alcohol)/chitosan asymmetrical membranes: Highly controlled morphology toward the ideal wound dressing. J. Membrane Sci. 2014; 469: 262–271.
65. Heilmann S, Kuchler S, Wischke C, Lendlein A, Stein C, Schafer-Korting M. A thermosensitive morphine-containing hydrogel for the treatment of large-scale skin wounds. Int. J. Pharm. 2013; 444: 96–102.
66. Du L, Tong L, Jin Y, Jia J, Liu Y, Su C, Yu S, Li X. A multifunctional in situ-forming hydrogel for wound healing. Wound Rep. Regen. 2012; 20: 904–910.
67. Han F, Dong Y, Song A, Yin R, Li S. Alginate/chitosan based bi-layer composite membrane as potential sustained-release wound dressing containing ciprofloxacin hydrochloride. Appl. Surf. Sci. 2014; 311: 626–634.
68. Chen H, Xing X, Tan H, Jia Y, Zhou T, Chen Y, Ling Z, Hu X. Covalently antibacterial alginate-chitosan hydrogel dressing integrated gelatin microspheres containing tetracycline hydrochloride for wound healing. Mater. Sci. Eng. C Mater. Biol. Appl. 2017; 70, Part 1: 287–295.
69. Jiang Q, zhou W, Wang J, Tang R, Di Zhang, Wang X. Hypromellose succinate-crosslinked chitosan hydrogel films for potential wound dressing. Int. J. Biol. Macromol. 2016; 91: 85–91.
70. Kim DW, Kim KS, Seo YG, Lee B-J, Park YJ, Youn YS, Kim JO, Yong CS, Jin SG, Choi H-G. Novel sodium fusidate-loaded film-forming hydrogel with easy application and excellent wound healing. Int. J. Pharm. 2015; 495: 67–74.
71. Li W, Dong K, Ren J, Qu X. A beta-lactamase-imprinted responsive hydrogel for the treatment of antibiotic-resistant bacteria. Angew. Chem. Int. Ed. 2016; 55: 8049–8053.

72. Neibert K, Gopishetty V, Grigoryev A, Tokarev I, Al-Hajaj N, Vorstenbosch J, Philip A, Minko S, Maysinger D. Wound-healing with mechanically robust and biodegradable hydrogel fibers loaded with silver nanoparticles. Adv. Healthcare Mater. 2012; 1: 621–630.
73. Archana D, Dutta J, Dutta PK. Evaluation of chitosan nano dressing for wound healing: characterization, in vitro and in vivo studies. Int. J. Biol. Macromol. 2013; 57: 193–203.
74. Archana D, Singh BK, Dutta J, Dutta PK. In vivo evaluation of chitosan-PVP-titanium dioxide nanocomposite as wound dressing material. Carbohydr. Polym. 2013; 95: 530–539.
75. Liakos I, Rizzello L, Scurr DJ, Pompa PP, Bayer IS, Athanassiou A. All-natural composite wound dressing films of essential oils encapsulated in sodium alginate with antimicrobial properties. Int. J. Pharm. 2014; 463: 137–145.
76. Konieczynska MD, Villa-Camacho JC, Ghobril C, Perez-Viloria M, Tevis KM, Blessing WA, Nazarian A, Rodriguez EK, Grinstaff MW. On-demand dissolution of a dendritic hydrogel-based dressing for second-degree burn wounds through thiol-thioester exchange reaction. Angew. Chem. Int. Ed. 2016; 55: 9984–9987.
77. Zhou G, A R, Ge H, Wang L, Liu M, Wang B, Su H, Yan M, Xi Y, Fan Y. Research on a novel poly(vinyl alcohol)/lysine/vanillin wound dressing: Biocompatibility, bioactivity and antimicrobial activity. Burns 2014; 40: 1668–1678.
78. Romic MD, Klaric MS, Lovric J, Pepic I, Cetina-Cizmek B, Filipovic-Grcic J, Hafner A. Melatonin-loaded chitosan/Pluronic® F127 microspheres as in situ forming hydrogel: An innovative antimicrobial wound dressing. Eur. J. Pharm. Biopharm. 2016; 107: 67–79.
79. Tan SP, McLoughlin P, O'Sullivan L, Prieto ML, Gardiner GE, Lawlor PG, Hughes H. Development of a novel antimicrobial seaweed extract-based hydrogel wound dressing. Int. J. Pharm. 2013; 456: 10–20.
80. Moritz S, Wiegand C, Wesarg F, Hessler N, Müller FA, Kralisch D, Hipler U-C, Fischer D. Active wound dressings based on bacterial nanocellulose as drug delivery system for octenidine. Int. J. Pharm. 2014; 471: 45–55.
81. Dissemond J, Augustin M, Eming SA, Goerge T, Horn T, Karrer S, Schumann H, Stucker M. Modern wound care - practical aspects of non-interventional topical treatment of patients with chronic wounds. J. Dtsch. Dermatol. Ges. 2014; 12: 541–554.

82. Baier G, Cavallaro A, Vasilev K, Mailander V, Musyanovych A, Landfester K. Enzyme responsive hyaluronic acid nanocapsules containing polyhexanide and their exposure to bacteria to prevent infection. Biomacromolecules 2013; 14: 1103–1112.
83. Wiegand C, Moritz S, Hessler N, Kralisch D, Wesarg F, Müller FA, Fischer D, Hipler U-C. Antimicrobial functionalization of bacterial nanocellulose by loading with polihexanide and povidone-iodine. J. Mater. Sci. Mater. Med. 2015; 26: 245.
84. Napavichayanun S, Amornsudthiwat P, Pienpinijtham P, Aramwit P. Interaction and effectiveness of antimicrobials along with healing-promoting agents in a novel biocellulose wound dressing. Mater. Sci. Eng. C Mater. Biol. Appl. 2015; 55: 95–104.
85. Prestwich GD. Hyaluronic acid-based clinical biomaterials derived for cell and molecule delivery in regenerative medicine. J. Control. Release 2011; 155: 193–199.
86. Notodihardjo PV, Morimoto N, Kakudo N, Matsui M, Sakamoto M, Liem PH, Suzuki K, Tabata Y, Kusumoto K. Gelatin hydrogel impregnated with platelet-rich plasma releasate promotes angiogenesis and wound healing in murine model. J. Artif. Organs 2015; 18: 64–71.
87. Kutlu B, Tigli Aydin RS, Akman AC, Gumusderelioglu M, Nohutcu RM. Platelet-rich plasma-loaded chitosan scaffolds: Preparation and growth factor release kinetics. J. Biomed. Mater. Res. Part B Appl. Biomater. 2013; 101: 28–35.
88. Borena BM, Martens A, Broeckx SY, Meyer E, Chiers K, Duchateau L, Spaas JH. Regenerative skin wound healing in mammals: State-of-the-art on growth factor and stem cell based treatments. Cell. Physiol. Biochem. 2015; 36: 1–23.
89. Goh M, Hwang Y, Tae G. Epidermal growth factor loaded heparin-based hydrogel sheet for skin wound healing. Carbohydr. Polym. 2016; 147: 251–260.
90. Han L, Zhang Y, Lu X, Wang K, Wang Z, Zhang H. Polydopamine nanoparticles modulating stimuli-responsive PNIPAM hydrogels with cell/tissue adhesiveness. ACS Appl. Mater. Interfaces 2016; 8: 29088–29100.
91. Li X, Ye X, Qi J, Fan R, Gao X, Wu Y, Zhou L, Tong A, Guo G. EGF and curcumin co-encapsulated nanoparticle/hydrogel system as potent skin regeneration agent. Int. J. Nanomedicine 2016; 11: 3993–4009.
92. Kim H, Kong WH, Seong K-Y, Sung DK, Jeong H, Kim JK, Yang SY, Hahn SK. Hyaluronate-epidermal growth factor conjugate for skin wound healing and regeneration. Biomacromolecules 2016; 17: 3694–3705.

93. Sakamoto M, Morimoto N, Ogino S, Jinno C, Taira T, Suzuki S. Efficacy of gelatin gel sheets in sustaining the release of basic fibroblast growth factor for murine skin defects. J. Surg. Res. 2016; 201: 378–387.
94. Xu D, Fu W, Chen, Huihua, Zou, Minji, Cai X, Xia W. Composite chitosan hydrogel dressing as well as preparation method and applications thereof (CN104707164 A); 2015.
95. Mohandas A, Anisha BS, Chennazhi KP, Jayakumar R. Chitosan-hyaluronic acid/ VEGF loaded fibrin nanoparticles composite sponges for enhancing angiogenesis in wounds. Colloid Surf. B Biointerfaces 2015; 127: 105–113.
96. Xie Z, Paras CB, Weng H, Punnakitikashem P, Su L-C, Vu K, Tang L, Yang J, Nguyen KT. Dual growth factor releasing multi-functional nanofibers for wound healing. Acta Biomater. 2013; 9: 9351–9359.
97. Busilacchi A, Gigante A, Mattioli-Belmonte M, Manzotti S, Muzzarelli RAA. Chitosan stabilizes platelet growth factors and modulates stem cell differentiation toward tissue regeneration. Carbohydr. Polym. 2013; 98: 665–676.
98. Lu B, Wang T, Li Z, Dai F, Lv L, Tang F, Yu K, Liu J, Lan G. Healing of skin wounds with a chitosan-gelatin sponge loaded with tannins and platelet-rich plasma. Int. J. Biol. Macromol. 2016; 82: 884–891.
99. La W-G, Yang HS. Heparin-conjugated poly(lactic-co-glycolic acid) nanospheres enhance large-wound healing by delivering growth factors in platelet-rich plasma. Artif. Organs 2015; 39: 388–394.
100. Spano R, Muraglia A, Todeschi MR, Nardini M, Strada P, Cancedda R, Mastrogiacomo M. Platelet rich plasma-based bioactive membrane as a new advanced wound care tool. J. Tissue Eng. Regen. Med. 2016; doi: 10.1002/term.2357.
101. Tsao C-T, Leung M, Chang JY-F, Zhang M. A simple material model to generate epidermal and dermal layers in vitro for skin regeneration. J. Mater. Chem. B Mater. Biol. Med. 2014; 2: 5256–5264.
102. Revi D, Paul W, Anilkumar TV, Sharma CP. Chitosan scaffold co-cultured with keratinocyte and fibroblast heals full thickness skin wounds in rabbit. J. Biomed. Mater. Res. A 2014; 102: 3273–3281.
103. Helary C, Zarka M, Giraud-Guille MM. Fibroblasts within concentrated collagen hydrogels favour chronic skin wound healing. J. Tissue Eng. Regen. Med. 2012; 6: 225–237.

104. Martin YH, Jubin K, Smalley S, Wong JPF, Brown RA, Metcalfe AD. A novel system for expansion and delivery of human keratinocytes for the treatment of severe cutaneous injuries using microcarriers and compressed collagen. J. Tissue Eng. Regen. Med. 2017; doi: 10.1002/term.2220.

105. Zhao X, Lang Q, Yildirimer L, Lin ZY, Cui W, Annabi N, Ng KW, Dokmeci MR, Ghaemmaghami AM, Khademhosseini A. Photocrosslinkable gelatin hydrogel for epidermal tissue engineering. Adv. Healthcare Mater. 2016; 5: 108–118.

106. Horch RE, Debus M, Wagner G, Stark GB. Cultured human keratinocytes on type I collagen membranes to reconstitute the epidermis. Tissue Eng. 2000; 6: 53–67.

107. Isakson M, Blacam C de, Whelan D, McArdle A, Clover AJP. Mesenchymal stem cells and cutaneous wound healing: Current evidence and future potential. Stem Cells Int. 2015; 2015: 831095.

108. Skardal A, Murphy SV, Crowell K, Mack D, Atala A, Soker S. A tunable hydrogel system for long-term release of cell-secreted cytokines and bioprinted in situ wound cell delivery. J. Biomed. Mater. Res. Part B Appl. Biomater. 2016; doi: 10.1002/jbm.b.33736.

109. Wang S, Yang H, Tang Z, Long G, Huang W. Wound dressing model of human umbilical cord mesenchymal stem cells-alginates complex promotes skin wound healing by paracrine signaling. Stem Cells Int. 2016; 2016: 3269267.

110. Chen S, Shi J, Zhang M, Chen Y, Wang X, Zhang L, Tian Z, Yan Y, Li Q, Zhong W, Xing M, Zhang L, Zhang L. Mesenchymal stem cell-laden anti-inflammatory hydrogel enhances diabetic wound healing. Sci. Rep. 2015; 5: 18104.

111. Tong C, Hao H, Xia L, Liu J, Ti D, Dong L, Hou Q, Song H, Liu H, Zhao Y, Fu X, Han W. Hypoxia pretreatment of bone marrow-derived mesenchymal stem cells seeded in a collagen-chitosan sponge scaffold promotes skin wound healing in diabetic rats with hindlimb ischemia. Wound Rep. Regen. 2016; 24: 45–56.

112. Dong Y, Hassan WU, Kennedy R, Greiser U, Pandit A, Garcia Y, Wang W. Performance of an in situ formed bioactive hydrogel dressing from a PEG-based hyperbranched multifunctional copolymer. Acta Biomater. 2014; 10: 2076–2085.

113. Chang Q, Gao H, Bu S, Zhong W, Lu F, Xing M. An injectable aldehyded 1-amino-3,3-diethoxy-propane hyaluronic acid-chitosan hydrogel as a carrier of adipose derived stem cells to enhance angiogenesis and promote skin regeneration. J. Mater. Chem. B 2015; 3: 4503–4513.

114. Kosaraju R, Rennert RC, Maan ZN, Duscher D, Barrera J, Whittam AJ, Januszyk M, Rajadas J, Rodrigues M, Gurtner GC. Adipose-derived stem cell-seeded hydrogels increase endogenous progenitor cell recruitment and neovascularization in wounds. Tissue Eng. Part A 2016; 22: 295–305.

115. Zonari A, Martins TMM, Paula ACC, Boeloni JN, Novikoff S, Marques AP, Correlo VM, Reis RL, Goes AM. Polyhydroxybutyrate-co-hydroxyvalerate structures loaded with adipose stem cells promote skin healing with reduced scarring. Acta Biomater. 2015; 17: 170–181.

116. Chan RK, Zamora DO, Wrice NL, Baer DG, Renz EM, Christy RJ, Natesan S. Development of a vascularized skin construct using adipose-derived stem cells from debrided burned skin. Stem Cells Int. 2012; 2012: 841203.

117. Natesan S, Zamora DO, Wrice NL, Baer DG, Christy RJ. Bilayer hydrogel with autologous stem cells derived from debrided human burn skin for improved skin regeneration. J. Burn Care Res. 2013; 34: 18–30.

118. Barrientos S, Brem H, Stojadinovic O, Tomic-Canic M. Clinical application of growth factors and cytokines in wound healing. Wound Rep. Regen. 2014; 22: 569–578.

119. Sweeney IR, Miraftab M, Collyer G. A critical review of modern and emerging absorbent dressings used to treat exuding wounds. Int. Wound J. 2012; 9: 601–612.

120. Koehler J, Wallmeyer L, Hedtrich S, Goepferich AM, Brandl FP. pH-modulating poly(ethylene glycol)/alginate hydrogel dressings for the treatment of chronic wounds. Macromol. Biosci. 2017; 17: 1600369.

121. Koehler J, Wallmeyer L, Hedtrich S, Brandl FP, Goepferich AM. Alkaline poly(ethylene glycol)-based hydrogels for a potential use as bioactive wound dressings. J. Biomed. Mater. Res. Part A 2017; doi: 10.1002/jbm.a.36177.

122. Sharpe JR, Booth S, Jubin K, Jordan NR, Lawrence-Watt DJ, Dheansa BS. Progression of wound pH during the course of healing in burns. J. Burn Care Res. 2013; 34: e201-e208.

123. Schreml S, Meier RJ, Kirschbaum M, Kong SC, Gehmert S, Felthaus O, Küchler S, Sharpe JR, Wöltje K, Weiß KT, Albert M, Seidl U, Schröder J, Morsczeck C, Prantl L, Duschl C, Pedersen SF, Gosau M, Berneburg M, Wolfbeis OS, Landthaler M, Babilas P. Luminescent dual sensors reveal extracellular pH-gradients and hypoxia on chronic wounds that disrupt epidermal repair. Theranostics 2014; 4: 721–735.

124. Schreml S, Szeimies R-M, Karrer S, Heinlin J, Landthaler M, Babilas P. The impact of the pH value on skin integrity and cutaneous wound healing. J. Eur. Acad. Dermatol. Venereol. 2010; 24: 373–378.

125. Percival SL, McCarty S, Hunt JA, Woods EJ. The effects of pH on wound healing, biofilms, and antimicrobial efficacy. Wound Repair Regen. 2014; 22: 174–186.

126. Gioia M, Fasciglione GF, Monaco S, Iundusi R, Sbardella D, Marini S, Tarantino U, Coletta M. pH dependence of the enzymatic processing of collagen I by MMP-1 (fibroblast collagenase), MMP-2 (gelatinase A), and MMP-14 ectodomain. J. Biol. Inorg. Chem. 2010; 15: 1219–1232.

Chapter 2

Antimicrobial Interpenetrating Polymer Network Hydrogels for an Application in Acute Wound Care

Abstract

Critical microbial colonialization of dermal wounds is a serious reason for impaired wound healing. Due to the rising threat of antibiotic resistant bacterial strains, the prevention of wound infections and the treatment of infected wounds are getting more and more challenging. Thus, the aim of this study was to develop alternative antimicrobial wound dressings with a universal field of action. To this end, the concept of interpenetrating polymer networks (IPNs) was applied to poly(ethylene glycol) diacrylate (PEGDA)/ alginate-based hydrogels, resulting in IPN materials with favorable wound dressing properties. The developed IPN hydrogels resisted a maximum tensile stress of 80 kPa with a maximum elasticity of 175%. Furthermore, the systematic alteration of the PEGDA network density enabled a significant enhancement of the hydrogel swelling capacity, from 2 to 40%. The most promising IPN hydrogel formulation, photopolymerized PEGDA 6 kDA/alginate with a precursor content of 9.5 and 0.5%, respectively, was successfully used as antimicrobial drug carrier. The achieved release of 3.4 mg poly(hexamethylene biguanide) per gram of hydrogel is comparable to the properties of commercially available antimicrobial wound care products.

1. Introduction

Infections are a big burden in wound care, because impaired healing and chronic wounds may result.[1,2] Endangered acute wound types are e.g. burns with a high amount of tissue loss, animal bites, gunshots, and contaminated surgical wounds. The adequate treatment of infected wounds is very challenging, since the traditional, antibiotic treatment methods bear the risk of developing bacterial resistance, and a rising number of resistant bacterial strains has been detected in recent years.[3] Therefore, antimicrobials are a valuable treatment alternative.[1] Nevertheless, some antimicrobials, including silver and chlorhexidine, are discussed to cause bacterial resistance as well or harm the human organism.[4–6] Yet, no resistant bacterial strains or harmful side-effects have been detected for poly(hexamethylene biguanide) hydrochloride (PHMB).[7] Its antimicrobial properties are based on the cationic molecular structure, which is similar to endogenous antimicrobial peptides (Scheme 1). Recently published data by Chindera et al. suggest, that its mechanism of action includes the condensation of bacterial chromosomes, whilst not entering the mammalian nuclei.[7] By this means, common wound site bacteria like *Staphylococcus Aureus* and in particular methicillin-resistant *S. Aureus* (MRSA), as well as *Pseudomonas Aeruginosa* can be defeated.[8–10]

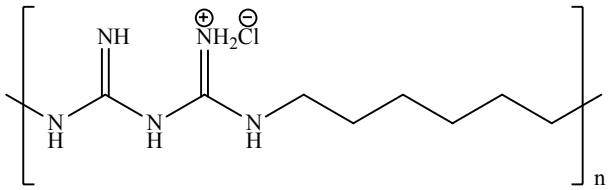

Scheme 1. Repeating unit of poly(hexamethylene biguanide) hydrochloride.

In this study, PHMB was incorporated in optimized interpenetrating polymer network (IPN) hydrogels. IPNs are a special class of hydrogels, consisting of two separate polymer networks that are combined in one material. The interpenetrating network structure enables numerous material variations by simple means. Thus, the hydrogel stability, the capacity of liquid uptake, the microstructure, and biochemical properties, such as cell adhesion and cytotoxicity, can be adapted to particular requirements.[11–14] Extensive research has focused on the remarkable IPN hydrogel mechanical properties.[15,16] Due to the combination of a rigid and a flexible polymer network, highly load bearing materials can be formed. Decisive factors for the mechanical performance of IPNs were identified to be the cross-linking density of both networks, the concentration and the ratio of the precursors, the

initiator concentrations, and environmental factors like the pH value and the salt concentration of the solvent.[11,17,18] Besides mechanical resistance during the application, wearing, and removal process, an appropriate wound dressing material must also provide low adherence to the wound site.[19] Furthermore, wound dressings should absorb excessive exudate, whilst maintaining a moist wound environment. For this purpose, a mechanically stable and moist material with a proper swelling capacity and gaseous exchange is required. Since hydrogels are very hydrophilic materials with a water content of around 90%, their fluid handling capacity qualifies them for this particular application. As described above, applying the IPN concept additionally guarantees a proper mechanical performance. Further advantageous dressing features, that can likewise be achieved with hydrogel materials, are active healing-supportive properties like the release of growth factors, stem cells, or antimicrobial drugs.[20–25]

In this study, IPN hydrogel wound dressings based on poly(ethylene glycol) diacrylate (PEGDA) as primary, dense network and alginate as secondary, loose network were developed. Both precursors are biocompatible and suitable for medical applications.[25,26] Additionally, alginate has a supportive healing effect, encouraging angiogenesis and cell migration.[27] The conducted material optimization focused on the mechanical and fluid handling properties of the IPN hydrogels. Moreover, the most promising PEGDA/alginate IPN formulation was examined for its suitability as PHMB release matrix.

2. Experimental Section

2.1 Materials

Toluene was purchased from Acros Organics (Geel, Belgium). Deuterated chloroform ($CDCl_3$) and deuterated water (D_2O) were obtained from Deutero GmbH (Kastellaun, Germany). 20% poly(hexamethylene biguanide) hydrochloride solution was purchased from Fagron (Barsbüttel, Germany). Alginate (Protanal® LF 10/60FT) was kindly provided by FMC BioPolymer (Wallingstown, Ireland). Dichloromethane (DCM), diethyl ether, and ethanol were obtained from CSC Jäcklechemie (Nürnberg, Germany). Phosphate buffered saline (PBS) was purchased from Life Technologies (Carlsbad, CA, USA). Hydrochloric acid, sodium acetate, sodium hydroxide, and triethylamine were obtained from Merck KGaA (Darmstadt, Germany). Poly(ethylene glycol) with a molecular weight of 4 kDa (PEG4k) was purchased from Riedel-de Haën (Seelze, Germany). Deionized water was obtained using a Milli-Q water purification system (Millipore, Schwabach, Germany). All

other chemicals were obtained from Sigma Aldrich (Taufkirchen, Germany). Poly(ethylene glycol) was dried by azeotropic distillation in toluene; all other chemicals were used as received.

2.2 Precursor Synthesis

Poly(ethylene glycol) diacrylate with a molecular weight of 6 kDa (PEGDA6k) was synthesized as previously described.[28] PEGDA with a molecular weight of 2 kDa (PEGDA2k) and 4 kDa (PEGDA4k) was synthesized in the same manner, though the amount of reactants was adapted as follows: 20.00 g PEG2k (10.00 mmol), combined with 2800 µL triethylamine (20.00 mmol) and 3250 µL acryloyl chloride (40.00 mmol); 25.01 g PEG4k (6.25 mmol), combined with 1742 µL triethylamine (12.50 mmol) and 2031 µL acryloyl chloride (25.00 mmol). A reaction yield of 66.9% (PEGDA2k), 61.6% (PEGDA4k), and 66.3% (PEGDA6k) was achieved.

^{1}H NMR PEGDA2k (300 MHz, $CDCl_3$, δ): 3.64 ppm (m, 99 H, -C*H*$_2$C*H*$_2$O-), 4.31 ppm (t, 2 H, -C*H*$_2$OC(O)-), 5.85 ppm (dd, 1 H, C*H*$_2$=CHC(O)O-), 6.16 ppm (dd, 1 H, CH_2=C*H*C(O)O-), 6.45 ppm (dd, 1 H, C*H*$_2$=CHC(O)O-).

^{1}H NMR PEGDA4k (300 MHz, $CDCl_3$, δ): 3.63 ppm (m, 197 H, -C*H*$_2$C*H*$_2$O-), 4.30 ppm (t, 2 H, -C*H*$_2$OC(O)-), 5.82 ppm (dd, 1 H, C*H*$_2$=CHC(O)O-), 6.14 ppm (dd, 1 H, CH_2=C*H*C(O)O-), 6.41 ppm (dd, 1 H, C*H*$_2$=CHC(O)O-).

^{1}H NMR PEGDA6k (300 MHz, $CDCl_3$, δ): 3.62 ppm (m, 310 H, -C*H*$_2$C*H*$_2$O-), 4.30 ppm (t, 2 H, -C*H*$_2$OC(O)-), 5.82 ppm (dd, 1 H, C*H*$_2$=CHC(O)O-), 6.13 ppm (dd, 1 H, CH_2=C*H*C(O)O-), 6.41 ppm (dd, 1 H, C*H*$_2$=CHC(O)O-).

Alginate methacrylate (AMA) was obtained from the reaction of alginate with methacrylic anhydride.[29] In brief, 5 N sodium hydroxide solution was added dropwise to 50 mL of an ice-cooled alginate solution (2 w%, 5.00 mmol) until pH 8 was reached. 2.965 mL of methacrylic anhydride (20.00 mmol) were slowly pipetted to the stirring solution and pH 8 was maintained for further 24 h. Then, AMA was precipitated in 250 mL ethanol, washed, and dried to yield 1.06 g (86.1%).

^{1}H NMR (300 MHz, D_2O, δ): 1.90 ppm (s, 0.40 H, -C(O)CC*H*$_3$), 3.20 - 5.20 ppm (m, alginate backbone including H-2 at 4.41 ppm (1.00 H)), 5.73 and 6.17 ppm (d, 0.14 H, =C*H*$_2$). The conversion rate of 14% was calculated from the ratio of the peak area at 5.73 (=CH_2) and 4.41 ppm (H-2).

For the synthesis of N-carboxyethylchitosan (CEC), 2.00 g medium molecular weight chitosan with an acetylation degree of approximately 80% was dissolved in 100 mL of an

aqueous acrylic acid solution (0.10 mol·L^{-1}). After stirring for 65 h at 50 °C, 11.00 mL of a 1 M sodium hydroxide solution were added dropwise. The product was precipitated in ice-cooled acetone, 50 h dialyzed against water (molecular weight cut-off 12000), dried under vacuum, and lyophilized to yield 2.01 g (85.0%).

^{1}H NMR (300 MHz, D_2O, δ): 2.03 ppm (s, 0.27 H, -NHC(O)C*H*$_3$), 2.37 ppm (m, 0.32 H, -NHCH$_2$C*H*$_2$-), 2.70 ppm (m, 0.41 H, -NH(CH$_2$C*H*$_2$-)$_2$), 3.02 - 4.10 ppm (m, H polysaccharide), 4.35 - 4.70 (m, 1 H, H-1 polysaccharide). A ratio of 63.8% -NH_2, 9.3% - NHC(O)CH_3, 16.2% -NHR and 10.7% -NR_2 with R = -NHCH$_2$CH$_2$- was calculated from the respective peak areas in relation to the peak area of H-1.

2.3 Preparation of Hydrogels

The components of the precursor mixture were successively blended in the following order: PEGDA solution, alginate/AMA solution (c = 41.68 mg·mL^{-1}) or CEC solution in deionized water (final PBS to water ratio = 0.849), $CaHPO_4 \cdot 2\ H_2O$ suspension, 2-hydroxy-4′-(2-hydroxyethoxy)-2-methylpropiophenone (HHMP) suspension, N,N,N',N'-tetra-methylethane-1,2-diamine (TEMED), gluconolactone solution (n(gluconolactone) = 2 n($CaHPO_4 \cdot 2\ H_2O$)), ammonium persulfate (APS) solution (m(APS) = 2 m(TEMED)). The respective formulations and amounts of cross-linking agent are displayed in Table 1, where m is the mass of the respective component in brackets.

Table 1. Amount of cross-linking agent in the examined hydrogel formulations.

Hydrogel	m(TEMED)/0.5 m(APS)	m($CaHPO_4 \cdot 2\ H_2O$)	m(HHMP)
3% alginate	-	0.13 m(alginate)	-
0.5% alginate 9.5% PEGDA	0.015 - 0.05 m(PEGDA)	0.13 m(alginate)	-
	-	0 or 0.13 m(alginate)	0.018 m(PEGDA)
0.5% AMA 9.5% PEGDA	-	-	0.018 m(monomer)
0.5% CEC 9.5% PEGDA	-	-	0.018 m(PEGDA)
10% PEGDA	0.018 m(PEGDA)	-	-
	-	-	0.018 m(PEGDA)

If not stated otherwise, PBS was used as solvent. The hydrogels had a total polymer ratio of 10 w% (including the amount of AMA, alginate, CEC, and PEGDA), except for pure

alginate gels with a polymer ratio of 3 w%. For water vapor transmission studies and tensile testing, 10 mL of the precursor solution were cast into rectangular silicon molds; for all other experiments, cylindrical glass molds (0.7 mL volume, 1 cm diameter) were used. HHMP induced polymerization was initiated by UV radiation (1 h, 366 nm, 6 W). In all other cases, the molds were covered with a glass plate and left at room temperature for 24 h.

2.4 Tensile Strength

Hydrogel sheets were cut into rectangular specimens of 8 cm length and 1 cm width (d). The thickness (h) of the specimens was determined using a MiniTest 600 gauge (ElektroPhysik, Köln, Germany). The maximum load (F_{max}) and elongation until failure were measured using an Instron 5542 load frame with two serrated grips (Instron GmbH, Darmstadt, Germany). The maximum tensile stress (σ_t) was calculated according to Equation (1).

$$\sigma_t = \frac{F_{max}}{h \cdot d} \qquad (1)$$

The elastic modulus (E_t) was calculated from the slope of the stress-strain curve between 0.05 and 0.15 strain. The data are presented as mean ± standard deviation (n = 4).

2.5 Swelling Capacity

Hydrogel cylinders were incubated in 10 mL of PBS at 37 °C in a shaking water bath. Every 24 h, the gels were blotted dry and weighed. The swelling capacity (Q_t) was calculated according to Equation (2)

$$Q_t = \frac{m_t - m_0}{m_0} \cdot 100\% \qquad (2)$$

where m_0 is the initial mass of the hydrogel and m_t is the mass of the gel at time point t.

2.6 Water Vapor Transmission Rate

The water vapor transmission rate (WVTR) was determined using the inverted water method (ASTM E96/E96M-12).[30] For this purpose, the hydrogel sheet was fixed at a circular WVTR test dish (test area A = 10.18 cm^2), filled with 5 mL of deionized water. Water loss at 21% relative humidity and 37 °C was measured gravimetrically every hour (0 – 10 h and ≥ 22 h) until a weight loss of 5 g had been be reached. The WVTR was

calculated from the average weight change per hour, corresponding to the slope of the time-water loss curve *G*, and the test area A, according to Equation (3).

$$WVTR = \frac{G}{A} \qquad (3)$$

2.7 Drug Release

PHMB loading was performed at 37 °C by incubating hydrogel cylinders in 10 mL of a PHMB solution (c = 2 mg·mL^{-1}) for 24 h. PHMB was dissolved either in water or saline. PHMB release was measured over a period of 7 days in 10 mL of PBS at 33 °C in a shaking water bath. 200 µL samples were taken at regular time intervals and replaced by fresh PBS. The samples were stored at 4 °C until the experiment was completed. Then, 200 µL of the diluted PHMB solution, 10 µL of a sodium acetate solution (10 w% in deionized H_2O), and 25 µL of an Eosin Y solution (0.025 w% in deionized H_2O) were pipetted in a 96-well plate for the colorimetric concentration assay. After 15 min under light exclusion, PHMB absorbance at 545 nm was measured with a FluoStar Omega micro plate reader (BMG Labtech, Ortenberg, Germany). The PHMB concentrations were calculated based on calibration measurements.[31] The amount of initial PHMB load was calculated from the remaining volume of PHMB incubation solution and its concentration.

2.8 Statistical Analysis

If not stated otherwise, the experiments were done in triplicate and the data are presented as mean ± standard deviation (SD). For statistical analysis, Brown Forsythe tests were run followed by one-way ANOVA/Tukey' test or Kruskal-Wallis-ANOVA. Differences were considered statistically significant at $p < 0.05$.

3. Results

3.1 Optimization of the PEGDA Network Cross-Linking Density

Alginate and poly(ethylene glycol) diacrylate with a molecular weight of 2 kDa were used as starting materials for the systematic development of antimicrobial IPN hydrogel wound dressing materials. First, the impact of the PEGDA network cross-linking density on the IPN hydrogel properties was evaluated. For this purpose, formulations consisting of 0.5% alginate and 9.5% PEGDA2k were polymerized by varying amounts of redox initiator TEMED/APS (1.5 – 5.0% TEMED; 3.0 – 10.0% APS) and the mechanical properties of the resulting hydrogels were examined under tensile load (Figure 1).

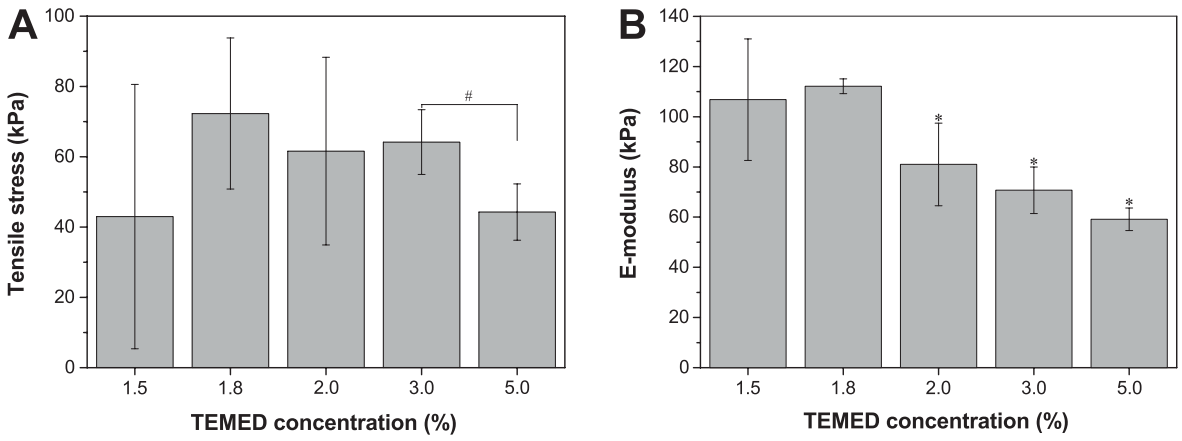

Figure 1. Tensile stress at maximum load (A) and calculated E-modulus (B) of 9.5% PEGDA2k/ 0.5% alginate hydrogels polymerized with different initiator concentrations. Data are expressed as mean ± SD (n = 4); * indicates statistically significant differences versus the 1.5% and 1.8% TEMED samples ($p < 0.05$); # indicates statistically significant differences between the groups ($p < 0.05$).

The brittle texture of the PEGDA2k/alginate IPN hydrogels hampered the sample preparation and handling. This resulted in high variations of the maximum tensile stress, σ_t, within each formulation (Figure 1A). Therefore, significant differences were only found between the σ_t values of 3.0%TEMED/6.0% APS and 5.0% TEMED/10.0% APS containing hydrogels. Further variations of the TEMED/APS content had no significant impact on the mechanical stability. However, regarding the absolute σ_t values, 1.8% TEMED/3.6% APS containing hydrogels seemed to be the strongest gels. The elastic modulus (E-modulus E_t), a parameter that characterizes the material stiffness, was calculated to be around 110 kPa for hydrogels that were polymerized with 1.5% TEMED/ 3.0% APS and 1.8% TEMED/3.6% APS, and significantly lower (60 - 80 kPa) for hydrogels that were polymerized with higher TEMED/APS concentrations (Figure 1B). Based on the data displayed in Figure 1, a radical initiator concentration of 1.8% TEMED/ 3.6% APS was used for further experiments.

Another method to optimize the PEGDA network cross-linking density in the examined IPN hydrogel systems is the variation of the PEGDA precursor molecular weight (PEGDA2k/4k/6k), whereas the mass fraction of PEGDA remains constant. The impact of the PEGDA molecular weight on the mechanical properties of the IPN system 9.5% PEGDA/0.5% alginate with 1.8% TEMED/3.6% APS was examined in tensile tests (Figure 2).

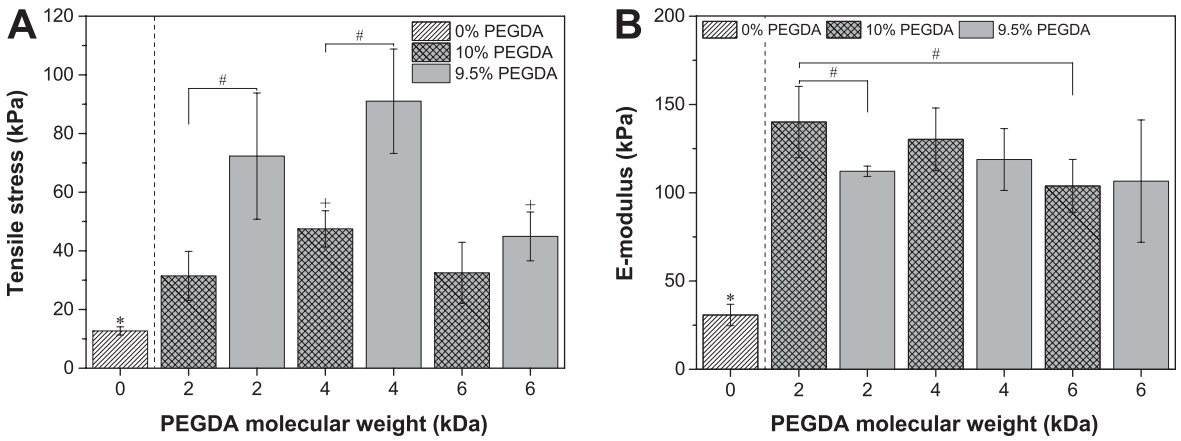

Figure 2. Tensile stress at maximum load (A) and calculated E-modulus (B) of pure alginate (0% PEGDA), pure 10% PEGDA, and 9.5% PEGDA/0.5% alginate IPN hydrogels (1.8% TEMED/3.6% APS content) with different PEGDA precursor molecular weights. Data are expressed as mean ± SD (n = 4); * indicates statistically significant differences versus all samples ($p < 0.05$); + indicates statistically significant differences versus the respective lower molecular weight samples ($p < 0.05$); # indicates statistically significant differences between the groups ($p < 0.05$).

All tested IPN hydrogels resisted a higher maximum tensile stress than pure alginate (0% PEGDA) and pure PEGDA (10% PEGDA) samples did (Figure 2A). The σ_t values of PEGDA2k/alginate and PEGDA4k/alginate IPNs were even higher than the summed σ_t values of the single component hydrogels. A modified PEGDA molecular weight resulted in the highest maximum tensile stress for PEGDA4k IPN samples, followed by PEGDA2k and 6k IPN samples. In contrast, the E-modulus of the examined PEGDA hydrogels was rather independent from the gel formulation (Figure 2B).

Besides sufficient mechanical stability and elasticity, an appropriate liquid uptake is an important parameter of wound dressing materials. Therefore, the TEMED/APS polymerized PEGDA/alginate IPN hydrogels were additionally examined for their swelling capacity in PBS (Figure 3).

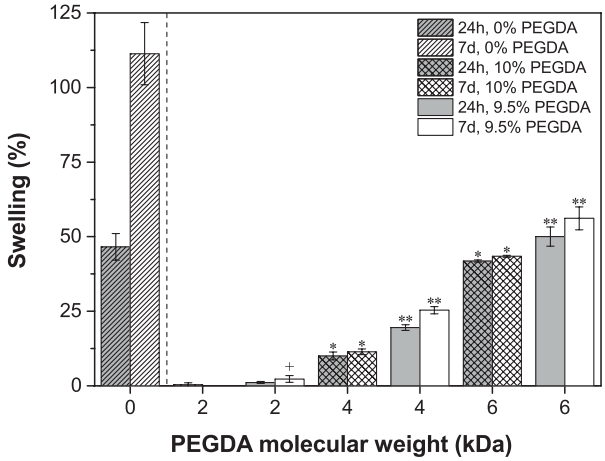

Figure 3. Swelling capacity of pure alginate (0% PEGDA), pure 10% PEGDA, and 9.5% PEGDA/ 0.5% alginate IPN hydrogels (1.8% TEMED/3.6% APS content) with different PEGDA molecular weights, after 24 h and 7 days of incubation. Data are expressed as mean ± SD (n = 3). + indicates statistically significant differences versus the respective alginate free samples ($p < 0.05$); * indicates statistically significant differences versus lower molecular weight samples ($p < 0.05$); ** indicates statistically significant differences versus the respective alginate free and lower molecular weight samples ($p < 0.05$).

The detected liquid uptake significantly increased with rising PEGDA molecular weight and by the incorporation of alginate, resulting in swelling capacities of 1 and 2% (PEGDA2k/alginate), 20 and 25% (PEGDA4k/alginate), and 50 and 56% (PEGDA6k/ alginate) for 24 hours and 7 days of incubation, respectively.

Considering the assessed swelling properties, PEGDA2k containing hydrogels were no longer regarded as valuable candidates for wound dressing applications, whereas further optimization on PEGDA4k and PEGDA6k containing IPNs appeared promising.

3.2 Optimization of the Initiator Type

A draw-back of the so far used initiator system TEMED/APS is its reaction time, taking around 24 hours for full completion.[32,33] For faster manufacturing, PEGDA polymerization with the UV-light sensitive initiator HHMP was examined. Furthermore, concerning the secondary network, the impact of additional ionic gelation with Ca^{2+} in comparison to pure physically entangled alginate polymer chains was evaluated.

The HHMP induced polymerization influenced the mechanical properties of the PEGDA4k and the PEGDA6k containing hydrogels in an opposite manner (Figure 4). The PEGDA4k/ alginate/HHMP hydrogels did not benefit from the characteristic IPN stabilizing effect described for the respective TEMED/APS polymerized hydrogels (see Figure 2 for comparison), whereas PEGDA6k/alginate IPNs showed a specific mechanical stabilization

(σ_t(PEGDA6k/alginate) > σ_t(alginate) + σ_t(PEGDA6k)) related to the use of HHMP. Yet, the calculated E-modulus decreased, independent from the hydrogel composition.

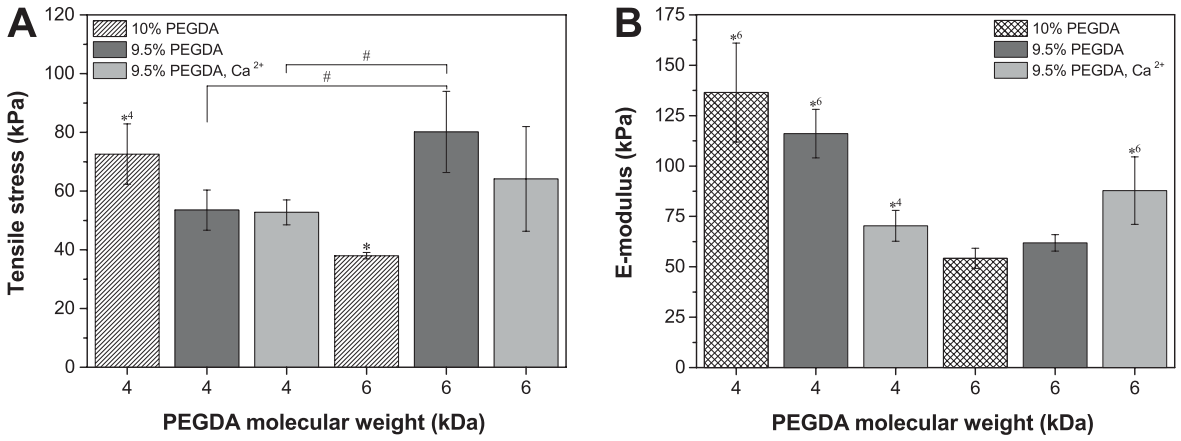

Figure 4. Tensile stress at maximum load (A) and calculated E-modulus (B) of pure 10% PEGDA and 9.5% PEGDA/0.5% alginate IPN hydrogels (1.8% HHMP content) with and without Ca^{2+} polymerization. Data are expressed as mean ± SD (n = 4); * indicates statistically significant differences versus all samples ($p < 0.05$); *4/*6 indicates statistically significant differences versus all PEGDA4k/6k samples ($p < 0.05$); # indicates statistically significant differences between the groups ($p < 0.05$).

The incorporation of divalent calcium ions for additional cross-linking influenced both, the hydrogel stability and stiffness (Figure 4). The E-modulus of Ca^{2+} containing PEGDA4k/ alginate IPNs (70.3 ± 7.7 kPa) was significantly lower compared to the E_t of Ca^{2+}-free PEGDA4k/alginate IPNs (116.1 ± 12.0 kPa). However, σ_t was around 53 kPa in both cases. In contrast, PEGDA6k/alginate IPNs showed more stable but stiffer behavior without Ca^{2+} polymerization. In further experiments, PEGDA6k/alginate IPNs were consequently prepared without Ca^{2+}.

Comparing the mechanical properties of the so far examined materials, no significant differences were found for the maximally achieved tensile stress of redox (σ_t(PEGDA4k/alginate + Ca^{2+}) = 91.0 ± 17.8 kPa) and UV-light (σ_t(PEGDA6k/alginate) = 80.1 ± 13.8 kPa) polymerized hydrogels. Since easy and fast manufacturing is preferred (HHMP instead of TEMED/APS initiator) and a sufficient liquid uptake (PEGDA6k instead of PEGDA4k containing IPNs) should be guaranteed, only PEGDA6k/alginate/ HHMP IPN hydrogels were further analyzed for their suitability as wound dressing material. First, their liquid handling characteristics were determined (Table 2).

Table 2. Liquid handling capacity of PEGDA6k/alginate/HHMP IPNs in comparison to the single component hydrogels.

Hydrogel	WVTR ($g \cdot h^{-1} \cdot m^{-2}$)	Q_{24h} (%)	Q_{7d} (%)
3.0% alginate	198.48 ± 1.13	46.6 ± 4.5	111.4 ± 10.4
10.0% PEGDA6k	175.35 ± 0.58	13.5 ± 0.4	15.5 ± 0.4
9.5% PEGDA6k 0.5% alginate	171.40 ± 0.30	40.0 ± 5.7	41.2 ± 5.7

The formation of an IPN system resulted in a significant enhancement of the swelling capacity (Q_{24h}) in comparison to the pure PEGDA6k hydrogels, and was comparable to Q_{24h} of pure alginate hydrogels. Extending the incubation time to 7 days did not alter the swelling capacity of PEGDA and PEGDA/alginate hydrogels, whereas pure alginate hydrogels could absorb approximately double the amount of liquid after 7 days. The water vapor transmission rate of PEGDA6k/alginate IPN hydrogels was 171.4 $g \cdot h^{-1} \cdot m^{-2}$, the WVTRs of the single components were 2 - 16% higher.

3.3 Optimization of the Drug Release Properties

The final goal of this study was the development of antimicrobial wound dressings. As potential antimicrobial drug, poly(hexamethylene biguanide) hydrochloride was therefore incorporated into PEGDA6k-based hydrogels. Antimicrobial hydrogels produced by two different loading processes, incubation in an aqueous and in a saline solution of PHMB, were analyzed for their release behavior. In comparison to pure PEGDA6k hydrogels, that showed a PHMB release of 83% for the water loading process, the PHMB release from PEGDA6k/alginate IPN hydrogels was much smaller (34%, Figure 5A). To understand the processes that limit the drug release from PEGDA6k/alginate IPN hydrogels, an exchange of the secondary network was conducted, facing the nature of its reactive functional groups. To this end, alginate, which carries carboxylic acid groups, was substituted by AMA, which has a lower amount of carboxylic acid groups, or N-carboxyethylchitosan (CEC), which offers carboxylic acid and amino groups. PEGDA/AMA IPNs showed a slightly increased maximum release (37% PHMB release) in comparison to the PEGDA/ alginate IPNs, whereas 53% release could be detected from PEGDA/CEC IPNs. Yet, all formulations released comparable absolute amounts of PHMB per gram of hydrogel (Figure 5B). The differences in percentage PHMB release were based on the initially incorporated PHMB mass, which varied between 2.7 and 6.2 mg.

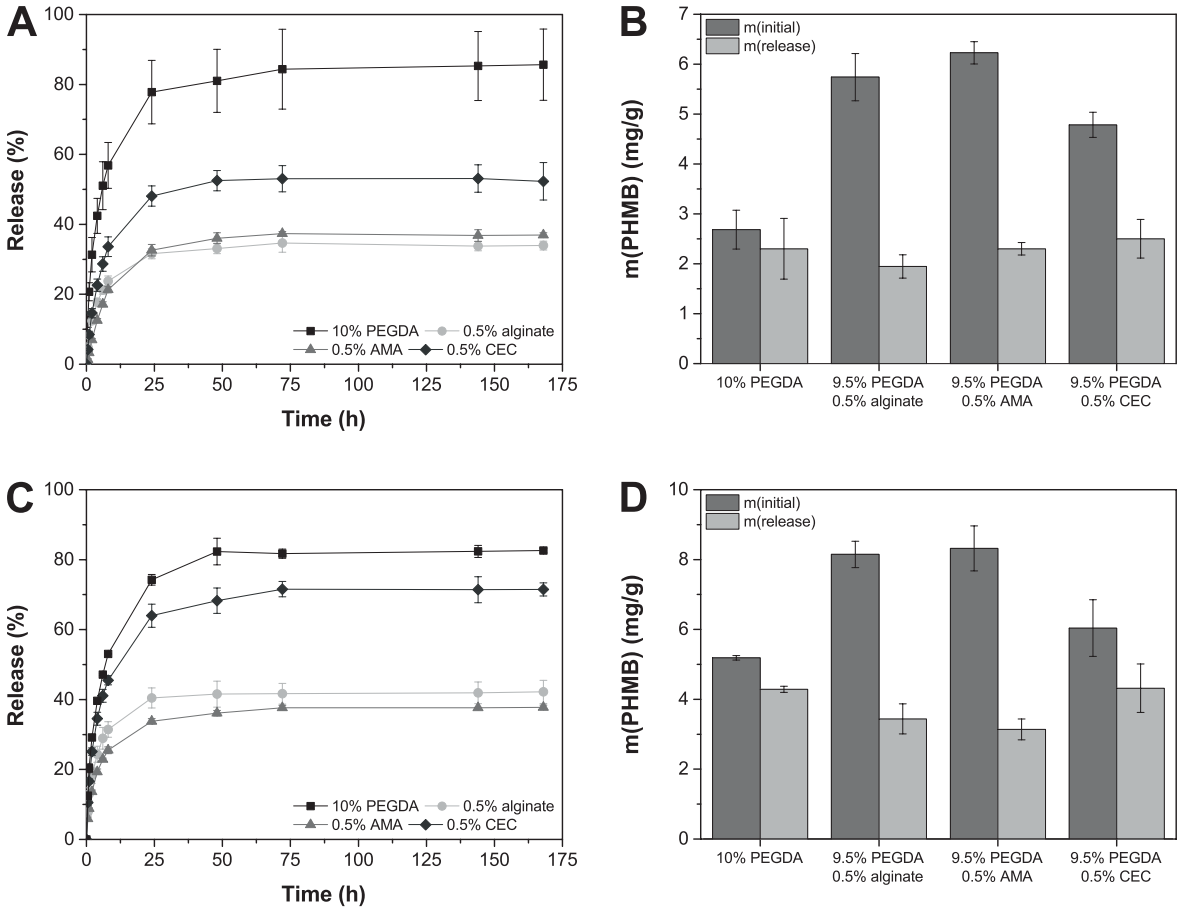

Figure 5. Relative release (A, C) and absolute load/release (B, D) of PHMB from different PEGDA6k-based hydrogels. PHMB was diluted in water (A, B) or saline (C, D). Data are expressed as mean ± SD (n = 3).

The PHMB release could be enhanced by drug loading in saline solution (Figure 5C). Especially alginate and CEC containing hydrogels showed substantially increased maximum release rates (42 and 71%, respectively). The initial PHMB load and the absolute amount of released PHMB increased for all hydrogel formulations (Figure 5D). The release kinetics was independent from the loading process and the hydrogel formulation; a burst release during the first 24 hours and marginal further release until day 3 were detected.

4. Discussion

The aim of this study was the precise network optimization of the IPN system PEGDA/ alginate, leading to a suitable wound dressing material for acute wounds. The reason for choosing an IPN system was, that favorable properties of the two polymer components (high swelling capacity of alginate hydrogels, hydrolysis resistance of PEGDA hydrogels) could be combined, and material issues (low mechanical stability and low hydrolysis

resistance of alginate hydrogels, rigidity and marginal liquid uptake of PEGDA hydrogels) could be compensated. By this means, an enhanced mechanical performance and sufficient liquid uptake should be available in one material. The cross-linking density of the primary (dense) network is known to have a high impact on the mechanical performance of IPN hydrogels.[11,17,34] It can be controlled by the initiator concentration of the primary network (*c*(TEMED/APS)) and the molecular weight of the precursors (*M*(PEGDA)). The optimal initiator concentration was found to be 1.8% TEMED/3.6% APS (Figure 1). Extensive initiator ratios might cause enhanced amounts of network irregularities, resulting in less stable (reduced σ_t values) and less stiff (reduced E_t values) hydrogels.[34] On the other hand, insufficient amounts of initiator enable polymer chain entanglements because of prolonged reaction times.[35] The thereby reduced mobility of the reactive sites consequently results in a lower degree of cross-linking, likewise leading to reduced σ_t values, but comparable E-moduli.

The characteristic stabilizing effect of IPN structures in contrast to single polymer networks (PEGDA2k and 4k/alginate/TEMED/APS IPNs in Figure 2) is caused by inter-network entanglements that enable a load transfer between the two interpenetrating polymer networks (see Figure 6 for illustration).[11]

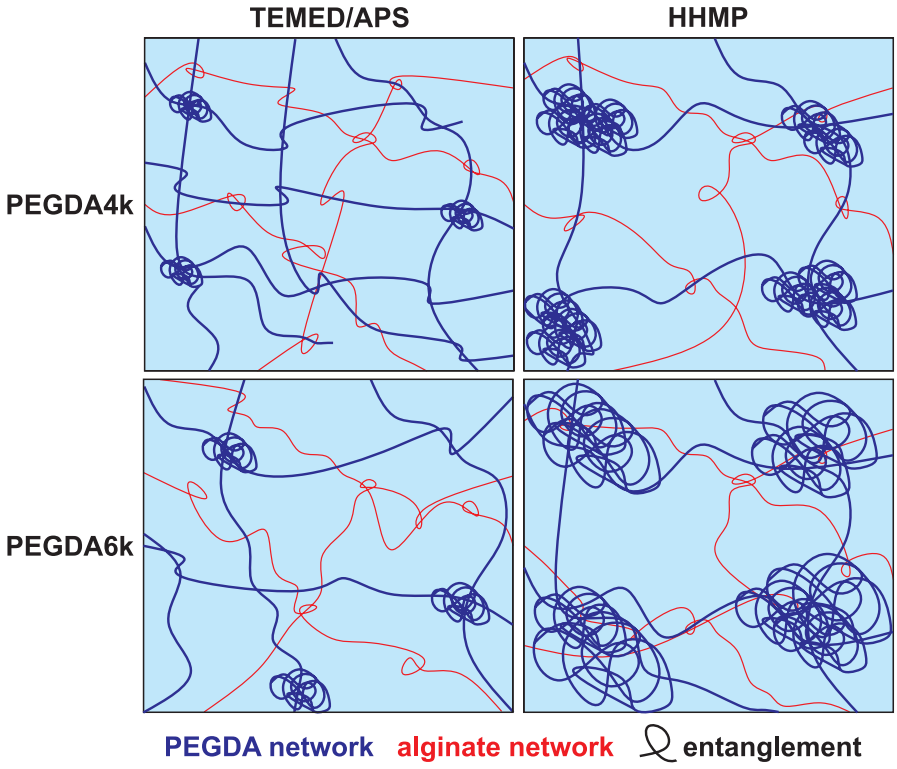

Figure 6. Schematic illustration of the suggested hydrogel network structure as a function of the initiator (TEMED/APS or HHMP) and the PEGDA molecular weight (PEGDA4k or 6k).

Apparently, insufficient entanglement occurs in PEGDA6k/alginate/TEMED/APS IPNs, as they had the same maximum tensile stress as pure PEGDA6k/TEMED/APS hydrogels (Figure 2). The reduced number of cross-links in the covalent PEGDA6k network (in comparison to the PEGDA4k network) is not responsible for this behavior, since the mechanical stability of pure PEGDA gels is hardly changing with altered PEGDA molecular weight. More likely, this effect is related to an increasing PEGDA mesh-size, favoring rather intra-network entanglement of alginate chains than inter-network entanglement of the two networks. The reduction in E-modulus with increasing molecular weight is in agreement with a decrease in cross-links, causing less stiff materials.[36]

The effect of the PEGDA molecular weight is considerably more pronounced concerning the swelling capacity of the respective hydrogels (Figure 3). As expected, a reduced number of covalent bonds by the altered PEGDA molecular weight, the partial substitution of PEGDA by alginate, and longer polymer chains between cross-links (PEGDA2k < 4k < 6k) enable a higher extent of hydrogel volume increase and therefore, higher liquid uptake.[37] A sufficient swelling capacity is mandatory for wound dressing materials. Yet, hard data on occurring exudate amounts are rarely recorded. Mostly, clinicians differentiate between “moderately”, “medium”, and “excessively” exuding wounds.[38,39] Based on recently published calculations, dressings with a swelling capacity of 57% or higher might be applied on excessively exuding wounds.[28] In regard to the swelling data displayed in Figure 3, PEGDA6k/alginate IPN hydrogels might be considered universally, whilst PEGDA4k/alginate IPNs might not be applied on strongly exuding wounds. PEGDA2k/alginate hydrogels (around 2% swelling) do not fulfill the requirements for exuding wounds in any case.

Besides offering advantageous material properties, wound dressings should also be cost-effective. A preparation process of 24 hours (TEMED/APS initiator) is economically less favorable than a polymerization reaction taking only 1 hour for full completion (UV induced reaction).[33] Besides, concerns about the TEMED/APS cytocompatibility were published recently, whereas no negative side-effects were found for HHMP.[40,41] Even though wound dressing materials are purified prior to the application, there is a risk of still remaining initiator. Therefore, further material optimization was conducted concerning the initiator system. Regarding UV cross-linked hydrogels, the incorporation of alginate had a favorable effect on PEGDA6k containing hydrogels only (Figure 4). This might be explained as follows. The shortened reaction time of HHMP has a great impact on the hydrogel structure (see Figure 6 for illustration). The number of kinetic chains is increased

whilst the chain length is reduced.[42] The resulting polymer structure provides numerous dense polymer zones (DPZs) in contrast to the more uniform network structure in redox hydrogels. In PEGDA4k containing hydrogels, the mesh size in the DPZs is expected to be even smaller, caused by the shorter distance between cross-links. Apparently, an inter-network entanglement in PEGDA4k/alginate/HHMP IPNs is therefore impeded, leading to hydrogels with reduced σ_t and E_t values, whereas beneficial entanglement occurs in the dense polymer zones of PEGDA6k/alginate/HHMP IPNs.

The exclusion of calcium ions has two contrary effects on the IPN structure. Missing ionic bonds between alginate macromolecules reduce the material stability and E-modulus.[43] On the other hand, more flexible alginate chains might facilitate an entanglement in the DPZs, resulting in rising σ_t and E_t values. These two effects were balanced out concerning σ_t(PEGDA4k/alginate). However, the E-modulus was higher in Ca^{2+}-free PEGDA4k/ alginate IPNs, since polymer chain entanglements have a stronger stiffening effect than ionic bonds.[44] The findings for PEGDA6k/alginate IPNs underlined the theory discussed above; network entanglements in DPZs are dominating with higher PEGDA molecular weight, leading to further increased σ_t values. Probably because of the already existing high number of entanglements in the DPZs of PEGDA6k/alginate + Ca^{2+} IPNs, the E-modulus is lower for only physically entangled Ca^{2+}-free samples.

With a maximum tensile stress of 80.1 ± 13.8 kPa and a maximum elasticity of 174.7 ± 22.9% (data not shown), the most favorable hydrogel formulation PEGDA6k/alginate/ HHMP/no Ca^{2+} possessed sufficient mechanical properties for an easy handling of the dressing sheets. In general, wound dressings need to be stable and flexible enough to sustain the forces applied during the application and wearing process, whilst adapting to the actual wound shape.[19] In view of the elasticity of the human skin (around 70%), the developed dressing materials provide sufficient ductility.[45] As hydrogels often serve as primary dressing covered by a secondary dressing with a stabilizing function, the requirements for these particular wound dressings are even lower.[46] Values of 1.5 to 5.0 kPa maximum tensile stress were described to already meet the requirements for wound dressing applications.[47,48]

The great advantage of an IPN hydrogel formulation is also visible in the liquid handling properties of the developed PEGDA6k/alginate IPN gels (Table 2). The presence of alginate, which is known for its excellent absorption properties, together with a slightly decreased PEGDA network density, which is caused by partial substitution of PEGDA by

alginate, resulted in a significantly increased swelling capacity.[43] Yet, it was a fast process and the maximum liquid uptake of the non-degrading PEGDA containing hydrogels had already been reached after 24 h. Further swelling of pure alginate gels is related to an ion exchange of the cross-linking Ca^{2+} ions by monovalent, non-cross-linking Na^{+} ions of the incubation medium.[49] A satisfying liquid handling capacity of wound dressings is also defined by the water vapor transmission rate, classifying the amount of excessive exudate that can be removed by evaporation or the ability of preventing tissue from desiccation.[50] The here detected values are in accordance with typical WVTRs of (hydrogel) wound dressings.[51] In comparison to water evaporation from uncovered surfaces (323.88 ± 1.39 $g \cdot h^{-1} \cdot m^{-2}$), the treatment with the examined hydrogel dressings reduced the water loss by 39 – 47%.

The need for antimicrobial dressings is founded on the high rate of wound infections and the related risk for serious healing issues.[3,52,53] Therefore, the favorable PEGDA6k/alginate IPN hydrogels were tested for their suitability as PHMB releasing antimicrobial dressing materials. The PHMB release was observed at 33 °C, which corresponds to the average wound bed temperature.[54] Fast and almost complete drug release from pure PEGDA6k hydrogels indicates a diffusion controlled mechanism.[55] Reduced release rates from PEGDA6k/alginate IPN hydrogels must therefore be caused by an interaction of the positively charged PHMB molecules and the negatively charged carboxylic acid groups of alginate. This theory could be verified by the examination of AMA and CEC containing PEGDA6k IPN hydrogels. A reduced amount of carboxylic acid groups in the drug carrier (alginate > AMA > CEC) and additional incorporation of potential positive charges ($-NH_2 \leftrightarrow -NH_3^+$; CEC) decreased the amount of interaction sites with PHMB (Table 3), and therefore significantly increased the release rates.

Table 3. Amount of functional groups per gram of hydrogel and impact of saline shielding.

	9.5% PEGDA6k 0.5% alginate	**9.5% PEGDA6k 0.5% AMA**	**9.5% PEGDA6k 0.5% CEC**
n(-COOH) (mmol)	0.0253	0.0210	0.0094
n($-NH_2$) (mmol)	-	-	0.0160
Effect of saline shielding on the % PHMB release	+ 24%	+ 2%	+ 37%

The percentage release from PEGDA6k/alginate gels was successfully enhanced by 24%, when the PHMB loading process was modified so that the positively charged PHMB imino groups were shielded by an increased number of chloride ions, and ionized alginate carboxylic groups were shielded by an increased number of sodium ions from the saline loading solution. The intensity of the saline induced shielding was dependent on the character of the secondary network (Table 3). This effect might be explained by differences in the steric hindrance around the respective carboxylic acid groups. In CEC containing hydrogels, the carboxyl groups are easily accessible as they have a $-NRCH_2CH_2$ spacer to the chitosan saccharide ring system. In alginate and AMA containing gels, the carboxyl groups are directly bound to the folded saccharide ring chains. Additional steric hindrance in AMA containing hydrogels is induced by chemical bonds between the AMA and PEGDA molecules. Nevertheless, PHMB release should also be evaluated regarding the absolute amount of PHMB release per gram of hydrogel. In accordance with the swelling capacity of the different formulations, PHMB uptake was highest in alginate and AMA containing IPNs (Figure 5).[56] The data on PHMB/saline loaded gels suggests that functional groups in the hydrogel do not only alter the release rate, but also influence the loading process. Commercially available wound dressings contain 0.1 – 0.5% PHMB (e.g. Suprasorb X + PHMB (Lohmann & Rauscher), Kendall (AMD), Prontosan (B. Braun Medical Ltd)). In the light of the facts, the here described PEGDA/alginate IPN hydrogels (0.8% maximal loading and 0.3% maximal release of PHMB) can therefore be seen as promising candidates for an antimicrobial wound dressing application.

5. Conclusion

Different approaches were taken to develop antimicrobial hydrogel wound dressings, consisting of interpenetrating alginate and poly(ethylene glycol) diacrylate polymer networks. The conducted research focused on a systematic optimization of the initiator system, using redox-, UV-, and ionically induced cross-linking. Furthermore, a variation of the polymer network cross-linking density enabled the adaption of important wound dressing properties, such as the liquid uptake and the mechanical stability. The photopolymerized hydrogel 9.5% PEGDA6k/0.5% alginate/HHMP was identified to be the most promising gel formulation. Its suitability for an antimicrobial drug release was furthermore proven, using poly(hexamethylene biguanide) hydrochloride as model

substance. Further research should focus on the evaluation of the hydrogel biocompatibility and its wound healing capacity, both in vitro and in vivo.

References

1. Butcher M. PHMB: An effective antimicrobial in wound bioburden management. Br. J. Nurs. 2012; 21: S16, S18-21.
2. Bjarnsholt T, Kirketerp-Moller K, Jensen PO, Madsen KG, Phipps R, Krogfelt K, Hoiby N, Givskov M. Why chronic wounds will not heal: A novel hypothesis. Wound Rep. Regen. 2008; 16: 2–10.
3. Bessa LJ, Fazii P, Di Giulio M, Cellini L. Bacterial isolates from infected wounds and their antibiotic susceptibility pattern: Some remarks about wound infection. Int. Wound J. 2015; 12: 47–52.
4. Finley PJ, Norton R, Austin C, Mitchell A, Zank S, Durham P. Unprecedented silver resistance in clinically isolated enterobacteriaceae: Major implications for burn and wound management. Antimicrob. Agents Chemother. 2015; 59: 4734–4741.
5. Randall CP, Gupta A, Jackson N, Busse D, O'Neill AJ. Silver resistance in Gram-negative bacteria: A dissection of endogenous and exogenous mechanisms. J. Antimicrob. Chemother. 2015; 70: 1037–1046.
6. Giannelli M, Chellini F, Margheri M, Tonelli P, Tani A. Effect of chlorhexidine digluconate on different cell types: A molecular and ultrastructural investigation. Toxicol. in Vitro 2008; 22: 308–317.
7. Chindera K, Mahato M, Sharma AK, Horsley H, Kloc-Muniak K, Kamaruzzaman NF, Kumar S, McFarlane A, Stach J, Bentin T, Good L. The antimicrobial polymer PHMB enters cells and selectively condenses bacterial chromosomes. Sci. Rep. 2016; 6: 23121.
8. Kirker KR, Fisher ST, James GA, McGhee D, Shah CB. Efficacy of polyhexamethylene biguanide-containing antimicrobial foam dressing against MRSA relative to standard foam dressing. Wounds 2009; 21: 229–233.
9. Kamaruzzaman NF, Firdessa R, Good L. Bactericidal effects of polyhexamethylene biguanide against intracellular Staphylococcus aureus EMRSA-15 and USA 300. J. Antimicrob. Chemother. 2016; 71: 1252–1259.
10. Werthen M, Davoudi M, Sonesson A, Nitsche DP, Morgelin M, Blom K, Schmidtchen A. Pseudomonas aeruginosa-induced infection and degradation of human wound fluid and skin proteins ex vivo are eradicated by a synthetic cationic polymer. J. Antimicrob. Chemother. 2004; 54: 772–779.

11. Myung D, Koh W, Ko J, Hu Y, Carrasco M, Noolandi J, Ta CN, Frank CW. Biomimetic strain hardening in interpenetrating polymer network hydrogels. Polymer 2007; 48: 5376–5387.
12. Waters DJ, Engberg K, Parke-Houben R, Ta CN, Jackson AJ, Toney MF, Frank CW. Structure and mechanism of strength enhancement in interpenetrating polymer network hydrogels. Macromolecules 2011; 44: 5776–5787.
13. Rennerfeldt DA, Renth AN, Talata Z, Gehrke SH, Detamore MS. Tuning mechanical performance of poly(ethylene glycol) and agarose interpenetrating network hydrogels for cartilage tissue engineering. Biomaterials 2013; 34: 8241–8257.
14. Tong X, Yang F. Engineering interpenetrating network hydrogels as biomimetic cell niche with independently tunable biochemical and mechanical properties. Biomaterials 2014; 35: 1807–1815.
15. Haque MA, Kurokawa T, Gong JP. Super tough double network hydrogels and their application as biomaterials. Polymer 2012; 53: 1805–1822.
16. Gong JP. Why are double network hydrogels so tough? Soft Matter 2010; 6: 2583–2590.
17. Nakajima T, Furukawa H, Tanaka Y, Kurokawa T, Osada Y, Gong JP. True chemical structure of double network hydrogels. Macromolecules 2009; 42: 2184–2189.
18. Anseth KS, Bowman CN, Brannon-Peppas L. Mechanical properties of hydrogels and their experimental determination. Biomaterials 1996; 17: 1647–1657.
19. Boateng JS, Matthews KH, Stevens HNE, Eccleston GM. Wound healing dressings and drug delivery systems: A review. J. Pharm. Sci. 2008; 97: 2892–2923.
20. Ågren M. Wound Healing Biomaterials: Volume 1; Therapies and Regeneration, 1st edn. Swaston, UK: Woodhead Publishing; 2016.
21. Zhu Y, Hoshi R, Chen S, Yi J, Duan C, Galiano RD, Zhang HF, Ameer GA. Sustained release of stromal cell derived factor-1 from an antioxidant thermoresponsive hydrogel enhances dermal wound healing in diabetes. J. Control. Release 2016; 238: 114–122.
22. Madhumathi K, Sudheesh Kumar PT, Abhilash S, Sreeja V, Tamura H, Manzoor K, Nair SV, Jayakumar R. Development of novel chitin/nanosilver composite scaffolds for wound dressing applications. J. Mater. Sci. Mater. Med. 2010; 21: 807–813.
23. Moura LIF, Dias AMA, Leal EC, Carvalho L, Sousa HC de, Carvalho E. Chitosan-based dressings loaded with neurotensin--An efficient strategy to improve early diabetic wound healing. Acta Biomater. 2014; 10: 843–857.

24. Hunt NC, Shelton RM, Grover L. An alginate hydrogel matrix for the localised delivery of a fibroblast/keratinocyte co-culture. Biotechnol. J. 2009; 4: 730–737.
25. Dong Y, Hassan WU, Kennedy R, Greiser U, Pandit A, Garcia Y, Wang W. Performance of an in situ formed bioactive hydrogel dressing from a PEG-based hyperbranched multifunctional copolymer. Acta Biomater. 2014; 10: 2076–2085.
26. Jeon O, Bouhadir KH, Mansour JM, Alsberg E. Photocrosslinked alginate hydrogels with tunable biodegradation rates and mechanical properties. Biomaterials 2009; 30: 2724–2734.
27. Lee W-R, Park J-H, Kim K-H, Kim S-J, Park D-H, Chae M-H, Suh S-H, Jeong S-W, Park K-K. The biological effects of topical alginate treatment in an animal model of skin wound healing. Wound Rep. Regen. 2009; 17: 505–510.
28. Koehler J, Wallmeyer L, Hedtrich S, Goepferich AM, Brandl FP. pH-modulating poly(ethylene glycol)/alginate hydrogel dressings for the treatment of chronic wounds. Macromol. Biosci. 2017; 17: 1600369.
29. Smeds KA, Grinstaff MW. Photocrosslinkable polysaccharides for in situ hydrogel formation. J. Biomed. Mater. Res. A 2001; 54: 115–121.
30. E96/E96M-12, Standard test methods for water vapor transmission of materials. West Conshohocken, PA, USA: ASTM International; 2012.
31. Müller G, Kramer A, Schmitt J, Harden D, Koburger T. Reduced cytotoxicity of polyhexamethylene biguanide hydrochloride (PHMB) by egg phosphatidylcholine while maintaining antimicrobial efficacy. Chem. Biol. Interact. 2011; 190: 171–178.
32. Nair LS. Injectable hydrogels for regenerative engineering. Hackensack, NJ: Imperial College Press; 2016.
33. Tokita M, editor. Gels: Structures, Properties, and Functions: Fundamentals and Applications. Progress in Colloid and Polymer Science 136. Berlin, Heidelberg: Springer-Verlag Berlin Heidelberg; 2009.
34. Nakajima T, Furukawa H, Gong JP, Lin EK, Wu W-l. A deformation mechanism for double-network hydrogels with enhanced toughness. Macromol. Symp. 2010; 291-292: 122–126.
35. van Dijk-Wolthuis WN, Franssen O, Talsma H, van Steenbergen MJ, Kettenes-van den Bosch, J. J., Hennink WE. Synthesis, characterization, and polymerization of glycidyl methacrylate derivatized dextran. Macromolecules 1995; 28: 6317–6322.

36. Beamish JA, Zhu J, Kottke-Marchant K, Marchant RE. The effects of monoacrylated poly(ethylene glycol) on the properties of poly(ethylene glycol) diacrylate hydrogels used for tissue engineering. J. Biomed. Mater. Res. A 2010; 92: 441–450.
37. Nguyen QT, Hwang Y, Chen AC, Varghese S, Sah RL. Cartilage-like mechanical properties of poly(ethylene glycol)-diacrylate hydrogels. Biomaterials 2012; 33: 6682–6690.
38. Moura LIF, Dias AMA, Carvalho E, Sousa HCd. Recent advances on the development of wound dressings for diabetic foot ulcer treatment-a review. Acta Biomater. 2013; 9: 7093–7114.
39. Dissemond J, Augustin M, Eming SA, Goerge T, Horn T, Karrer S, Schumann H, Stucker M. Modern wound care - practical aspects of non-interventional topical treatment of patients with chronic wounds. J. Dtsch. Dermatol. Ges. 2014; 12: 541–554.
40. Desai ES, Tang MY, Ross AE, Gemeinhart RA. Critical factors affecting cell encapsulation in superporous hydrogels. Biomed. Mater. 2012; 7: 24108.
41. Hu X, Gao C. Photoinitiating polymerization to prepare biocompatible chitosan hydrogels. J. Appl. Polym. Sci. 2008; 110: 1059–1067.
42. Jansen J, Ghaffar A, van der Horst, Thomas N S, Mihov G, van der Wal S, Feijen J, Grijpma DW. Controlling the kinetic chain length of the crosslinks in photo-polymerized biodegradable networks. J. Mater. Sci. Mater. Med. 2013; 24: 877–888.
43. Goh CH, Heng PWS, Chan LW. Cross-linker and non-gelling Na^+ effects on multi-functional alginate dressings. Carbohydr. Polym. 2012; 87: 1796–1802.
44. Sun TL, Luo F, Kurokawa T, Karobi SN, Nakajima T, Gong JP. Molecular structure of self-healing polyampholyte hydrogels analyzed from tensile behaviors. Soft Matter 2015; 11: 9355–9366.
45. Hansen B, Jemec GBE. The mechanical properties of skin in osteogenesis imperfecta. Arch. Dermatol. 2002; 138: 909–911.
46. Dutta J, Ghosh D, Majumdar AS, Dwivedi G, Viswanathan C. Hydrogel composition (WO2010067378 A2); 2010.
47. Ajji Z, Othman I, Rosiak JM. Production of hydrogel wound dressings using gamma radiation. Nucl. Instrum. Meth. B 2005; 229: 375–380.
48. Razzak MT, Darwis D, Zainuddin, Sukirno. Irradiation of polyvinyl alcohol and polyvinyl pyrrolidone blended hydrogel for wound dressing. Radiat. Phys. Chem. 2001; 62: 107–113.

49. Lee KY, Mooney DJ. Alginate: Properties and biomedical applications. Prog. Polym. Sci. 2012; 37: 106–126.
50. Xu R, Luo G, Xia H, He W, Zhao J, Liu B, Tan J, Zhou J, Liu D, Wang Y, Yao Z, Zhan R, Yang S, Wu J. Novel bilayer wound dressing composed of silicone rubber with particular micropores enhanced wound re-epithelialization and contraction. Biomaterials 2015; 40: 1–11.
51. Sahraro M, Yeganeh H, Sorayya M. Guanidine hydrochloride embedded polyurethanes as antimicrobial and absorptive wound dressing membranes with promising cytocompatibility. Mater. Sci. Eng. C Mater. Biol. Appl. 2016; 59: 1025–1037.
52. Stevens DL, Bisno AL, Chambers HF, Dellinger EP, Goldstein EJC, Gorbach SL, Hirschmann JV, Kaplan SL, Montoya JG, Wade JC. Practice guidelines for the diagnosis and management of skin and soft tissue infections: 2014 update by the infectious diseases society of America. Clin. Infect. Dis. 2014; 59: 147–159.
53. van Walraven C, Musselman R. The surgical site infection risk score (SSIRS): A model to predict the risk of surgical site infections. PLoS One 2013; 8: e67167.
54. McGuiness W, Vella E, Harrison D. Influence of dressing changes on wound temperature. J. Wound Care 2004; 13: 383–385.
55. Dilamian M, Montazer M, Masoumi J. Antimicrobial electrospun membranes of chitosan/poly(ethylene oxide) incorporating poly(hexamethylene biguanide) hydrochloride. Carbohydr. Polym. 2013; 94: 364–371.
56. Guo B, Yuan J, Yao L, Gao Q. Preparation and release profiles of pH/temperature-responsive carboxymethyl chitosan/P(2-(dimethylamino) ethyl methacrylate) semi-IPN amphoteric hydrogel. Colloid Polym. Sci. 2007; 285: 665–671.

Chapter 3

pH-Modulating Poly(ethylene glycol)/ Alginate Hydrogel Dressings for the Treatment of Chronic Wounds

This chapter was published as: Koehler J, Wallmeyer L, Hedtrich S, Goepferich AM, and Brandl FP. Macromol. Biosci. 2017; 17: 1600369. Data which were not obtained or analyzed by J. Koehler are highlighted at the appropriate points.

Abstract

The development of chronic wounds has been frequently associated with alkaline pH values. The application of pH-modulating wound dressings could, therefore, be a promising treatment option to promote normal wound healing. This study reports on the development and characterization of acidic hydrogel dressings based on interpenetrating poly(ethylene glycol) diacrylate/acrylic acid/alginate networks. The incorporation of ionizable carboxylic acid groups results in high liquid uptake up to 500%. The combination of two separate polymer networks significantly improves the tensile and compressive stability. In a 2D cell migration assay, the application of hydrogels (0 to 1.5% acrylic acid) results in complete "wound" closure; hydrogels with 0.25% acrylic acid significantly increase the cell migration velocity to 19.8 ± 1.9 $\mu m \cdot h^{-1}$. The most promising formulation (hydrogels with 0.25% acrylic acid) is tested on 3D human skin constructs, increasing keratinocyte ingrowth into the wound by 164%.

1. Introduction

Normal wound healing proceeds in three major stages. Directly after coagulation and clot formation, neutrophils and monocytes enter the wound site. This process is mediated by cytokines and growth factors and marks the beginning of the inflammatory phase.[1] During the proliferative phase, epithelial cells, fibroblasts, and keratinocytes migrate to the injured area and start to proliferate. This phase is characterized by the synthesis of collagen and the formation of blood vessels.[2,3] In the remodeling phase, final healing occurs by tissue strengthening and replacement of provisional tissue.[2,4] This sequence is disrupted in non-healing or chronic wounds. Wounds that do not heal over a period of several months or years affect 2% of the population of the United States and generate costs of more than 50 billion U.S. dollar per year.[5] Finding new treatment options for chronic wounds is, therefore, a pressing problem in healthcare.

Clinical studies indicate that chronic wounds are often characterized by elevated pH values,[6,7] which may have a strong impact on different processes in the healing cascade.[8,9] At elevated pH, the availability of oxygen is reduced; this may affect the proliferation of fibroblasts and impair the synthesis of extracellular matrix (ECM).[10,11] Furthermore, bacterial colonialization and biofilm formation are facilitated under these conditions.[9] Effects of the pH have also been described on the level of protein conformation. For example, the conformation of vitronectin, an important ECM protein, changes with the pH of the environment. This alters the ability of vitronectin to bind endothelial cells and osteonectin, which is an important factor for fibroblast migration and collagen synthesis.[12,13] Furthermore, the activity of several enzymes depends on the wound pH.[14] In particular, the concentration and activity of matrix metalloproteinases (MMPs) is increased in chronic wounds, whereas tissue inhibitors of metalloproteinases (TIMPs) are suppressed. This imbalance between MMPs and TIMPs favors the degradation of ECM and growth factors.

Recent approaches tackle, amongst others, the problems of bacterial colonization and reduced oxygen levels; this has resulted in the development of advanced, rather expensive wound dressing materials.[15] Restoring the physiological pH (pH 7.4) could be an alternative, more economical way to bring chronic wounds back to the natural healing cascade.[7,8] For the development of pH-modulating wound dressings, physically cross-linked alginate was combined with a chemically cross-linked network consisting of poly(ethylene glycol) diacrylate (PEGDA) and acrylic acid (AA). Alginate is a naturally

occurring polysaccharide consisting of 1,4-linked β-D-mannuronic acid and α-L-guluronic acid repeating units; it is widely used for the development of medical products.[16–18] The hydrophilicity, excellent biocompatibility, and huge liquid absorbing capacity make alginate an attractive base material for wound dressings. Poly(ethylene glycol), on the other hand, is a synthetic hydrogel precursor that is widely used in the biomedical field, e.g., for cell encapsulation.[19–21] By using different starting materials, different properties can be combined in one single material. In comparison with wound dressings made from a single polymer, these composite materials have shown superior mechanical properties and liquid handling capacity, and resulted in improved wound healing.[15] In particular, alginate and PEGDA form an interpenetrating polymer network (IPN), which is characterized by enhanced mechanical stability.[22–24] The incorporated AA groups are responsible for pH regulation and act, together with functional groups of alginate, as interconnection between the two networks. Different PEGDA and AA concentrations were used; their impact on the swelling capacity, mechanical properties, and base neutralizing capacity of the formed hydrogels was assessed. Furthermore, the performance of the IPN hydrogels was evaluated in two-dimensional (2D) cell culture and three-dimensional (3D) human skin constructs.

2. Experimental Section

2.1 Preparation of Hydrogels

The synthesis of PEGDA is described in the supporting information. For hydrogel preparation, PEGDA was dissolved in phosphate buffered saline (PBS). To initiate polymerization, 2-hydroxy-4′-(2-hydroxyethoxy)-2-methylpropiophenone was suspended in PBS and added to the stirred solution. Afterwards, the required amounts of alginate (solution in PBS, c = 41.7 mg·mL^{-1}) and acrylic acid (AA) were added drop-wise. The PEGDA concentration ranged from 5.0 to 10.0%; the AA concentration was varied between 0 and 4.5%; the alginate concentration was either 0 or 0.5%. The overall concentration of all three components was 10.0% in all groups; the initiator concentration was 1.8%, based on the total monomer mass. For tensile testing and water vapor transmission studies, 8 mL of the solution were cast into rectangular silicon molds; for skin construct healing assays, 1.4 mL of the solution were cast into a 6-well plate. For all other experiments, cylindrical glass molds (1 cm diameter, 0.7 mL volume) were used. All samples were irradiated with UV light (366 nm, 6 W) for 1 h. If not stated otherwise, the hydrogels (initial weight m_0) were placed in 10 mL of deionized water to leach out the

initiator and unreacted monomers. The gels were removed after 24 h of incubation at 37 °C. To remove the absorbed water, the gels were partially dried by exposing them to a stream of compressed air. The drying process was stopped after m_0 had been reached; in this way, the water content (90%) was kept constant throughout all experiments.

2.2 Swelling Capacity

Hydrogel cylinders were prepared as described above (without pre-incubation in water) and incubated in 10 mL of PBS at 37 °C in a shaking water bath. Over a period of 7 days, the liquid was decanted every 24 h; the gels were blotted dry using a filter paper and weighed. The swelling capacity (Q_t) was calculated according to Equation (1)

$$Q_t = \frac{m_t - m_0}{m_0} \cdot 100\% \qquad (1)$$

where m_t is the mass of the gel cylinder at time point t, and m_0 is the initial mass of the gel.

2.3 Water Vapor Transmission Rate

The water vapor transmission rate (WVTR) was determined according to the ASTM E96/E96M-12 inverted water method.[25] Hydrogel sheets were prepared as described above and fixed at a circular WVTR test dish carrying 5 mL of deionized water. Water loss at 37 °C and 21% relative humidity was measured gravimetrically every hour (0 – 10 h and ≥ 24 h) until a weight loss of 5 g had been be reached. The WVTR was calculated according to Equation (2)

$$WVTR = \frac{G}{A \cdot 1\text{h}} \qquad (2)$$

where G is the slope of the time–water loss curve, and A is the test area (10.18 cm^2).

2.4 Tensile Strength

Hydrogel sheets were prepared as described above (without pre-incubation in water) and cut into rectangular specimens of 1 cm width (d) and 8 cm length. Prior to mechanical testing, the thickness (h) of the specimens (around 550 μm) was determined using a MiniTest 600 gauge (ElektroPhysik, Köln, Germany). Tensile testing was performed using an Instron 5542 load frame with two serrated grips (Instron GmbH, Darmstadt, Germany). The specimens were stretched until failure with a tensile velocity of 15 $mm \cdot min^{-1}$ and the

maximum load ($F_{max,\,t}$) and elongation (l_{max}) were measured. The tensile stress (σ_t) was calculated according to Equation (3).

$$\sigma_t = \frac{F_{max,t}}{h \cdot d} \qquad (3)$$

The elastic modulus (E_t) was calculated from the slope of the stress-strain curve between 0.05 and 0.15 strain. The data are presented as mean ± standard deviation (SD), based on the test results of $n = 4$ specimens.

2.5 Compressive Strength

Hydrogel cylinders were prepared as described above (with and without pre-incubation in water). Height (h) and diameter (d) of the gel cylinders were determined using a caliper (BORT GmbH, Weinstadt-Benzach, Germany). Compressive testing was carried out using an Instron 5542 load frame equipped with two cylindrical platens. The hydrogel cylinders were compressed at 0.5 mm·min^{-1} until a strain of 95% had been reached. Compressive stress (σ_c) and elastic modulus of compression (E_c) were calculated as described above.

2.6 Scanning Electron Microscopy

Hydrogel cylinders were shock-frozen in liquid nitrogen, lyophilized and coated with gold. The microstructure was examined by using a Crossbeam XB 340 scanning microscope (Zeiss, Jena, Germany) at an extra high tension voltage level of 3.0 kV.

2.7 Base Neutralizing Capacity

Hydrogel cylinders were prepared as described above and placed in 15 mL of a 0.1 M sodium chloride solution. To determine the base neutralizing capacity (BNC), a 0.1 M sodium hydroxide solution was added over 24 h using a TitroLine 7000 dosage system equipped with a BlueLine glass electrode (SI Analytics GmbH, Mainz, Germany); the pH was kept constant at 7.4 during the experiment (static pH titration). The BNC was calculated from the amount of neutralized sodium hydroxide, n(NaOH), and the initial mass of the gel cylinder, m_0, according to Equation (4).

$$BNC = \frac{n(\mathrm{NaOH})}{m_0} \qquad (4)$$

2.8 Cell Viability

The cell viability was determined according to ISO 10993-5 using adult human dermal fibroblasts (HDFa).[26,27] A detailed description of the methods and experimental conditions can be found in the supporting information.

2.9 Cell Migration Assay

Cell culture inserts (Ibidi GmbH, Martinsried, Germany) were placed in a fibronectin-coated 6-well plate (Corning, Corning, NY, USA); then, 140 µL of a HDFa suspension (300000 cells·mL^{-1}) were pipetted into the inserts. After 24 h of incubation under standard cell culture conditions, the inserts were removed; 8 mL of pH-modified medium (medium 199 : utrient mixture F12 (F12) 3 : 1, 10% fetal bovine serum (FBS), 1.10 mM hydrocortisone, adjusted to pH 8 with 1 M NaOH) were added. Hydrogels were placed in netwell inserts (Corning, Corning, NY, USA) and inserted into the cell culture plate. Every 12 h, pH adjusted cell culture medium was replaced by fresh medium. The cell migration was observed over 48 h using a Leica DM IRB microscope (Leica Microsystems GmbH, Wetzlar, Germany) connected to a DS-5M digital camera (Nikon GmbH, Düsseldorf, Germany). The area of cell migration was calculated using the Eclipsenet software (Nikon GmbH, Düsseldorf, Germany); cell migration velocity was calculated from the slope of the area closure/time curve.

2.10 3D Human Skin Constructs and Healing Assay*

Normal human skin constructs were generated according to previously published procedures.[28–30] Briefly, normal primary human keratinocytes and fibroblasts were isolated from juvenile foreskin, the remainder of circumcision surgery (with ethical consent) and cultivated according to standard protocols until skin construction. Fibroblasts ($3.0 \cdot 10^5$/skin construct), FBS, Hank's balanced salt solution and bovine collagen I were brought to neutral pH and poured into cell culture inserts with a growth area of 4.2 cm^2. After cultivation for 2 h at 37 °C, keratinocyte growth medium (KGM) was added and the system was transferred to an incubator with 5% CO_2 and 95% humidity for further 2 h. Primary keratinocytes ($4.2 \cdot 10^6$/skin construct) resuspended in KGM were added on top of the collagen matrix. Skin constructs were lifted to the air-liquid interface 24 h later and a

* 3D human skin constructs were generated at the Institute of Pharmacy, Pharmacology and Toxicology, Freie Universität Berlin, with support and based on the method of S. Hedtrich and L. Wallmeyer.

high glucose Dulbecco's modified eagle medium (DMEM)-based differentiation medium was added.

After 2 days of skin construct cultivation, a wound was induced by cutting the epidermal layer with a scalpel. For reproducibility, defect size and operating person remained unchanged in all samples. The injured constructs were incubated with pH–defined medium, containing 2.5% hydroxyethyl cellulose to enhance the viscosity. In order to maintain induced pH variations during the healing assay, the differentiation medium was modified by substituting DMEM with medium 199 with reduced bicarbonate. Medium was adjusted to pH 8.0 by dropwise addition of 2 M NaOH.[11] The respective hydrogels were punched out in circular shape (1 cm diameter) and applied onto the wound area. The pH-defined medium was changed every day and the hydrogels were replaced 2 days after wound induction. Injured constructs without hydrogels applied served as control. After further 2 days, the hydrogels were carefully removed from the skin constructs. The constructs were punched, embedded in tissue freezing medium (Leica Biosystems, Nussloch, Germany), and shock-frozen using liquid nitrogen. Subsequently, the skin constructs were cut vertically into slices (7 µm) using a Leica CM1510 S cryotome (Leica Biosystems, Nussloch, Germany) and stained with conventional hematoxylin and eosin (H&E) according to standard protocols. After picture capturing (BZ-8000 microscope, Keyence, Neu-Isenburg, Germany), the length of cell ingrowth was determined using ImageJ (National Institutes of Health, Bethesda, Maryland, USA).

3. Results

Interpenetrating polymer networks were prepared by radical polymerization of poly(ethylene glycol) diacrylate (PEGDA) and acrylic acid (AA) in combination with alginate.[31] The resulting hydrogels had water contents of 90%, thus showing a flexible but stable texture.

Table 1. Composition of the examined hydrogel formulations.

Formulation	PEGDA (%)	AA (%)	Alginate (%)
PEGDA	10.00	–	–
PEGDA/alginate	9.50	–	0.50
PEGDA/AA/alginate	5.00 – 9.25	0.25 – 4.50	0.50

The AA content ranged from 0 to 4.5% (Table 1); raising the AA concentration above 4.5% was not possible. At low pH values, AA forms complexes with PEGDA via hydrogen bonds. These became visible as white precipitate when high volumes of AA ($c \geq 3.5\%$) were added to aqueous PEGDA solutions during precursor mixing.[32,33]

3.1 Liquid Uptake and Water Vapor Transmission

The swelling capacity of PEGDA, PEGDA/alginate, and PEGDA/AA/alginate hydrogels was calculated after 24 h and 7 days; the value determined after 7 days was regarded as equilibrium swelling ratio (Figure 1). Compared to pure PEGDA hydrogels, the addition of 0.5% alginate caused a significant change in the swelling ratio, which increased from 15 to 40% regardless of the incubation time. With the incorporation of AA, the swelling capacity further increased. After 24 h of incubation, the swelling ratio ranged from 63% (0.25% AA) to 253% (4.5% AA). After the equilibrium had been reached, swelling ratios between 64 and 501% could be measured.

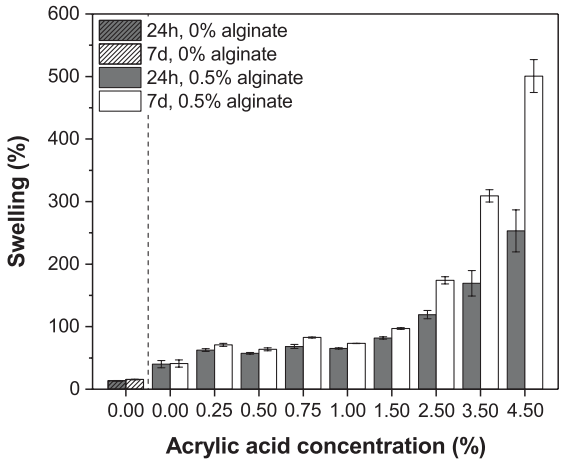

Figure 1. Swelling capacity of PEGDA/AA/alginate hydrogels with different monomer concentrations after 24 h and 7 days of incubation. Data are expressed as mean ± SD (n = 3).

Exemplarily, the water vapor transmission rate of PEGDA, PEGDA/alginate and PEGDA/AA/alginate (0.25% acrylic acid) hydrogels was determined; the measured values were 175.35 ± 0.58, 171.40 ± 0.30 and 182.35 ± 0.38 $g \cdot h^{-1} \cdot m^{-2}$, respectively.

3.2 Mechanical Properties and Microstructure

To evaluate the mechanical properties of the developed hydrogels, their behavior in tensile and compressive testing was examined. The tensile stress at maximum load (σ_t) ranged from 38.0 ± 1.1 kPa (pure PEGDA hydrogels) to 80.1 ± 13.8 kPa (PEGDA/alginate gels,

Figure 2A); the compressive stress at maximum load (σ_c) ranged from 0.43 ± 0.16 MPa to 2.85 ± 0.68 MPa, respectively (Figure 2C). The incorporation of AA had little effect on the tensile stress, which ranged between 65.5 and 91.5 kPa (Figure 2A). The compressive stress, on the other hand, was clearly influenced by the AA content; higher amounts of AA resulted in lower values of σ_c (Figure 2C).

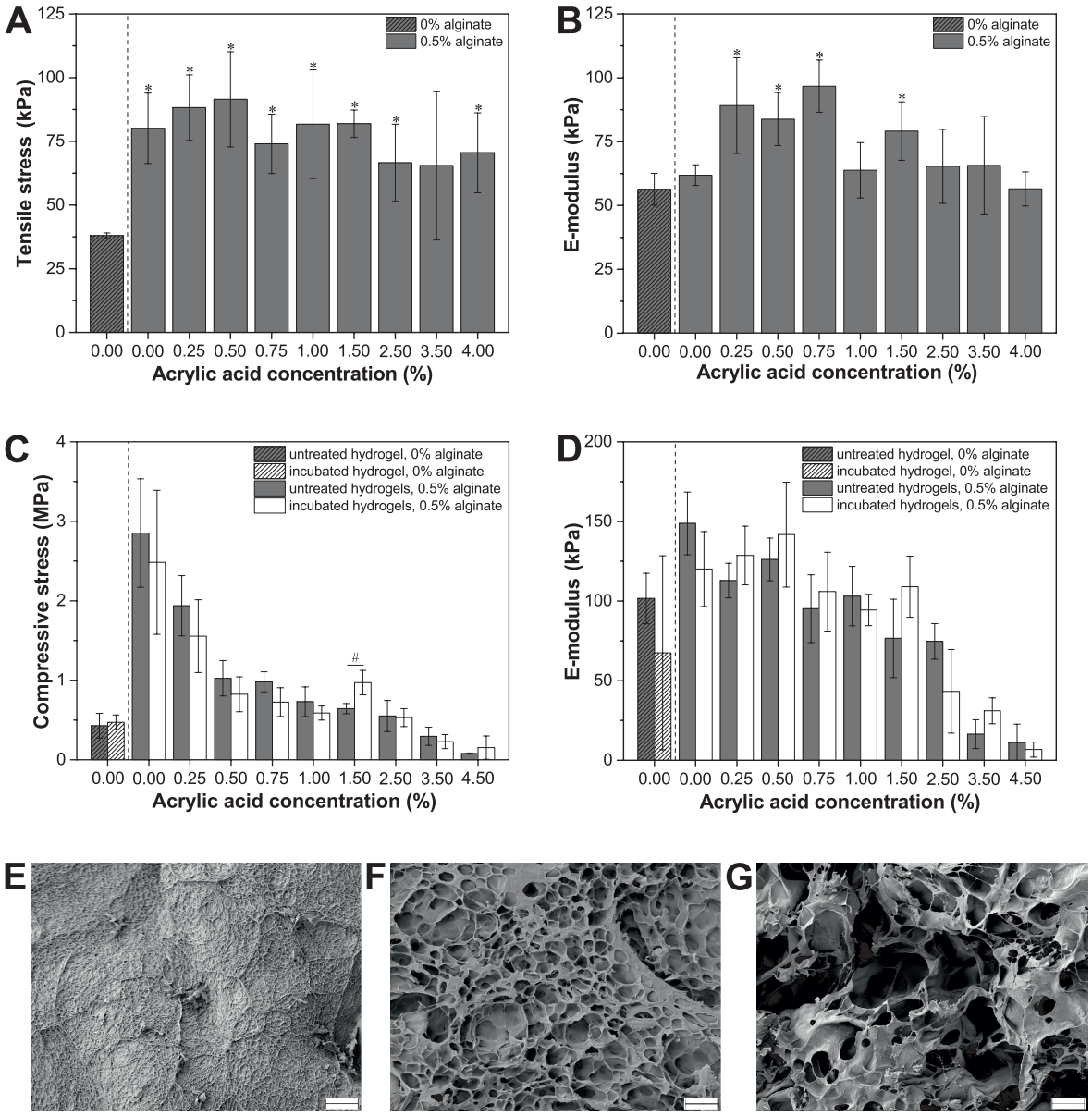

Figure 2. Mechanical properties and microstructure of different PEGDA/AA/alginate hydrogels. Tensile stress at maximum load (A) and calculated E-modulus (B); compressive stress at maximum load (C) and calculated E-modulus (D). Data are expressed as mean ± SD (n = 4); * indicates statistically significant differences versus the control ($p < 0.05$); # indicates statistically significant differences between the groups ($p < 0.05$). SEM images of lyophilized PEGDA (E), PEGDA/alginate (F), and PEGDA/AA/alginate (G) hydrogels. The length of the scale bars is 10 μm.

In tensile testing, the elastic modulus (E_t) increased by approximately 45% when low concentrations of AA (0.25 to 0.75%) were incorporated into PEGDA/alginate hydrogels (Figure 2B). Further increasing the AA content resulted in lower values of E_t similar to those of pure PEGDA/alginate hydrogels. In contrast to that, E_c showed the same trend as σ_c in compressive testing (Figure 2D). The compressive testing was repeated after incubating the gels in deionized water to check whether purification results in altered mechanical properties. As shown in Figure 2C and D, neither σ_c nor E_c changed significantly upon incubation in water. The investigation of the hydrogel microstructure was performed by scanning electron microscopy (SEM). Pure PEGDA gels had a low porosity, whereas PEGDA/alginate IPNs showed a considerable amount of pores at the surface (diameter around 4 μm; Figure 2E and F). The addition of AA generated fibrous structures and irregular pores with a high variation in diameter (0.5 – 30 μm, Figure 2G).

3.3 Base Neutralizing Capacity

The capacity for proton donation is an important parameter of pH-modulating wound dressings that can be estimated by the base neutralizing capacity (BNC).[34,35] As it was expected, the BNC of the tested hydrogels increased with increasing AA content (Figure 3). Depending on the AA content, 0.012 to 0.88 mmol of sodium hydroxide were neutralized per gram hydrogel.

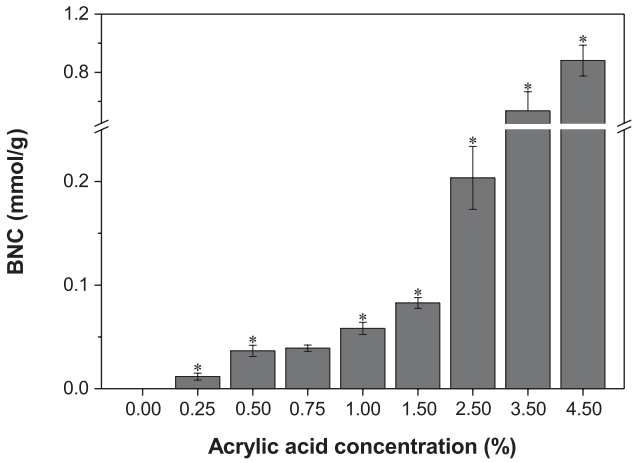

Figure 3. Base neutralizing capacity of PEGDA/AA/alginate hydrogels with different monomer concentrations. Data are expressed as mean ± SD (n = 3); * indicates statistically significant differences versus the lower concentrated samples ($p < 0.05$).

3.4 Cell Viability Testing

The cytotoxicity of the developed hydrogels was evaluated by a MTT assay. Since high AA concentrations gave rather fragile hydrogels (see Figure 2 for comparison), the cell viability testing was only performed on hydrogels with AA contents up to 2.5%. The results presented in Figure 4 demonstrate that hydrogels with AA concentrations between 0 and 1.0% did not significantly affect the cell viability, independent from the hydrogel incubation time (12 – 48 h). However, hydrogels with AA concentrations between 1.5 and 2.5% reduced the cell viability by approximately 20% during the first 12 h of incubation. Nevertheless, the cell viability was generally between 77 and 127%; therefore, all tested hydrogels were regarded as non-cytotoxic.[26]

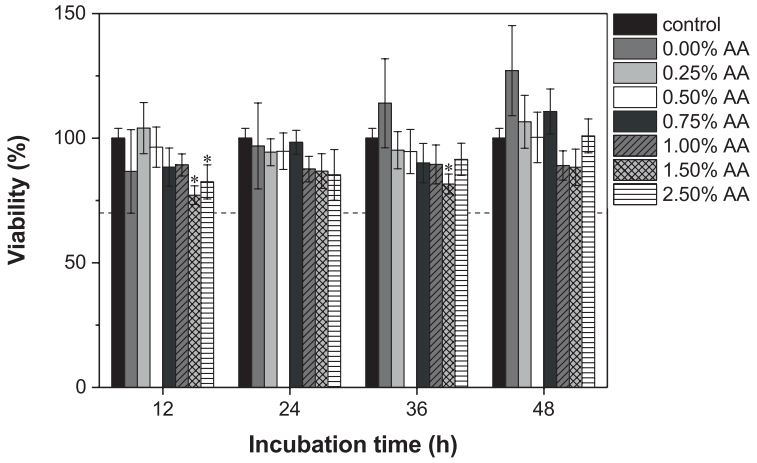

Figure 4. Viability of HDFa in contact with different PEGDA/AA/alginate hydrogel extracts. The broken line (---) marks the critical value of 70% cell viability.[21] Data are expressed as mean ± SD (n = 6); * indicates statistically significant differences versus the untreated control ($p < 0.05$).

3.5 2D Cell Migration Assay

The effects of pH-modulating hydrogels on cells were studied in 2D migration assays.[11,36] During the duration of the experiment, cells treated with PEGDA/alginate and PEGDA/AA/alginate hydrogels (0.25 – 1.5% AA concentration) showed a complete gap closure (Figure 5A). However, when hydrogels with an AA concentration of 2.5% were applied, the percentage of gap closure decreased; the measured values were significantly lower than in the control group. Moreover, the application of PEGDA/alginate and individual PEGDA/AA/alginate hydrogels (0.25 and 0.50% AA concentration) significantly increased the cell migration velocity in comparison to the control group (Figure 5B). The maximum migration velocity (19.8 ± 1.9 $\mu m \cdot h^{-1}$) was measured when PEGDA/AA/alginate gels with an AA content of 0.25% were applied.

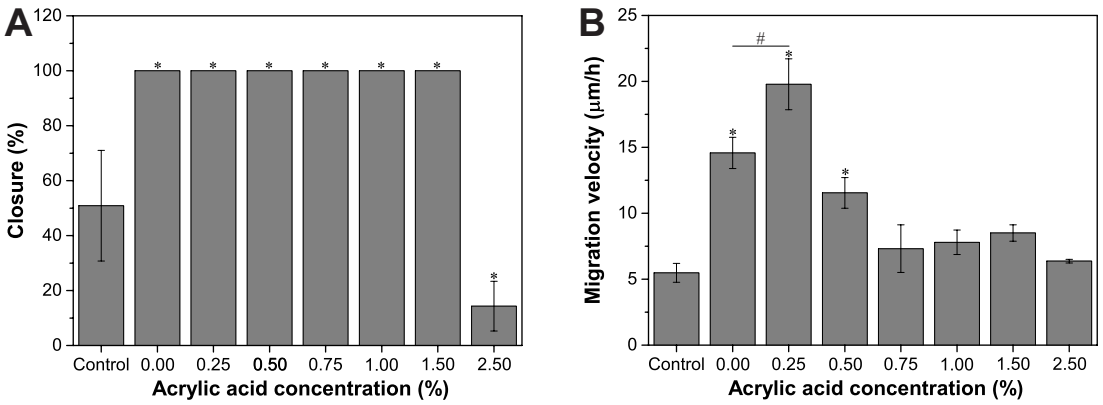

Figure 5. Percentage of gap closure (A) and cell migration velocity (B) in 2D migration experiments with different PEGDA/AA/alginate hydrogels applied. Data are expressed as mean ± SD (n = 3); * indicates statistically significant differences versus the untreated control ($p < 0.05$); # indicates statistically significant differences between the groups ($p < 0.05$).

3.6 3D Human Skin Constructs and Healing Assay

As a proof of concept, the developed hydrogels were applied on wounded human skin constructs supplied with alkaline cell culture medium (pH 8).[28] To this end, the damaged stratum corneum (layer S in Figure 6) and epidermis (layer E in Figure 6) were covered with PEGDA/alginate or PEGDA/AA/alginate hydrogels (0.25% AA concentration); the degree of "wound healing" was evaluated by measuring the ingrowth of cells.

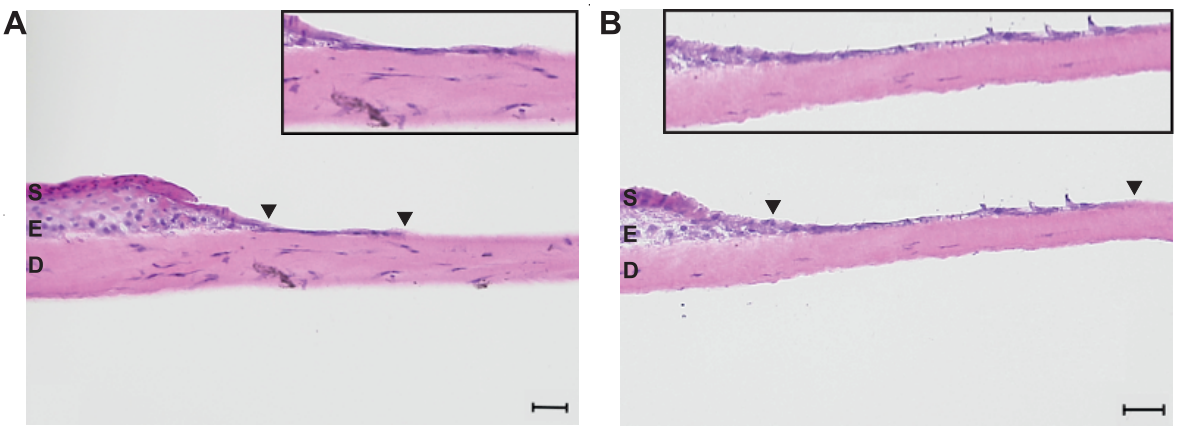

Figure 6. H&E stained histological images of injured skin constructs after a healing period of 4 days. The untreated control is shown on the left (A); a skin construct treated with a PEGDA/AA/alginate hydrogel (0.25% AA content) is shown on the right (B). Stratum corneum (S), epidermis (E), and dermis equivalent (D) are clearly visible. The length of cell ingrowth is indicated by triangles; the insets show a magnification of this area. The length of the scale bars is 50 µm.

In comparison to untreated constructs, the cell ingrowth increased significantly when PEGDA/AA/alginate hydrogels with an AA content of 0.25% were applied (Figure 7); the

keratinocyte ingrowth could be enhanced by 164%. On the other hand, the application of hydrogels without pH-modulating properties (PEGDA/alginate) did not have any effect on "wound healing".

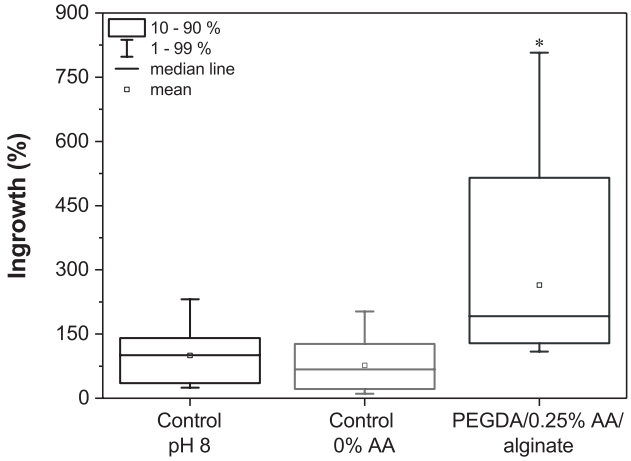

Figure 7. Ingrowth length in the untreated control at pH 8 (mean set as 100%), skin constructs treated with PEGDA/alginate gels, and skin constructs treated with PEGDA/AA/alginate hydrogels (0.25% AA content). Data are expressed as boxplot (10 - 90%); * indicates statistically significant difference versus the untreated control ($p < 0.05$).

4. Discussion

The treatment of chronic wounds is a great challenge in health care.[5] Numerous studies indicate that impaired healing is often correlated with alkaline pH values of the wound. To neutralize the alkaline pH and stimulate the healing of chronic wounds, pH-modulating hydrogels consisting of poly(ethylene glycol) diacrylate, acrylic acid and alginate were developed. These hydrogels must meet strict requirements regarding swelling capacity, mechanical properties, and biocompatibility. For example, a sufficient swelling capacity is mandatory for wound dressings. In particular chronic wounds secrete large amounts of wound exudate, which should be absorbed by the dressing material. If not removed, excessive exudate can inhibit cell proliferation; furthermore, wound exudate contains high concentrations of cytokines and MMPs, which can cause degradation of the surrounding tissue and promote inflammation.[2,37,38] For most wounds, exudate amounts between 1 and 12 $L \cdot m^{-2}$ per day have been described in the literature.[39,40] Transferring these values to the herein examined gel cylinders (approximate surface area: 4.37 cm^2), the material should be able to absorb at least 0.4 mL of liquid to act as a dressing for heavily exuding wounds. Taking the volume of the hydrogel cylinders (approximately 0.7 mL) into account, a swelling capacity of at least 57% is required. As shown in Figure 1, the developed

PEGDA/AA/alginate IPN hydrogels exhibited swelling ratios between 57.4 ± 1.5 and 253.1 ± 33.6% after 24 h. The swelling capacity increased with increasing AA content, most likely due to the increasing charge density. A high charge density translates into strong repulsive forces within the polymer network; hence, there is a strong osmotic force directed into the hydrogel, which results in extensive swelling.[41] The swelling capacity of hydrogel dressings usually depends on the composition of the material; furthermore, different ways of calculating the swelling capacity are used, which makes the available data difficult to compare.[18,42,43] For example, the swelling ratio of PEG-based hydrogels is typically not exceeding 30%.[42,44] Chen et al. reported the preparation of chitosan-based wound dressings with extremely high liquid absorbing capacity;[43] however, the calculation of the swelling ratio (approximately 1000) was based on the mass of the dry polymer. Another parameter characterizing the fluid handling capacity of wound dressings is the water vapor transmission rate. The WVTR of commercially available products ranges from 3.75 to 390 $g \cdot h^{-1} \cdot m^{-2}$, depending on the composition.[45] The herein described hydrogels (WVTR around 175 $g \cdot h^{-1} \cdot m^{-2}$) are, therefore, suitable for wound coverage.

The mechanical properties of the developed hydrogels were characterized by tensile and compressive testing. As it has been described by Gong et al.,[22] the tensile strength of hydrogels, expressed as tensile stress at maximum load (σ_t), can be enhanced by generating interpenetrating polymer networks. In our study, the addition of alginate to PEGDA networks increased the tensile strength by 111%. This is remarkable since an increase by only 32% is expected from the sum of σ_t(alginate) and σ_t(PEGDA). The addition of AA is expected to change the architecture of the PEGDA network. Acrylic acid only contributes to chain growth, which typically results in less densely cross-linked networks with reduced mechanical strength.[46,47] Indeed, changes in the hydrogel structure were identified on the microscopic scale, as can be seen in SEM images (Figure 2E – F). However, with regard to the tensile strength, the inserted carboxylic acid groups apparently counteract this effect. As already discussed before, carboxylic acid groups engage in hydrogen bonds with PEGDA (see Figure 8 for illustration).[32,33] These interactions were found to contribute to the stability of hydrogels under tensile load.[48] Furthermore, alginate might also engage in hydrogen bonds with PEGDA and AA, given the large number of hydroxyl and carboxylic acid groups of the molecule (see Figure 8 for illustration).[49] The effect might be comparable to the formation of alginic acid gels at acidic pH.[31] Apparently, the reduced cross-linking density of PEGDA/AA/alginate hydrogels is compensated by the stabilizing

effects of hydrogen bonds. As a result, the tensile strength and the E-modulus of PEGDA/AA/alginate hydrogels were almost independent from the AA content (Figure 2A and B).

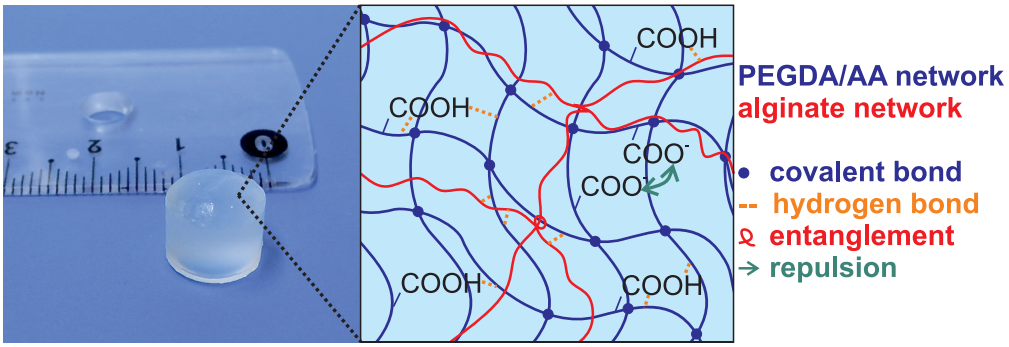

Figure 8. Schematic representation showing the proposed network architecture of PEGDA/AA/alginate hydrogels with all relevant interactions.

In contrast to the tensile strength, the compressive strength of PEGDA/AA/alginate hydrogels (expressed as stress at maximum load, σ_c) was clearly dependent on the AA concentration. Increasing the amount of AA resulted in significantly reduced compressive strength (Figure 2C); similarly, the elastic modulus (E_c) decreased with increasing AA content (Figure 2D). This behavior can be explained as follows. PEGDA/AA/alginate hydrogels have a pH of approximately 4.6 (data not shown), as measured using a luminescent pH sensor.* At this pH, the carboxylic acid groups (pK_a = 4.25) are partially ionized and carry a negative charge. During compressive testing, the polymer chains are approaching and repulsive forces between negatively charged groups get more and more important (see Figure 8 for illustration); as a result, material failure might occur rather than polymer chain entanglement. Furthermore, the reverse of strain hardening might have an effect in compressive testing. Strain hardening describes the increased strength of a material under tensile load; it is explained by the better accessibility of hydrogen bonding functional groups in stretched polymer chains.[48] During compression, the accessibility of these groups is declining; as a consequence, entanglements between polymer chains are no longer reinforced by hydrogen bonds and the compressive strength is decreasing.

The obtained results are in line with previous reports indicating an inverse relationship between the E-modulus and hydrogel swelling (see Figure 1 and 2 for comparison).[50] Hydrogels with lower E-modulus are typically characterized by more flexible polymer chains, which result in higher swelling capacity. Besides the swelling capacity, further

* pH sensor data were obtained and analyzed by R. Meier, Institute of Analytical Chemistry, Chemo- and Biosensors, University of Regensburg, according to the method of Schreml et al.[11]

aspects need to be considered when defining the required mechanical strength of hydrogel dressings. Wound dressings should be both tough and flexible to withstand the mechanical forces occurring during application, wearing and removal; at the same time, the material should adapt to the irregular shape of the wound.[2,47] The elasticity of the human skin, which lies between 70 and 100%, can be taken as a reference value.[51,52] The herein described PEGDA/AA/alginate IPN hydrogels showed an elongation at break of around 170%, which should be sufficient for wound dressings. Both fragile and tough wound dressings have been described in the literature. Several groups reported on PEG-based hydrogels with mechanical properties comparable to the herein described hydrogels. The tensile stress at maximum load (σ_t) typically ranged between 4 and 220 kPa; values between 0.04 and 3.73 MPa were reported for the compressive stress (σ_c). The maximum strain at break was 41 – 460% (tensile testing) and 40 – 95% (compressive testing), respectively.[53–56] On the other hand, materials with a strength of up to 50.9 MPa have also been described in the literature.[57,58]

Since it was our aim to develop pH-modulating wound dressings, the base neutralizing capacity of PEGDA/AA/alginate hydrogels was determined. The physiological pH of human tissue (pH 7.4) was taken as target value. The results presented in Figure 3 show that the BNC of PEGDA/AA/alginate hydrogels was proportional to the amount of incorporated AA. This means that the capacity for proton donation, and hence the pH-modulating effect, can be easily adjusted. However, the wound pH varies among the different wound types; furthermore, the specific needs in wound care are changing from patient to patient and over time.[6,59] In clinical application, measurements of the wound pH (e.g., by using suitable pH sensors)[11] can be used as supportive tool to choose the appropriate wound dressing.

As a consequence, the safety and effectiveness of pH-modulating wound dressings must be carefully evaluated in organotypic cell culture models. In a first experiment, the cell viability after exposure to hydrogel extracts was evaluated by MTT assay. Although exposure to hydrogel extracts was generally well tolerated, the cell viability was significantly lower when hydrogels with AA contents of 1.5 and 2.5% were applied. As it can be expected from the high concentration of carboxylic acid groups, the pH of the cell culture medium dropped to 6.2 and 6.1, respectively (data not shown). The reduced cell viability is in accordance with the literature, which also showed reduced fibroblast proliferation and viability at pH $\leq$ 6.5.[11,60] A more detailed study of the effects of pH-modulating hydrogels on primary human skin cells was done in 2D cell migration

experiments, which can be regarded as simplified wound models. As it can be seen from Figure 5B, alginate could promote cell migration in vitro. Alginate has been reported to modulate the concentration of cytokines and growth factors, which is, among others, related to fibroblast proliferation.[61,62] Since PEGDA/alginate hydrogels had no detectable influence on the pH of the medium (data not shown), additional effects were expected from pH-modulating hydrogels. Indeed, the cell migration velocity further increased when PEGDA/AA/alginate hydrogels with an AA content of 0.25% were applied (pH shift to 7.4). The application of hydrogels with AA contents of 0.5% and above reduced the cell migration velocity in comparison to PEGDA/alginate and PEGDA/AA/alginate (0.25% AA content) treated samples. Their capacity for proton donation is apparently not appropriate; consequently, the pH of the medium dropped to 5.8 - 6.8 (data not shown). Finally, the most promising formulation (PEGDA/AA/alginate hydrogel with 0.25% AA content) was tested in contact with 3D human skin constructs. Since the human skin is structurally different from the skin of commonly used laboratory animals, such as rodents, human skin constructs are regarded as promising in vitro alternative to animal testing.[63–65] Furthermore, animal models of chronic wounds are difficult to generate and often non-reproducible, especially in combination with altered wound pH.[66] To simulate the conditions of chronic wounds, we decided to supply the skin constructs with an alkaline cell culture medium. When pH-modulating PEGDA/AA/alginate IPN hydrogels (0.25% AA content) were applied, the ingrowth of keratinocytes increased by 164% as compared with the untreated control (Figure 7). In this experiment, the pH of the medium seemed to be the predominant factor, since the application of PEGDA/alginate gels did not have any positive effects on keratinocyte ingrowth. These results confirm the above-described findings. PEGDA/AA/alginate hydrogels proved to be biocompatible; the application of pH-modulating hydrogels is, therefore, regarded as promising option for the treatment of chronic wounds.

5. Conclusion

Since chronic wounds have been associated with alkaline pH values, the application of pH-modulating wound dressings could be a promising treatment option. Herein, we reported the development and characterization of novel pH-regulating hydrogel dressings based on alginate, PEGDA, and AA. Alginate and PEGDA form an interpenetrating polymer network, which is characterized by superior mechanical strength. Important

properties of wound dressings, such as swelling capacity and mechanical strength, can be adjusted by varying the AA concentration. The developed PEGDA/AA/alginate IPN hydrogels are both tough and flexible to withstand the mechanical forces occurring during application, wearing, and removal. Similarly, the base neutralizing capacity, which characterizes the pH-modulating effect, can be controlled by increasing or decreasing the AA content. The results of cell viability studies and cell migration assays indicate that the application of PEGDA/AA/alginate hydrogels is a promising strategy to overcome pH-related wound healing problems. More particularly, hydrogels with an AA concentration of 0.25% can increase the cell migration velocity and percentage of gap closure in a simplified 2D model for chronic wounds. These findings are corroborated by further tests involving human skin constructs supplied with an alkaline cell culture medium. Future research should focus on the incorporation and release of antiseptic drugs such as polyhexanide. Such hydrogels could be valuable for the treatment of infected wounds, which is another challenging problem in wound care.

6. Supporting Information

6.1 Materials

Toluene was obtained from Acros Organics (Geel, Belgium). Bovine collagen I (PureCol®) was purchased from Advanced BioMatrix (San Diego, USA). Cell culture inserts were obtained from BD Bioscience (Heidelberg, Germany). Fetal bovine serum for skin constructs was purchased from Biochrom (Berlin, Germany). Formaldehyde solution (4%) and reagents for hematoxylin and eosin staining were obtained from Carl Roth (Karlsruhe, Germany). Deuterated chloroform ($CDCl_3$) was purchased from Deutero GmbH (Kastellaun, Germany). Alginate (Protanal® LF 10/60FT) was kindly provided by FMC BioPolymer (Wallingstown, Ireland). Dichloromethane (DCM), diethyl ether, and ethanol were purchased from CSC Jäcklechemie (Nürnberg, Germany). Hydroxyethyl cellulose was purchased from Fagron (Barsbüttel, Germany). Dulbecco's modified eagle medium/nutrient mixture F-12 (DMEM/F12), high glucose DMEM, Hank's balanced salt solution, nutrient mixture F-12, penicillin–streptomycin, and PBS were obtained from Life Technologies (Carlsbad, CA, USA). Keratinocyte basal medium (KBM) and keratinocyte growth medium supplements were purchased from Lonza (Basel, Switzerland). Dimethyl sulfoxide (DMSO), glacial acetic acid, hydrochloric acid, sodium hydroxide, and triethylamine were purchased from Merck KGaA (Darmstadt, Germany). Deionized water

was obtained using a Milli-Q water purification system (Millipore, Schwabach, Germany). All other chemicals were purchased from Sigma Aldrich (Taufkirchen, Germany). Poly(ethylene glycol) with a molecular mass of 6 kDa (PEG6k) was dried by azeotropic distillation in toluene before use. All other chemicals were used as received.

6.2 Synthesis of Poly(ethylene glycol) diacrylate

Poly(ethylene glycol) diacrylate with a molecular mass of 6 kDa (PEGDA) was synthesized as previously described.[67] In brief, 25.2 g of dried PEG6k (4.2 mmol) was dissolved in 100 mL of anhydrous DCM. The solution was cooled to 0 °C; then, 1400 µL of triethylamine (10.0 mmol) and 1625 µL of acryloyl chloride (20.0 mmol) were added drop-wise. The reaction mixture was stirred overnight under argon atmosphere, filtered, washed with 2 M potassium carbonate solution, and dried over anhydrous magnesium sulfate. The product was precipitated in ice-cold diethyl ether and dried under vacuum to yield 17.02 g (66.3%).

^{1}H NMR (300 MHz, $CDCl_3$, δ): 3.62 ppm (m, 310 H, -C*H*$_2$C*H*$_2$O-), 4.30 ppm (t, 2 H, -C*H*$_2$OC(O)-), 5.82 ppm (dd, 1 H, C*H*$_2$=CHC(O)O-), 6.13 ppm (dd, 1 H, CH_2=C*H*C(O)O-), 6.41 ppm (dd, 1 H, C*H*$_2$=CHC(O)O-).

6.3 Cell Culture

Adult human dermal fibroblasts (HDFa, Life Technologies, Carlsbad, CA, USA) were cultured in DMEM/F12 containing 10% FBS and 1% penicillin-streptomycin. Primary fibroblasts from juvenile foreskin were cultured in high glucose DMEM supplemented with 10% FBS. Primary keratinocytes from juvenile foreskin were cultured in KBM with keratinocyte growth medium supplements (KGM). HDFa were used in passage 3 to 7; juvenile foreskin cells were used in passage 2.

6.4 Cell Viability

Hydrogel cylinders were incubated in pH-modified medium (medium 199 : F12 3 : 1, 10% FBS, 1.10 mM hydrocortisone, adjusted to pH 8 with 1 M NaOH) for 48 h at 37 °C. The ratio of the hydrogel mass to the volume of the medium was approximately 0.1 g·mL^{-1}. Every 12 h, the extracts were collected and replaced with fresh pH-modified medium, yielding 32 mL of extract per sample. HDFa (8000 cells per well) were seeded in a 96-well plate (Corning, Corning, NY, USA) and incubated for 24 h under standard cell culture conditions (37 °C, 5% CO_2, 95% relative humidity). The cell culture medium was

aspirated and replaced with 100 µL of the hydrogel extracts; pH-modified cell culture medium served as a control. The plate was incubated for 24 h at 37 °C. The medium was removed; then, 50 µL of a 3-(4,5-dimethylthiazol-2-yl)-2,5-diphenyltetrazolium bromide (MTT) solution (c = 2.5 mg·mL^{-1} in PBS), 130 µL of DMEM/F12, and 20 µL of FBS were added. After 4 h of incubation, the solution was gently aspirated; then, 100 µL of a sodium dodecyl sulfate solution (c = 0.35 mmol·mL^{-1} in glacial acetic acid : DMSO 1 : 159) were added. The absorbance (A) at 570 and 690 nm was measured after 3 h of incubation at room temperature using a FluoStar Omega micro plate reader (BMG Labtech, Ortenberg, Germany). The cell viability (v) was calculated according to Equation (S1).

$$v = \frac{A_{570,gel} - A_{690,gel}}{A_{570,ctrl} - A_{690,ctrl}} \cdot 100\% \qquad \text{(S1)}$$

The data are presented as mean ± SD, based on the test results of n = 6 samples.

6.5 Statistical Analysis

If not stated otherwise, the experiments were done in triplicate and the data are presented as mean ± standard deviation. For statistical analysis, Brown Forsythe tests were run followed by one-way ANOVA/Tukey' test or Kruskal-Wallis-ANOVA. Differences were considered statistically significant at $p < 0.05$.

References

1. Menke NB, Ward KR, Witten TM, Bonchev DG, Diegelmann RF. Impaired wound healing. Clin. Dermatol. 2007; 25: 19–25.
2. Boateng JS, Matthews KH, Stevens HNE, Eccleston GM. Wound healing dressings and drug delivery systems: A review. J. Pharm. Sci. 2008; 97: 2892–2923.
3. Moura LIF, Dias AMA, Carvalho E, Sousa HCd. Recent advances on the development of wound dressings for diabetic foot ulcer treatment-a review. Acta Biomater. 2013; 9: 7093–7114.
4. Schreml S, Szeimies R-M, Prantl L, Landthaler M, Babilas P. Wound healing in the 21st century. J. Am. Acad. Dermatol. 2010; 63: 866–881.
5. Fife CE, Carter MJ. Wound care outcomes and associated cost among patients treated in US outpatient wound centers: Data from the US wound registry. Wounds 2012; 24: 10–17.
6. Sharpe JR, Booth S, Jubin K, Jordan NR, Lawrence-Watt DJ, Dheansa BS. Progression of wound pH during the course of healing in burns. J. Burn Care Res. 2013; 34: e201-e208.
7. Schneider LA, Korber A, Grabbe S, Dissemond J. Influence of pH on wound-healing: A new perspective for wound-therapy? Arch. Dermatol. Res. 2007; 298: 413–420.
8. Nagoba BS, Suryawanshi NM, Wadher B, Selkar S. Acidic environment and wound healing: A review. Wounds 2015; 27: 5–11.
9. Percival SL, McCarty S, Hunt JA, Woods EJ. The effects of pH on wound healing, biofilms, and antimicrobial efficacy. Wound Repair Regen. 2014; 22: 174–186.
10. Strohal R, Gerber V, Kröger K, Kurz P, Läuchli S, Protz K, Uttenweiler S, Dissemond J. Expert consensus to practical aspects of wound therapy with hemoglobin spray. Wund Management 2016; 10: 276–284.
11. Schreml S, Meier RJ, Kirschbaum M, Kong SC, Gehmert S, Felthaus O, Küchler S, Sharpe JR, Wöltje K, Weiß KT, Albert M, Seidl U, Schröder J, Morsczeck C, Prantl L, Duschl C, Pedersen SF, Gosau M, Berneburg M, Wolfbeis OS, Landthaler M, Babilas P. Luminescent dual sensors reveal extracellular pH-gradients and hypoxia on chronic wounds that disrupt epidermal repair. Theranostics 2014; 4: 721–735.
12. Bernards MT, Jiang S. pH-induced conformation changes of adsorbed vitronectin maximize its bovine aortic endothelial cell binding ability. J. Biomed. Mater. Res. A 2008; 87: 505–514.

13. Sullivan MM, Puolakkainen PA, Barker TH, Funk SE, Sage EH. Altered tissue repair in hevin-null mice: Inhibition of fibroblast migration by a matricellular SPARC homolog. Wound Repair Regen. 2008; 16: 310–319.
14. Gioia M, Fasciglione GF, Monaco S, Iundusi R, Sbardella D, Marini S, Tarantino U, Coletta M. pH dependence of the enzymatic processing of collagen I by MMP-1 (fibroblast collagenase), MMP-2 (gelatinase A), and MMP-14 ectodomain. J. Biol. Inorg. Chem. 2010; 15: 1219–1232.
15. Boateng J, Catanzano O. Advanced therapeutic dressings for effective wound healing--A review. J. Pharm. Sci. 2015; 104: 3653–3680.
16. Matai I, Gopinath P. Chemically crosslinked hybrid nanogels of alginate and PAMAM dendrimers as efficient anticancer drug delivery vehicles. ACS Biomater. Sci. Eng. 2016; 2: 213–223.
17. Lee JY, Chung J, Chung W-J, Kim G. Fabrication and in vitro biocompatibilities of fibrous biocomposites consisting of PCL and M13 bacteriophage-conjugated alginate for bone tissue engineering. J. Mater. Chem. B Mater. Biol. Med. 2016; 4: 656–665.
18. Jin SG, Kim KS, Kim DW, Kim DS, Seo YG, Go TG, Youn YS, Kim JO, Yong CS, Choi H-G. Development of a novel sodium fusidate-loaded triple polymer hydrogel wound dressing: Mechanical properties and effects on wound repair. Int. J. Pharm. 2016; 497: 114–122.
19. Li Y, Fukushima K, Coady DJ, Engler AC, Liu S, Huang Y, Cho JS, Guo Y, Miller LS, Tan JPK, Ee PLR, Fan W, Yang YY, Hedrick JL. Broad-spectrum antimicrobial and biofilm-disrupting hydrogels: Stereocomplex-driven supramolecular assemblies. Angew. Chem. Int. Ed. 2013; 52: 674–678.
20. Dong Y, Hassan WU, Kennedy R, Greiser U, Pandit A, Garcia Y, Wang W. Performance of an in situ formed bioactive hydrogel dressing from a PEG-based hyperbranched multifunctional copolymer. Acta Biomater. 2014; 10: 2076–2085.
21. Cantu DA, Kao WJ. Combinatorial biomatrix/cell-based therapies for restoration of host tissue architecture and function. Adv. Healthcare Mater. 2013; 2: 1544–1563.
22. Gong JP, Katsuyama Y, Kurokawa T, Osada Y. Double-network hydrogels with extremely high mechanical strength. Adv. Mater. 2003; 15: 1155–1158.
23. Matricardi P, Di Meo C, Coviello T, Hennink WE, Alhaique F. Interpenetrating polymer networks polysaccharide hydrogels for drug delivery and tissue engineering. Adv. Drug Deliver. Rev. 2013; 65: 1172–1187.

24. Cao Z, Yang Q, Fan C, Liu L, Liao L. Biocompatible, ionic-strength-sensitive, double-network hydrogel based on chitosan and an oligo(trimethylene carbonate)-poly(ethylene glycol)-oligo(trimethylene carbonate) triblock copolymer. J. Appl. Polym. Sci. 2015; 132: 42459.
25. E96/E96M-12, Standard test methods for water vapor transmission of materials. West Conshohocken, PA, USA: ASTM International; 2012.
26. 10993-5:2009, Biological evaluation of medical devices - Part 5: Tests for in vitro cytotoxicity. Geneva, Switzerland: International Organization for Standardization; 2009.
27. 10993-12:2009, Biological evaluation of medical devices - Part 12: Sample preparation and reference materials. Geneva, Switzerland: International Organization for Standardization; 2009.
28. Küchler S, Henkes D, Eckl K-M, Ackermann K, Plendl J, Korting H-C, Hennies H-C, Schäfer-Korting M. Hallmarks of atopic skin mimicked in vitro by means of a skin disease model based on FLG knock-down. ATLA-Altern. Lab. Anim. 2011; 39: 471–480.
29. Eckl K-M, Alef T, Torres S, Hennies HC. Full-thickness human skin models for congenital ichthyosis and related keratinization disorders. J. Invest. Dermatol. 2011; 131: 1938–1942.
30. Wallmeyer L, Lehnen D, Eger N, Sochorova M, Opalka L, Kovacik A, Vavrova K, Hedtrich S. Stimulation of PPARalpha normalizes the skin lipid ratio and improves the skin barrier of normal and filaggrin deficient reconstructed skin. J. Dermatol. Sci. 2015; 80: 102–110.
31. Andriamanantoanina H, Rinaudo M. Relationship between the molecular structure of alginates and their gelation in acidic conditions. Polym. Int. 2010; 59: 1531–1541.
32. Waters DJ, Engberg K, Parke-Houben R, Ta CN, Jackson AJ, Toney MF, Frank CW. Structure and mechanism of strength enhancement in interpenetrating polymer network hydrogels. Macromolecules 2011; 44: 5776–5787.
33. Myung D, Waters D, Wiseman M, Duhamel P-E, Noolandi J, Ta CN, Frank CW. Progress in the development of interpenetrating polymer network hydrogels. Polym. Adv. Technol. 2008; 19: 647–657.
34. Ibanez JG, Hernandez-Esparza M, Doria-Serrano C, Fregoso-Infante A, Singh MM. Environmental Chemistry: Fundamentals. New York, NY, USA: Springer Science & Business Media; 2010.

35. Kerkhof NJ, Vanderlaan RK, White JL, Hem SL. pH-stat titration of aluminum hydroxide gel. J. Pharm. Sci. 1977; 66: 1528–1533.
36. Manca ML, Castangia I, Zaru M, Nácher A, Valenti D, Fernàndez-Busquets X, Fadda AM, Manconi M. Development of curcumin loaded sodium hyaluronate immobilized vesicles (hyalurosomes) and their potential on skin inflammation and wound restoring. Biomaterials 2015; 71: 100–109.
37. Wild T, Auböck J, editors. Manual der Wundheilung: Chirurgisch-dermatologischer Leitfaden der modernen Wundbehandlung. Wien: Springer-Verlag; 2007.
38. Bianchi J. The effective management of exudate in chronic wounds. Wounds Int. 2012; 3: 14–16.
39. Cutting KF. Wound exudate: Composition and functions. Brit. J. Community Nurs. 2003; 8: 4–9.
40. Argenta LC, Morykwas MJ. Vacuum-assisted closure: A new method for wound control and treatment: Clinical experience. Ann. Plast. Surg. 1997; 38: 563–576.
41. Ebara M, Kotsuchibashi Y, Narain R, Idota N, Kim Y-J, Hoffman JM, Uto K, Aoyagi T. Smart Biomaterials. Tokyo, Japan: Springer Japan; 2014.
42. Xie Z, Aphale NV, Kadapure TD, Wadajkar AS, Orr S, Gyawali D, Qian G, Nguyen KT, Yang J. Design of antimicrobial peptides conjugated biodegradable citric acid derived hydrogels for wound healing. J. Biomed. Mater. Res. A 2015; 103: 3907–3918.
43. Chen Y, Zhang Y, Wang F, Meng W, Yang X, Li P, Jiang J, Tan H, Zheng Y. Preparation of porous carboxymethyl chitosan grafted poly(acrylic acid) superabsorbent by solvent precipitation and its application as a hemostatic wound dressing. Mater. Sci. Eng. C Mater. Biol. Appl. 2016; 63: 18–29.
44. Mathur AM, Hammonds KF, Klier J, Scranton AB. Equilibrium swelling of poly(methacrylic acid-g-ethylene glycol) hydrogels. J. Control. Release 1998; 54: 177–184.
45. Sahraro M, Yeganeh H, Sorayya M. Guanidine hydrochloride embedded polyurethanes as antimicrobial and absorptive wound dressing membranes with promising cytocompatibility. Mater. Sci. Eng. C Mater. Biol. Appl. 2016; 59: 1025–1037.
46. Wu C-J, Wilker JJ, Schmidt G. Robust and adhesive hydrogels from cross-linked poly(ethylene glycol) and silicate for biomedical use. Macromol. Biosci. 2013; 13: 59–66.

47. Hrynyk M, Martins-Green M, Barron AE, Neufeld RJ. Alginate-PEG sponge architecture and role in the design of insulin release dressings. Biomacromolecules 2012; 13: 1478–1485.
48. Myung D, Koh W, Ko J, Hu Y, Carrasco M, Noolandi J, Ta CN, Frank CW. Biomimetic strain hardening in interpenetrating polymer network hydrogels. Polymer 2007; 48: 5376–5387.
49. Cao B, Tang Q, Li L, Humble J, Wu H, Liu L, Cheng G. Switchable antimicrobial and antifouling hydrogels with enhanced mechanical properties. Adv. Healthcare Mater. 2013; 2: 1096–1102.
50. Haque MA, Kurokawa T, Gong JP. Lamellar–micelle transition in a hydrogel induced by polyethylene glycol grafting. Soft Matter 2013; 9: 5223–5230.
51. Hansen B, Jemec GBE. The mechanical properties of skin in osteogenesis imperfecta. Arch. Dermatol. 2002; 138: 909–911.
52. Silver FH, Christiansen DL. Biomaterials Science and Biocompatability. New York, NY, USA: Springer; 1999.
53. Chang C-W, van Spreeuwel A, Zhang C, Varghese S. PEG/clay nanocomposite hydrogel: A mechanically robust tissue engineering scaffold. Soft Matter 2010; 6: 5157–5164.
54. Ajji Z, Othman I, Rosiak JM. Production of hydrogel wound dressings using gamma radiation. Nucl. Instrum. Meth. B 2005; 229: 375–380.
55. Hou Y, Schoener CA, Regan KR, Munoz-Pinto D, Hahn MS, Grunlan MA. Photo-cross-linked PDMSstar-PEG hydrogels: Synthesis, characterization, and potential application for tissue engineering scaffolds. Biomacromolecules 2010; 11: 648–656.
56. Yu F, Cao X, Li Y, Zeng L, Zhu J, Wang G, Chen X. Diels–Alder crosslinked HA/PEG hydrogels with high elasticity and fatigue resistance for cell encapsulation and articular cartilage tissue repair. Polym. Chem. 2014; 5: 5116–5123.
57. Mohamad N, Mohd Amin, Mohd Cairul Iqbal, Pandey M, Ahmad N, Rajab NF. Bacterial cellulose/acrylic acid hydrogel synthesized via electron beam irradiation: Accelerated burn wound healing in an animal model. Carbohydr. Polym. 2014; 114: 312–320.
58. Pereira R, Carvalho A, Vaz DC, Gil MH, Mendes A, Bártolo P. Development of novel alginate based hydrogel films for wound healing applications. Int. J. Biol. Macromol. 2013; 52: 221–230.

59. Ono S, Imai R, Ida Y, Shibata D, Komiya T, Matsumura H. Increased wound pH as an indicator of local wound infection in second degree burns. Burns 2015; 41: 820–824.
60. Sharpe JR, Harris KL, Jubin K, Bainbridge NJ, Jordan NR. The effect of pH in modulating skin cell behaviour. Br. J. Dermatol. 2009; 161: 671–673.
61. Wiegand C, Heinze T, Hipler U-C. Comparative in vitro study on cytotoxicity, antimicrobial activity, and binding capacity for pathophysiological factors in chronic wounds of alginate and silver-containing alginate. Wound Repair Regen. 2009; 17: 511–521.
62. Lee W-R, Park J-H, Kim K-H, Kim S-J, Park D-H, Chae M-H, Suh S-H, Jeong S-W, Park K-K. The biological effects of topical alginate treatment in an animal model of skin wound healing. Wound Rep. Regen. 2009; 17: 505–510.
63. Groeber F, Holeiter M, Hampel M, Hinderer S, Schenke-Layland K. Skin tissue engineering - In vivo and in vitro applications. Adv. Drug Deliver. Rev. 2011; 63: 352–366.
64. Hayden PJ, Bachelor M, Ayehunie S, Letasiova S, Kaluzhny Y, Klausner M, Kandárová H. Application of MatTek in vitro reconstructed human skin models for safety, efficacy screening, and basic preclinical research. Appl. In Vitro Toxicol. 2015; 1: 226–233.
65. Xie Y, Rizzi SC, Dawson R, Lynam E, Richards S, Leavesley DI, Upton Z. Development of a three-dimensional human skin equivalent wound model for investigating novel wound healing therapies. Tissue Eng. Part C 2010; 16: 1111–1123.
66. Nunan R, Harding KG, Martin P. Clinical challenges of chronic wounds: Searching for an optimal animal model to recapitulate their complexity. Dis. Model. Mech. 2014; 7: 1205–1213.
67. Elbert DL, Hubbell JA. Conjugate addition reactions combined with free-radical cross-linking for the design of materials for tissue engineering. Biomacromolecules 2001; 2: 430–441.

Chapter 4

Systematic Structural Modification of the Interpenetrating Polymer Network System Poly(ethylene glycol)/Acrylic Acid/ Alginate

Abstract

Interpenetrating polymer network (IPN) hydrogels are appropriate candidates for wound dressing applications, as the optimization of their material properties focuses directly on their wound healing capacity. In particular, the mechanical properties and the swelling capacity of IPN hydrogels can be adapted by structural changes in the dual network architecture, thereby influencing the humidity of the wound milieu and the wearing comfort. In this study, the IPN hydrogel formulation poly(ethylene glycol) diacrylate (PEGDA)/acrylic acid (AA)/alginate was examined. The conducted systematic network modification focused on the impact of the PEGDA molecular weight and variations in the initiator system and the cross-linking reaction. PEGDAs with lower molecular weight and additional ionic cross-linking of alginate appeared as promising approaches. The recently postulated high importance of ionized AA carboxylic acid groups for the outstanding PEGDA/AA/alginate hydrogel properties was proven by comparatively analyzing neutral poly(ethylene glycol) diacrylate/2-hydroxyethyl methacrylate (HEMA)/alginate IPN hydrogels; the uncharged HEMA containing gels showed a significantly reduced swelling capacity and mechanical stability.

1. Introduction

In general, hydrogels can be polymerized by two different types of cross-linking reaction. Physical cross-linking by molecular entanglements, ionic interactions, or hydrogen bonds, and chemical cross-linking by covalent bonds (initiated for example by UV-light, click-reactions, or redox systems) can be used to form polymer networks.[1,2] In classical interpenetrating polymer network (IPN) hydrogels, a rigid and densely cross-linked primary network and a flexible and loosely cross-linked secondary network are combined. This special polymer structure results in a superior new hydrogel material in comparison to the single component hydrogels, especially concerning their mechanical performance.[3,4] In this study, a chemically cross-linked network of poly(ethylene glycol) diacrylate (PEGDA) and acrylic acid (AA) and a physically cross-linked network of alginate were combined. Recently, these pH-modulating IPN hydrogels were reported to be promising candidates for wound dressing applications.[5] Amongst others, high liquid uptake, mechanical stability, and convincing in vitro wound healing properties were found for a formulation carrying 9.25% PEGDA with a molecular weight of 6 kDa (PEGDA6k), 0.25% AA, and 0.5% alginate.

Nevertheless, further optimization of the established system should be aspired. Numerous formulation parameters are known to have a significant impact on the IPN hydrogel properties. Amongst others, the molecular weight of the precursors, their concentration, the mass ratio of the primary to the secondary network, and the network cross-linking densities can affect the material performance.[3,6–11] A systematic adjustment of the listed parameters enables the identification of the most favorable IPN formulation in regard to its mechanical stability, flexibility, and liquid handling properties. Besides, all listed material characteristics have a direct or indirect impact on wound healing.[12] Sufficient liquid uptake prevents tissue degeneration caused by excessive exudate, whereas an appropriate mechanical stability of the dressing material is required during its application and wearing. Consequently, the effects of specific structural modifications concerning the interpenetrating polymer networks of PEGDA/AA/alginate hydrogels were examined in more detail. Optimizations concerning the cross-linking density of the two networks were conducted by 1) changing the time scale of the PEGDA/AA polymerization reaction, 2) using PEGDAs with different molecular weight, and 3) analyzing the impact of divalent calcium ions as gelling reactant. To gain further insights into the driving forces of the PEGDA/AA/alginate IPN hydrogel properties, the decisive interactions between the

individual network components were examined. For this purpose, AA was replaced by the carboxylic acid group free monomer 2-hydroxyethyl methacrylate (HEMA) and the properties of the resulting neutral IPNs were analyzed.

2. Experimental Section

2.1 Materials

Toluene was purchased from Acros Organics (Geel, Belgium). Deuterated chloroform ($CDCl_3$) was obtained from Deutero GmbH (Kastellaun, Germany). Alginate (Protanal® LF 10/60FT) was kindly provided by FMC BioPolymer (Wallingstown, Ireland). Phosphate buffered saline (PBS) was purchased from Life Technologies (Carlsbad, CA, USA). Hydrochloric acid, sodium hydroxide, and triethylamine were obtained from Merck KGaA (Darmstadt, Germany). Poly(ethylene glycol) with a molecular weight of 4 kDa (PEG4k) was purchased from Riedel-de Haën (Seelze, Germany). Deionized water was obtained using a Milli-Q water purification system (Millipore, Schwabach, Germany). All other chemicals were purchased from Sigma Aldrich (Taufkirchen, Germany). Poly(ethylene glycol) was dried by azeotropic distillation in toluene; all other chemicals were used as received.

2.2 Precursor Synthesis

PEGDA6k was synthesized as previously reported.[5] PEGDA4k was synthesized analogously, however, the ratio of PEG4k (25.01 g, 6.25 mmol) to triethylamine (1742 μL, 12.50 mmol) and acryloyl chloride (2031 μL, 25.00 mmol) was adapted. The reaction yielded 15.82 g PEGDA4k (61.6%).

^{1}H NMR PEGDA4k (300 MHz, $CDCl_3$, δ): 3.63 ppm (m, 197 H, -CH_2CH_2O-), 4.30 ppm (t, 2 H, -CH_2OC(O)-), 5.82 ppm (dd, 1 H, CH_2=CHC(O)O-), 6.14 ppm (dd, 1 H, CH_2=C*H*C(O)O-), 6.41 ppm (dd, 1 H, CH_2=CHC(O)O-).

^{1}H NMR PEGDA6k (300 MHz, $CDCl_3$, δ): 3.62 ppm (m, 310 H, -CH_2CH_2O-), 4.30 ppm (t, 2 H, -CH_2OC(O)-), 5.82 ppm (dd, 1 H, CH_2=CHC(O)O-), 6.13 ppm (dd, 1 H, CH_2=C*H*C(O)O-), 6.41 ppm (dd, 1 H, CH_2=CHC(O)O-).

2.3 Preparation of Hydrogels

Precursor mixtures for UV-polymerized hydrogels were prepared as follows: PEGDA was dissolved in PBS and mixed with a 2-hydroxy-4′-(2-hydroxyethoxy)-2-methylpropio-

phenone (HHMP) suspension in PBS, a solution of alginate in PBS (c = 41.68 mg·mL^{-1}), and the respective amount of AA or HEMA. If required, a solution of gluconolactone (GL) in PBS and a suspension of $CaHPO_4 \cdot 2\ H_2O$ in PBS were pipetted to the stirring mixture. Precursor mixtures for N,N,N',N'-tetramethylethane-1,2-diamine (TEMED)/ammonium persulfate (APS) polymerized hydrogels were produced in the same way, except that the HHMP suspension was replaced by TEMED and a solution of APS in PBS. The utilized amounts of initiator were 0.180% HHMP, 0.067% gluconolactone, and 0.130% $CaHPO_4 \cdot 2\ H_2O$. The respective mass of TEMED, *m(TEMED)*, was calculated according to Equation (1)

$$m(TEMED) = 0.0180\, m(PEGDA) + 0.2635\, m(AA) \qquad (1)$$

where *m(PEGDA)* is the mass of PEGDA and *m(AA)* is the mass of acidic acid in the hydrogel formulation; the amount of APS was two times *m(TEMED)*. The hydrogel water content was 90% in all cases; further information on the exact hydrogel compositions is displayed in Table 1.

Table 1. Composition and cross-linking agents of the examined hydrogels.

PEGDA4k (%)	PEGDA6k (%)	AA (%)	HEMA (%)	Alginate (%)	Cross-linking agents
10.00	0	0	0	0	HHMP
9.50	0	0	0	0.50	$CaHPO_4$/GL, HHMP
8.75	0	1.00	0	0.25	HHMP
8.75	0	1.00	0	0.25	$CaHPO_4$/GL, HHMP
5.00 – 9.25	0	0.25 – 4.50	0	0.50	$CaHPO_4$/GL, HHMP
8.00 – 9.00	0	0	0.50 – 1.50	0.50	$CaHPO_4$/GL, HHMP
0	9.25	0.25	0	0.50	TEMED/APS
0	9.25	0.25	0	0.50	HHMP
0	8.75	1.00	0	0.25	HHMP
0	8.75	1.00	0	0.25	$CaHPO_4$/GL, HHMP
0	8.50 – 9.00	0	0.50 – 1.00	0.50	HHMP

For tensile testing, 8 mL of the precursor mixture were cast into rectangular silicon molds; for all other experiments, cylindrical glass molds (1 cm diameter, 0.7 mL volume) were used. The polymerization reaction was either initiated by UV-light (HHMP containing

gels) at 366 nm for 1 h, or thermally by storing the covered molds at room temperature for 24 h (TEMED/APS containing gels).

2.4 Tensile Strength

Rectangular specimens of 1 cm width (d), 8 cm length, and a thickness h (measured with a MiniTest 600 gauge, ElektroPhysik, Köln, Germany) were stretched until failure with a tensile velocity of 15 mm·min^{-1}. The tensile strain (ε_t) and the maximum load (F_{max}) were measured using an Instron 5542 load frame (Instron GmbH, Darmstadt, Germany). The tensile stress (σ_t) was calculated according to Equation (2).

$$\sigma_t = \frac{F_{max}}{h \cdot d} \qquad (2)$$

The elastic modulus of tension (E_t) was calculated from the slope of the stress-strain curve between 0.05 and 0.15 strain.

2.5 Swelling Capacity

Hydrogel cylinders (initial mass m_0) were incubated in 10 mL of PBS at 37 °C in a shaking water bath. The mass of the gels (m_t) was measured every 24 h. The swelling capacity (Q_t) was calculated according to Equation (3).

$$Q_t = \frac{m_t - m_0}{m_0} \cdot 100\% \qquad (3)$$

2.6 Compressive Strength

If required, the hydrogel cylinders were purified in 10 mL of deionized water for 24 h at 37 °C. Afterwards, the purified hydrogels were partially dried by a stream of compressed air to assure a constant water content of 90% throughout all experiments. Unmodified and purified hydrogel cylinders with a height h and a diameter d (measured with a caliper, BORT GmbH, Weinstadt-Benzach, Germany) were compressed at 0.5 mm·min^{-1} using an Instron 5542 load frame. The maximum compressive stress (σ_c) and elastic modulus of compression (E_c) were calculated according to Section 2.4.

2.7 Base Neutralizing Capacity

Static pH titration at pH 7.4 was conducted with purified hydrogel cylinders in 15 mL of a 0.1 M sodium chloride solution. A 0.1 M sodium hydroxide solution was added over 24 h using a BlueLine glass electrode (SI Analytics GmbH, Mainz, Germany) connected to a

TitroLine 7000 dosage system (SI Analytics GmbH, Mainz, Germany). The base neutralizing capacity (BNC) was calculated from the amount of substance of neutralized sodium hydroxide n(NaOH) and the initial mass of the gel cylinder m_0, according to Equation (4).

$$BNC = \frac{n(\mathrm{NaOH})}{m_0} \qquad (4)$$

2.8 Statistical Analysis

The data are presented as mean ± standard deviation (SD). The number of samples n was 3 to 6, dependent on the conducted experiment. For statistical analysis, Brown Forsythe tests were run followed by one-way ANOVA/Tukey' test or Kruskal-Wallis-ANOVA. Differences were considered statistically significant at $p < 0.05$.

3. Results

3.1 Modification of the Network Forming Reaction

One possibility to alter the network architecture and therefore the material properties of IPN hydrogels is a modification of the network forming reaction. Decelerated polymerization by the redox system TEMED/APS was examined as an alternative to the instantly occurring polymerization induced by HHMP (Table 2).[13]

Table 2. Maximum tensile stress σ_t, strain ε_t, and E-modulus E_t of PEGDA6k/0.25% AA/alginate IPN hydrogels, polymerized with different initiators. Data are expressed as mean ± SD (n = 6).

Initiator	σ_t (kPa)	E_t (kPa)	ε_t (%)
TEMED/APS	48.78 ± 9.17	98.31 ± 18.28	60.89 ± 22.10
HHMP	88.21 ± 12.85	89.11 ± 18.76	161.37 ± 22.32

Yet, TEMED/APS polymerized hydrogels were less stable (lower tensile stress σ_t) and less elastic (higher E-modulus E_t and lower elasticity ε_t) than HHMP polymerized gels. Therefore, further research was exclusively conducted with HHMP polymerized hydrogels. Moreover, the effect of additional ionic cross-linking with divalent calcium ions was examined under tensile load. Besides testing the recently described PEGDA6k IPN hydrogels,[5] analogous IPN hydrogels containing PEGDA4k were assessed. The acidic PEGDA4k IPN gels showed higher σ_t values with additional Ca^{2+} gelation, whereas the acidic PEGDA6k IPN gels were significantly more stable without Ca^{2+} incorporation

(Figure 1). The E-modulus was slightly higher for Ca^{2+} containing gels in both cases. Consequently, only PEGDA4k containing IPNs should thenceforth be polymerized in the presence of calcium ions.

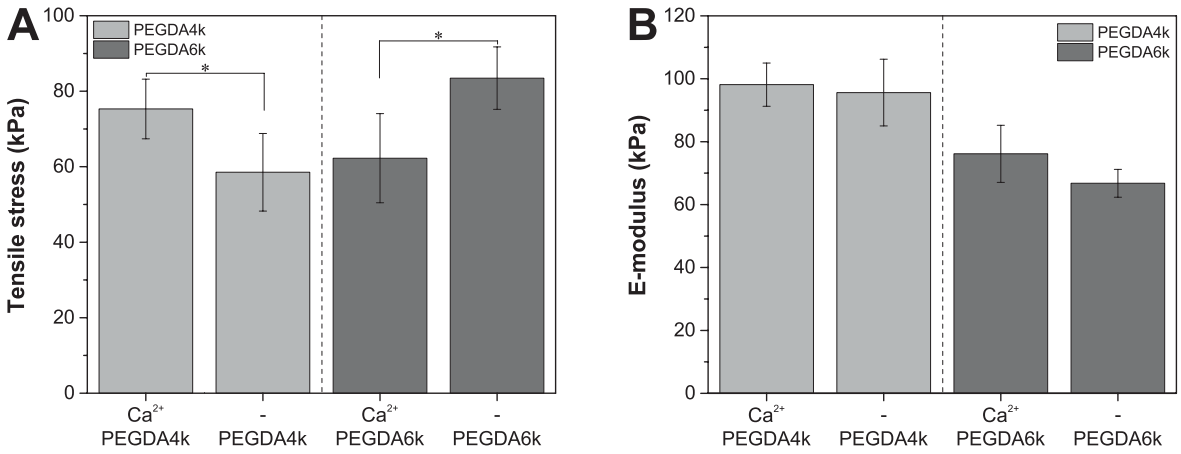

Figure 1. Tensile stress at maximum load (A) and correlated E-modulus (B) of PEGDA/1.00% AA/alginate hydrogels with and without Ca^{2+} polymerization. Data are expressed as mean ± SD (n = 5); * indicates statistically significant differences between the selected groups ($p < 0.05$).

Regarding the mechanical properties, PEGDA4k containing IPN hydrogels are equivalent to the already described PEGDA6k containing gels (see Chapter 3 for comparison). Therefore, further research focused on the impact of the PEGDA molecular weight with regard to the requirements for a potential wound dressing application.

3.2 Modification of the PEGDA Molecular Weight

The covalent hydrogel network of the IPN system PEGDA/AA/alginate was modified by using PEGDA with a molecular weight of 4 instead of 6 kDa. A comprehensive analysis concerning mechanical and fluid handling properties was run to gain comparable data for an evaluation in contrast to the recently described PEGDA6k/AA/alginate IPN hydrogels.[5] Regarding the swelling capacity of PEGDA4k/AA/alginate IPN hydrogels, the liquid uptake was strongly dependent on the amount of incorporated acrylic acid (Figure 2). Increasing AA concentrations enabled enhanced swelling, up to 328 ± 62% after one day and up to 594 ± 43% after 7 days of incubation. In contrast, pure PEGDA4k (1%) and PEGDA4k/alginate (18%) hydrogels had a rather low swelling capacity.

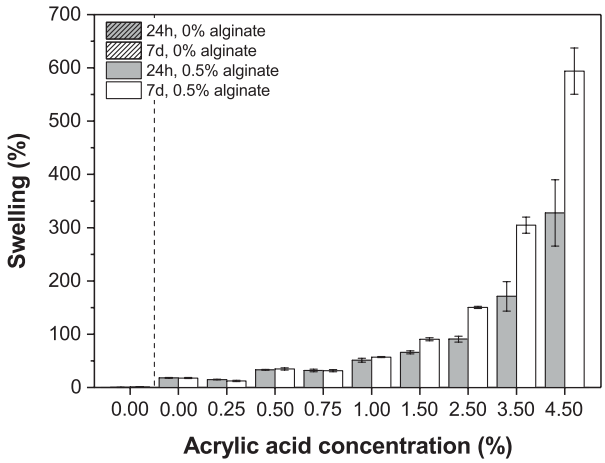

Figure 2. Swelling capacity of PEGDA4k/AA/alginate hydrogels with different AA concentrations after 24 hours and 7 days of incubation. Data are expressed as mean ± SD (n = 3).

The mechanical behavior of PEGDA4k/AA/alginate hydrogels with altering AA content was completely different, comparing the effects of tensile and compressive load. The tensile stress at maximum load, σ_t, remains consistent for all samples (around 75 kPa), except for the most stable formulation carrying 0.5% AA (Figure 3A). On the other hand, the compressive stress, σ_c, significantly increased with the addition of alginate (Figure 3C). The σ_c values of acidic IPN hydrogels were dependent on the amount of AA, which generally had a weakening effect. The calculated E-modulus was related to the AA concentration in all cases. Under tensile load, the E_t(PEGDA4k/AA/alginate) values were lower than E_t(PEGDA4k), except for 4.5% AA containing hydrogels (Figure 3B). Under compressive load, high AA concentrations caused a reduction of the E-modulus (Figure 3D).

In this context, special consideration should also be given to the potential impact of initial hydrogel purification, which is required for biomedical applications. By incubation in water, remaining initiator and precursor molecules can be removed, which further assures the biocompatibility of the developed material. Yet, purification did not have any impact on the mechanical performance of the examined hydrogels (Figure 3C and D).

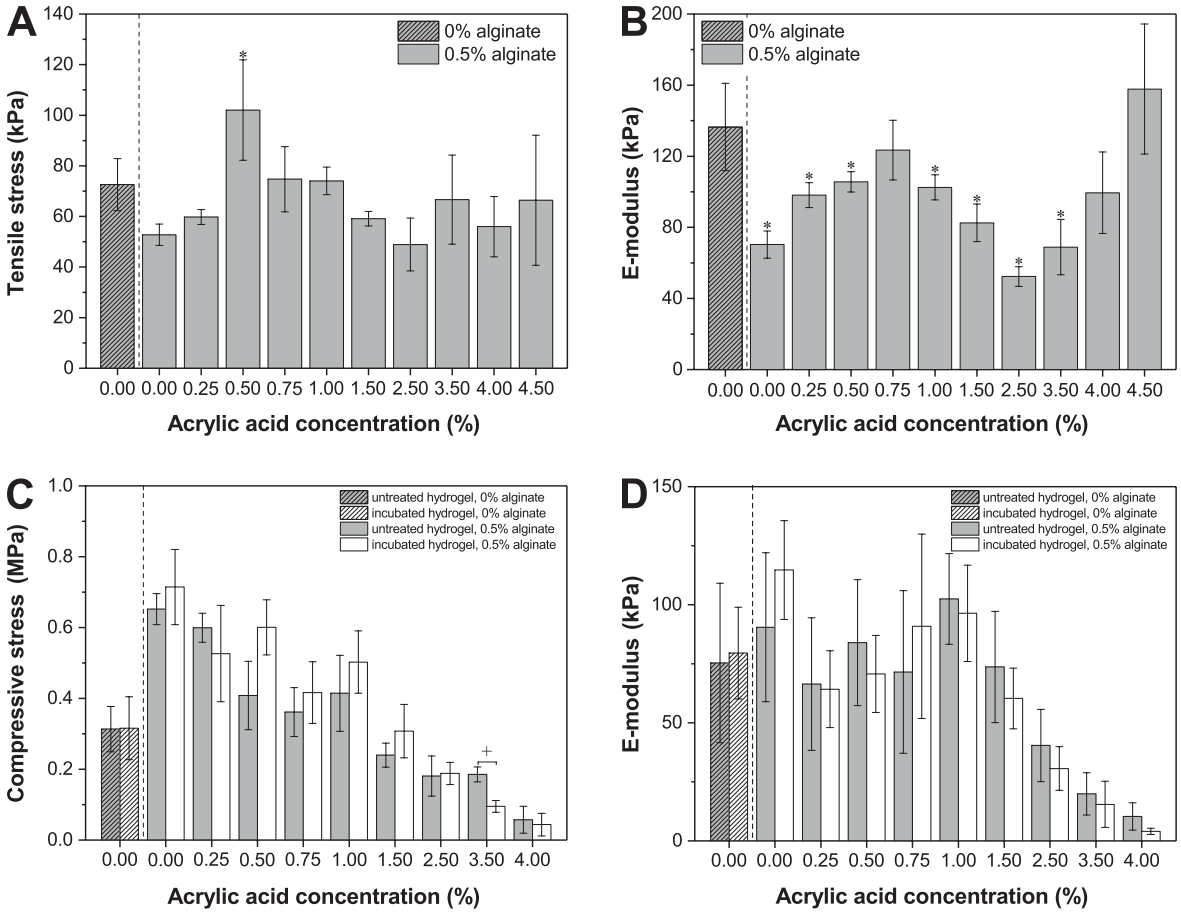

Figure 3. Tensile stress at maximum load (A) and correlated E-modulus (B), compressive stress at maximum load (C) and correlated E-modulus (D) of PEGDA4k/AA/alginate hydrogels with different AA concentrations. Samples were tested as prepared, and after purification in water (C, D: "incubated hydrogels"). Data are expressed as mean ± SD (n = 4); * indicates statistically significant differences versus the control PEGDA ($p < 0.05$); + indicates statistically significant differences between the groups ($p < 0.05$).

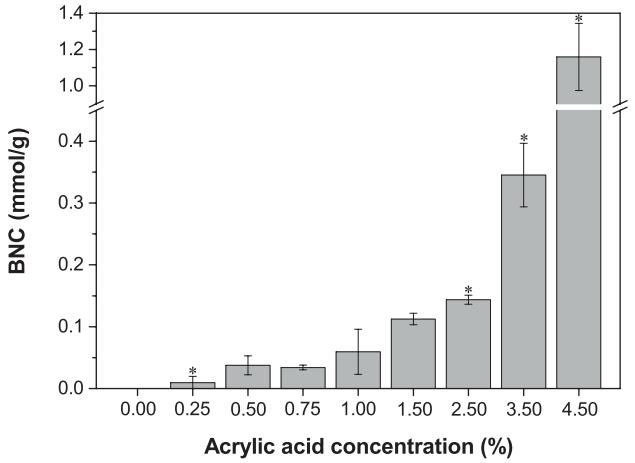

Figure 4. Base neutralizing capacity of PEGDA4k/AA/alginate hydrogels with different AA concentrations. Data are expressed as mean ± SD (n = 3); * indicates statistically significant differences versus the lower concentrated samples ($p < 0.05$).

The base neutralizing capacity of AA containing PEGDA4k IPN hydrogels, a parameter that characterizes their buffer capacity in an alkaline environment, ranged between 0.009 and 1.159 mmol per gram of hydrogel (Figure 4). Rising AA concentrations resulted in rising BNCs; PEGDA/alginate hydrogels had no impact on the environmental pH.

3.3 Modification of the Charge Density

Finally, the hydrogel charge density was altered by replacing AA with HEMA. HEMA is structurally comparable to AA, yet it does not carry an ionizable functional group (Scheme 1). Thus, the investigation of the resulting PEGDA/HEMA/alginate IPN hydrogels allowed drawing conclusions about the role of incorporated charges in the respective AA containing hydrogels.

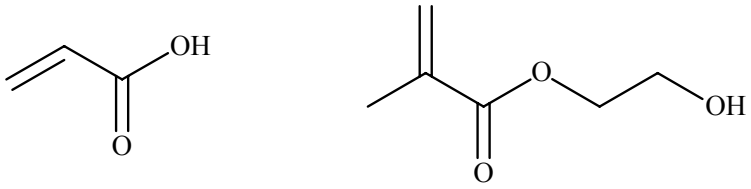

Scheme 1. Chemical structure of AA (on the left) and HEMA (on the right).

In swelling experiments, HEMA containing IPN hydrogels showed a significantly lower liquid uptake than the respective AA containing hydrogels, regardless of the AA/HEMA content (Figure 5). Increasing amounts of HEMA only had a little effect on the amount of hydrogel swelling.

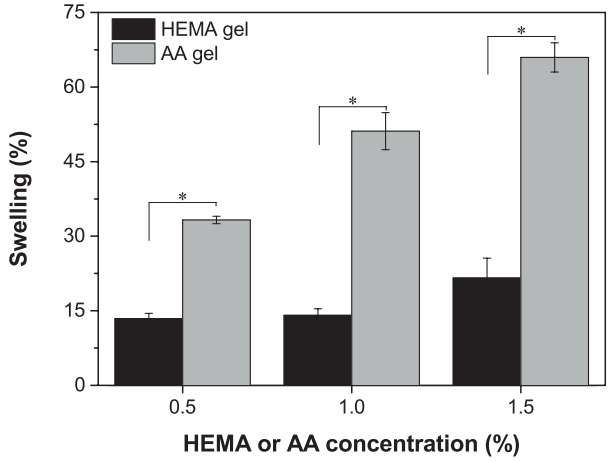

Figure 5. Swelling capacity of PEGDA4k/alginate hydrogels with different HEMA or AA concentrations. Data are expressed as mean ± SD (n = 3). * indicates statistically significant differences between the groups ($p < 0.05$).

The impact of ionizable carboxylic acid groups on the mechanical performance of the developed IPN hydrogels was examined for both, PEGDA4k and PEGDA6k formulations (Figure 6).

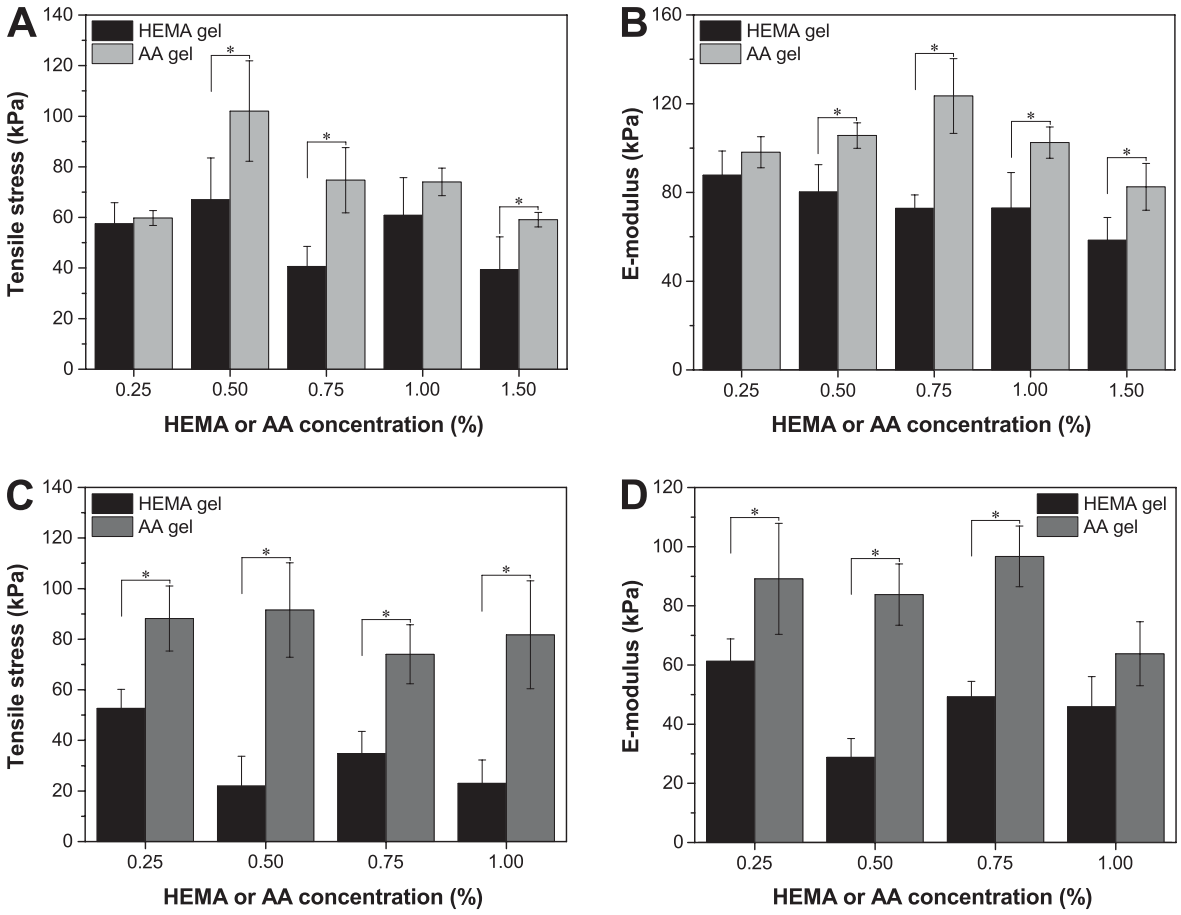

Figure 6. Tensile stress at maximum load (A, C) and correlated E-modulus (B, D) of PEGDA/alginate hydrogels with different HEMA or AA concentrations. PEGDA with a molecular weight of 4 kDA (A, B) and 6 kDa (C, D) was used. Data are expressed as mean ± SD (n = 4); * indicates statistically significant differences between the respective HEMA and AA containing hydrogels ($p < 0.05$).

The conducted experiments demonstrated that the stabilizing effect of AA incorporation was more pronounced in PEGDA6k IPNs (Figure 6C). PEGDA6k/HEMA/alginate gels could maximally bear 22 to 53 kPa under tensile load, in contrast to PEGDA6k/AA/ alginate gels with σ_t = 82 – 92 kPa. Regarding PEGDA4k IPNs, the stabilizing effect was dependent on the amount of substituted PEGDA (Figure 6A). Only little impact on the mechanical stability could be detected for hydrogels with 0.25 and 1.0% HEMA/AA content. The E-modulus showed similar tendencies to the described σ_t performance, independent from the PEGDA molecular weight (Figure 6B and D).

4. Discussion

Different structural modifications of the recently described IPN hydrogel formulation PEGDA/AA/alginate were conducted to obtain a further improved wound dressing material.[5] First, the alternative initiator system TEMED/APS was examined. TEMED/APS is known to give an overall slower reaction in comparison to the HHMP/UV-light induced polymerization, which leads to more entangled polymer chains.[13–15] Yet, the spatial approach of the reactive sites might consequently be impeded, resulting in less cross-linked and therefore, less stable hydrogel materials (Table 1). In a second approach, additional ionic cross-linking by calcium ions was evaluated. The different outcomes for Ca^{2+} containing PEGDA4k and PEGDA6k IPN hydrogels in tensile tests might likewise be related to the primary network mesh size.[6,7] Generally, a bigger average mesh size in UV-polymerized hydrogels is assumed to facilitate an entanglement of the IPNs (PEGDA6k > PEGDA4k; see Chapter 2 for comparison). Calcium ion addition generates Ca^{2+}/alginate/AA complexes,[5,16] which in contrast might impede this entanglement. Additionally, a reduced fluidity of the secondary network was described to reduce the mechanical stability of IPN materials.[3] Assuming that PEGDA4k/AA/alginate IPNs have less entangled networks, load transfer between the two networks and internal slipping would play a less important role. Therefore, additional Ca^{2+} induced cross-links should enhance the mechanical stability of PEGDA4k containing gels, whereas it should have a weakening effect on PEGDA6k containing gels (see Figure 1 for comparison).

A reduced PEGDA molecular weight, combined with an increased number of chemical cross-links (the applied PEGDA mass ratio stayed unchanged), was systematically examined concerning all relevant material properties of wound dressings. The impact of different acrylic acid concentrations on PEGDA6k/AA/alginate IPN hydrogels was discussed lately.[5] The here examined PEGDA4k IPNs exhibited comparable tendencies concerning the swelling capacity, the compressive properties, and the BNC. In brief, increasing repulsive forces between a rising amount of negatively charged carboxylic acid groups in the hydrogel network favor hydrogel swelling.[17] Furthermore, rising repulsive forces during compression encourage material failure, and the amount of carboxylic acid groups is proportional to the number of released protons (BNC). Surprisingly, no stabilizing effect due to the formation of a double network hydrogel (PEGDA4k/alginate) was visible under tensile load (Figure 3A). However, this further confirms the above considered reduced ability of PEGDA4k containing IPNs to form network entanglements. The significantly increased maximum tensile stress of PEGDA4k/0.5% AA/alginate IPN hydrogels might be explained by a combination of opposing effects concerning the

hydrogel structure. With rising AA concentrations, the primary network structure is more suitable for entanglements and the increasing amount of (protonated) carboxylic acid groups (of alginate and AA) enables additional inter- and intra-network bonds.[8,18] In contrast, mechanical weakening is induced by the lowered three-dimensional linkage in PEGDA/AA/alginate in comparison to PEGDA/alginate gels.[19,20] The ratio of all structural effects seems to be optimal in the case of 0.5% AA containing IPN hydrogels.[9] Correlating findings were published by Myung et al., who described a low fracture stress for PEGDA/poly(acrylic acid) IPNs with small and high AA ratios, and the highest maximum tensile stress for an intermediate AA concentration.[8] The loss of cross-links in the primary network is also responsible for the enhanced flexibility (ε(PEGDA4k) = 72.1%, ε(PEGDA4k/AA/alginate) around 104.2%, data not shown), resulting in reduced values of the calculated E-modulus.

Even though the consequences of altered AA concentrations in PEGDA4k and PEGDA6k IPN hydrogels were the same (see Chapter 3 for comparison), the absolute values differed among each other. The overall predominant factor in this context is the difference in molecular weight between cross-links, which is connected to numerous material properties.[7,21,22] Hence, PEGDA4k IPN hydrogels with a low AA content showed lower swelling capacities than the respective PEGDA6k IPNs. With rising AA content, this effect is balanced out or even reversed by the increasing amount of polymer chains (AA), substituting the three-dimensionally cross-linked PEGDA network. Concerning the compressive properties, the applied load can be transferred more easily to the surrounding network in flexible IPNs (PEGDA6k), whereas material failure occurs more probably in rigid and less entangled networks (PEGDA4k).[6] The findings on the tensile stability of differently composed PEGDA4k/AA/alginate IPNs emphasize the above discussed ability of Ca^{2+} ions to overcome weakening effects, induced by the change in PEGDA molecular weight. In contrast, no clear tendency could be identified for the base neutralizing capacity of PEGDA4k and PEGDA6k IPNs. Comparable BNC vales were expected, as the "release" of protons should not be affected by a change in mesh size.

The importance of carboxylic acid groups for the IPN hydrogel properties was finally proven by comparing PEGDA/HEMA/alginate to PEGDA/AA/alginate IPN hydrogels. The effect of polymer chain (HEMA, AA) instead of polymer network (PEGDA) formation stayed unaffected, allowing conclusions about the chemical structure induced effects only. Due to the loss of incorporated negative charges, the swelling ability of the HEMA containing hydrogels decreased drastically, underlining that repulsion between

carboxylic acid groups plays the major role in the liquid uptake process. Analyzing the outcomes of tensile tests with PEGDA4k and 6k/HEMA/alginate IPN hydrogels verified that negative charges/additional hydrogen bonding sites are responsible for the superior mechanical properties.[5] Again, the stabilizing impact on PEGDA6k IPNs was stronger than on PEGDA4k IPNs. Effects of a reduced number of cross-links, associated with rising HEMA concentrations, are mainly pronounced in PEGDA6k hydrogels (Figure 6C). Both results are probably connected to a change in the polymer mesh sizes, as already discussed above.

Despite the detected differences in the PEGDA4k and PEGDA6k IPN's performance concerning mechanical and liquid handling properties, the developed PEGDA4k/AA/ alginate hydrogels can likewise be regarded as potential wound dressing materials. Therefore, future experiments should focus on the biological evaluation of the altered IPN structure.

5. Conclusion

Taking all findings concerning structurally modified PEGDA/AA/alginate IPN hydrogels into account, PEGDA4k-based IPNs are promising candidates for wound dressing applications. Analogous to the recently described PEGDA6k/AA/alginate hydrogels,[5] they fulfill important wound dressing requirements such as mechanical stability and sufficient liquid uptake. Yet, no advantageous material properties have been detected in contrast to the PEGDA6k-based IPN hydrogels (see Chapter 3 for comparison). Nevertheless, further research should assess the wound healing capacity of the here described PEGDA4k/AA/ Ca^{2+} alginate IPNs, as a release of Ca^{2+} ions can potentially enhance cell migration and proliferation, leading to improved wound healing.[23] Further changes of the IPN hydrogel structure did not have any positive impact on the material properties. However, additional information on the polymer network interactions in the IPN hydrogels could be revealed. Based on HEMA containing IPN gels, the importance of AA carboxylic acid groups for the hydrogel stability and liquid uptake was proven.

References

1. Hoffman AS. Hydrogels for biomedical applications. Adv. Drug Deliver. Rev. 2002; 54: 3–12.
2. Du Ko Y, Shinde UP, Yeon B, Jeong B. Recent progress of in situ formed gels for biomedical applications. Prog. Polym. Sci. 2013; 38: 672–701.
3. Gong JP, Katsuyama Y, Kurokawa T, Osada Y. Double-network hydrogels with extremely high mechanical strength. Adv. Mater. 2003; 15: 1155–1158.
4. Haque MA, Kurokawa T, Gong JP. Super tough double network hydrogels and their application as biomaterials. Polymer 2012; 53: 1805–1822.
5. Koehler J, Wallmeyer L, Hedtrich S, Goepferich AM, Brandl FP. pH-modulating poly(ethylene glycol)/alginate hydrogel dressings for the treatment of chronic wounds. Macromol. Biosci. 2017; 17: 1600369.
6. Rennerfeldt DA, Renth AN, Talata Z, Gehrke SH, Detamore MS. Tuning mechanical performance of poly(ethylene glycol) and agarose interpenetrating network hydrogels for cartilage tissue engineering. Biomaterials 2013; 34: 8241–8257.
7. Temenoff JS, Athanasiou KA, LeBaron RG, Mikos AG. Effect of poly(ethylene glycol) molecular weight on tensile and swelling properties of oligo(poly(ethylene glycol) fumarate) hydrogels for cartilage tissue engineering. J. Biomed. Mater. Res. 2002; 59: 429–437.
8. Myung D, Waters D, Wiseman M, Duhamel P-E, Noolandi J, Ta CN, Frank CW. Progress in the development of interpenetrating polymer network hydrogels. Polym. Adv. Technol. 2008; 19: 647–657.
9. Nakajima T, Furukawa H, Tanaka Y, Kurokawa T, Osada Y, Gong JP. True chemical structure of double network hydrogels. Macromolecules 2009; 42: 2184–2189.
10. Myung D, Koh W, Ko J, Hu Y, Carrasco M, Noolandi J, Ta CN, Frank CW. Biomimetic strain hardening in interpenetrating polymer network hydrogels. Polymer 2007; 48: 5376–5387.
11. Sun J-Y, Zhao X, Illeperuma WRK, Chaudhuri O, Oh KH, Mooney DJ, Vlassak JJ, Suo Z. Highly stretchable and tough hydrogels. Nature 2012; 489: 133–136.
12. Boateng J, Catanzano O. Advanced therapeutic dressings for effective wound healing--A review. J. Pharm. Sci. 2015; 104: 3653–3680.
13. Nair LS. Injectable Hydrogels for Regenerative Engineering. Hackensack, NJ: Imperial College Press; 2016.

14. Tokita M, editor. Gels: Structures, Properties, and Functions: Fundamentals and Applications. Progress in Colloid and Polymer Science 136. Berlin, Heidelberg: Springer-Verlag Berlin Heidelberg; 2009.
15. van Dijk-Wolthuis WN, Franssen O, Talsma H, van Steenbergen MJ, Kettenes-van den Bosch, J. J., Hennink WE. Synthesis, characterization, and polymerization of glycidyl methacrylate derivatized dextran. Macromolecules 1995; 28: 6317–6322.
16. Pawar SN, Edgar KJ. Alginate derivatization: A review of chemistry, properties and applications. Biomaterials 2012; 33: 3279–3305.
17. Ebara M, Kotsuchibashi Y, Narain R, Idota N, Kim Y-J, Hoffman JM, Uto K, Aoyagi T. Smart Biomaterials. Tokyo, Japan: Springer Japan; 2014.
18. Waters DJ, Engberg K, Parke-Houben R, Ta CN, Jackson AJ, Toney MF, Frank CW. Structure and mechanism of strength enhancement in interpenetrating polymer network hydrogels. Macromolecules 2011; 44: 5776–5787.
19. Wu C-J, Wilker JJ, Schmidt G. Robust and adhesive hydrogels from cross-linked poly(ethylene glycol) and silicate for biomedical use. Macromol. Biosci. 2013; 13: 59–66.
20. Hrynyk M, Martins-Green M, Barron AE, Neufeld RJ. Alginate-PEG sponge architecture and role in the design of insulin release dressings. Biomacromolecules 2012; 13: 1478–1485.
21. Peppas NA, Keys KB, Torres-Lugo M, Lowman AM. Poly(ethylene glycol)-containing hydrogels in drug delivery. J. Control. Release 1999; 62: 81–87.
22. Lu S, Anseth KS. Release behavior of high molecular weight solutes from poly(ethylene glycol)-based degradable networks. Macromolecules 2000; 33: 2509–2515.
23. Lansdown ABG. Calcium: A potential central regulator in wound healing in the skin. Wound Rep. Regen. 2002; 10: 271–285.

Chapter 5

Alkaline Poly(ethylene glycol)-Based Hydrogels for a Potential Use as Bioactive Wound Dressings

This chapter was published as: Koehler J, Wallmeyer L, Hedtrich S, Brandl FP, and Goepferich AM. J. Biomed. Mater. Res. Part A 2017; doi: 10.1002/jbm.a.36177; Data which were not obtained or analyzed by J. Koehler are highlighted at the appropriate points.

Abstract

The number of patients with chronic wounds is increasing constantly in today's aging society. However, little work has been done so far tackling the associated disadvantageous shift of the wound pH. In our study, we developed two different approaches on pH-modulating wound dressing materials, namely bioactive interpenetrating polymer network hydrogels based on poly(ethylene glycol) diacrylate/N-vinylimidazole/alginate (named VI_x) and poly(ethylene glycol) diacrylate/2-dimethylaminoethyl methacrylate/ N-carboxyethylchitosan (named $DMAEMA_x$). Both formulations were cytocompatible and showed a good wound healing capacity in vitro. The developed dressing materials significantly increased the cell ingrowth in wounded human skin constructs, by 364% and 313% due to VI_x and $DMAEMA_x$ hydrogel treatment, respectively. Additionally, VI_x hydrogels were found to be suitable scaffolds for superficial cell attachment. Our research on the material properties suggests, that ionic interactions and hydrogen bonds are the driving forces for the mechanical and swelling properties of the examined hydrogels. High amounts of positively charged amino groups in $DMAEMA_x$ hydrogels caused increased liquid uptake (around 190%), whereas VI_x hydrogels showed a tenfold higher maximum compressive stress in comparison to hydrogels without ionizable functional groups.

1. Introduction

Impaired wound healing is a pressing problem in health care.[1] Several underlying diseases, like diabetes mellitus or venous insufficiency, as well as external causes, like large-scale burns, can be a trigger for the retardation or even the lack of wound healing.[2,3] One contributing factor for impaired healing is the wound pH. The pH value influences decisive processes like cell proliferation, cell migration, bacterial colonialization, and enzyme activity.[4] The direction of the pH shift in chronic wounds (either too acidic or too alkaline for a successful healing process) is dependent inter alia on the sort and the amount of bacterial load.[5] In the past, researchers mainly focused on the impact and the treatment of strongly alkaline wounds.[3] Yet, Schreml et al. recently identified an acidic pH around 6.5 at the wound edges being responsible for a reduced cell proliferation and migration into the wound area.[6] To the best of our knowledge, hardly any work has been done so far concerning the development of pH-modulating dressing materials for acidic non-healing wounds.[7] The application of alkaline wound dressings, which are capable to bring the pH back to physiological values (around 7.0 - 7.4), might be a potential treatment option.

In our work, we focused on the development of alkaline interpenetrating polymer network (IPN) hydrogels. IPN hydrogels are suitable wound dressing materials as they provide a moist healing environment.[8] Moreover, important wound dressing properties such as sufficient exudate uptake and mechanical stability can be adapted easily by changes in the dual network architecture.[9] The primary polymer network of the here examine IPN systems consisted of poly(ethylene glycol) diacrylate (PEGDA), combined with the alkaline precursor N-vinylimidazole (VI). Horta et al. found that VI containing hydrogels act as weak bases (pK_a = 7.0) that neutralize the surrounding medium, whilst avoiding to create an alkaline environment, which would likewise cause impaired healing.[10]

However, an alkaline environment is particularly beneficial for the successful healing of skin grafted wounds. Skin grafting is an important treatment option for non-healing wounds with severe tissue loss, for example in the case of full-thickness burns.[11] The take rate of skin grafts is often impaired by low vascularization and insufficient cellular in/outgrowth. Yet, both issues can be tackled in alkaline environment ($\geq$ 7.4).[3,6,12,13] Therefore, a second approach on alkaline IPN dressings was taken, including the strong base 2-dimethylaminoethyl methacrylate (DMAEMA; pK_a = 8.4) as alkaline part of the primary network.[14] Alginate or modified chitosan were used as secondary network in the IPN hydrogels. Both polysaccharides enhance wound healing by encouraging cell

proliferation and increasing collagen deposition, amongst others.[15,16] Additionally, chitosan is a weak base that exhibits a favorable antimicrobial effect.[17]

The alkaline IPN hydrogel wound dressings were developed by a bottom-up approach; different PEGDA/VI/alginate and PEGDA/DMAEMA/chitosan hydrogels were examined for their wound healing ability under acidic conditions in wound healing assays, by their ability to serve as cell scaffold and by their impact on wounded human skin constructs. As the structure of the human skin is significantly different from typically used animal models and the establishment of reproducible and pH-shifted in vivo chronic wound models is rather difficult, the use of such wounded human skin constructs is regarded as a valuable alternative.[18–20] Based on the in vitro experiments, the most promising formulations were further characterized for their material properties such as their microstructure, the mechanical performance, and the swelling capacity.

2. Experimental Section

2.1 Preparation of Hydrogels

A detailed description of the N-carboxyethylchitosan (CEC) and the PEGDA synthesis can be found in the supporting information. To prepare the precursor mixtures, a suspension of the radical initiator 2-hydroxy-4′-(2-hydroxyethoxy)-2-methylpropiophenone (2.5%, based on the total monomer mass) was pipetted to a PEGDA solution in phosphate buffered saline (PBS). Depending on the gel formulation, either a solution of alginate in PBS (c = 41.7 mg·mL^{-1}) or a CEC solution in water (final PBS to water ratio = 0.849) was added. Afterward, the required amount of VI, DMAEMA, or the neutral control 2-hydroxyethyl methacrylate (HEMA) was added drop-wise. The examined formulations are listed in Table 1. For skin construct healing assays, 1.4 mL of the precursor mixture were cast into a 6 well-plate; for cell adhesion experiments, 1.2 mL of the precursor mixture were cast into a 24 well-plate. For all other experiments, cylindrical glass molds (1 cm diameter, 0.7 mL volume) were used. All samples were irradiated with UV light (1 h 15, 366 nm, 6 W). If not stated otherwise, the hydrogels (with initial weight m_0) were purified in 10 mL of deionized water for 24 h. To ensure a constant water content of 90% throughout all experiments, the purified cylinders were exposed to a stream of compressed air until the initial weight m_0 had been reached again. The partial drying process was controlled gravimetrically.

Table 1. Composition of the examined hydrogel formulations with a total monomer concentration of 10%.

PEGDA (%)	pH-modulating component/ neutral control*	Secondary network (0.5%)
10	-	-
9.5	-	CEC or alginate 10/60
7.0 – 9.0	0.5 – 2.5% DMAEMA	CEC or alginate 10/60 or alginate 200
7.5	2.0% HEMA*	CEC
6.0 – 8.5	1.0 – 3.5% VI	alginate 10/60
6.0	3.5% HEMA*	alginate 10/60

2.2 Cell Viability

The cell viability (v) was determined according to the ISO 10993-5 extract method.[21] In brief, extraction was performed in pH-adjusted medium (medium 199 : nutrient mixture F-12 (F12) 3 : 1, 10% fetal bovine serum (FBS), 1.10 mM hydrocortisone, adjusted to pH 6.5 with 1 M HCl) for 48 h; the extraction medium was exchanged every 12 h. Then, 24 h cultured adult human dermal fibroblasts (HDFa, Life Technologies, Carlsbad, CA, USA; 8000 cells per well) were treated with 100 µL of hydrogel extracts; pH-adjusted cell culture medium served as a control. After 24 h of incubation under standard cell culture conditions, the extraction medium was removed; 130 µL of Dulbecco's modified eagle medium (DMEM)/F12, 20 µL of FBS, and 50 µL of a 3-(4,5-dimethylthiazol-2-yl)-2,5-diphenyltetrazolium bromide (MTT) solution (c = 2.5 mg·mL^{-1} in PBS) were added. The resulting blue dye was dissolved in 100 µL of a sodium dodecyl sulfate solution and its absorbance (A) at 570 and 690 nm was measured using a FluoStar Omega micro plate reader (BMG Labtech, Ortenberg, Germany). The cell viability was calculated according to Equation (1). Data are presented as mean ± standard deviation (SD), based on n = 6 samples.

$$v = \frac{A_{570,gel} - A_{690,gel}}{A_{570,ctrl} - A_{690,ctrl}} \cdot 100\% \qquad (1)$$

2.3 2D Cell Migration Assay

For two-dimensional (2D) cell migration assays, 140 µL of a HDFa suspension (300000 cells·mL^{-1}) were pipetted into cell culture inserts (Ibidi GmbH, Martinsried,

Germany) adhered to a fibronectin-coated 6-well plate. After 24 h of incubation under standard cell culture conditions, the inserts were removed and 8 mL of pH-adjusted medium were added. Hydrogels were placed in netwell inserts (Corning, Corning, NY, USA) and added to the cells; untreated cells served as a control. Every 12 h, the pH-adjusted cell culture medium was replaced. The cell migration was observed over 48 h using an Axiovert 200 microscope combined with a LSM 510 laser-scanning device (Zeiss, Jena, Germany). The area of cell migration was calculated using the LSM image browser (Zeiss, Jena, Germany); the cell migration velocity was calculated from the slope of the area closure/time curve.

2.4 3D Human Skin Constructs and Healing Assay*

Human skin constructs were built according to previously published methods.[22] Briefly, bovine collagen I, Hank's balanced salt solution, FBS, and primary fibroblasts ($3.0 \cdot 10^5$/construct) were brought to neutral pH and poured into cell culture inserts (BD Bioscience, Heidelberg, Germany). After 2 h at 37 °C, keratinocyte growth medium (KGM) was added and the system was transferred to an incubator (37 °C, 5% CO_2 and 95% humidity) for further 2 h. Primary keratinocytes ($4.2 \cdot 10^6$/construct) resuspended in KGM were pipetted on top. After 24 h, skin constructs were lifted to the air-liquid interface and KGM was replaced by a differentiation medium (based on high glucose DMEM). After 2 days of cultivation, the skin constructs were wounded by cutting the epidermal layer with a scalpel. For reproducibility, the operating person and the defect size remained unchanged. The injured constructs were incubated with pH-adjusted medium (pH 6.5) containing 2.5% hydroxyethyl cellulose. For this purpose, DMEM of the differentiation medium was substituted by medium 199 and the pH was adjusted with 1 M HCl.[6] The respective hydrogels were punched out in circular shape (1 cm diameter) and applied onto the wound. The medium was changed daily and the dressings were exchange after 2 days. After 4 days, the constructs were embedded in tissue freezing medium, cut vertically into slices (7 µm) using a Leica CM1510 S cryotome (Leica Biosystems, Nussloch, Germany) and stained with conventional hematoxylin and eosin (H&E) according to standard protocols. The length of cell ingrowth was measured with ImageJ (National Institutes of Health, Bethesda, Maryland, USA).

* 3D human skin constructs were generated at the Institute of Pharmacy, Pharmacology and Toxicology, Freie Universität Berlin, with support and based on the method of S. Hedtrich and L. Wallmeyer.

2.5 Cell Adhesion

HDFa (27400 cells/well) were seeded on the hydrogel surface and were incubated at standard cell culture conditions. After 24 h, the cells were stained with SYTO-13 (2.5 μM) and dead cells were stained with propidium iodide (1.5 μM). The fluorescence was measured at 488 and 543 nm using an Axiovert 200 microscope combined with a LSM 510 laser-scanning device (Zeiss, Jena, Germany).

2.6 Scanning Electron Microscopy

Hydrogel cylinders were shock-frozen in liquid nitrogen and lyophilized. The dried cylinders were coated with gold and examined using a Crossbeam XB 340 scanning electron microscope (Zeiss, Jena, Germany) at a working voltage of 3.0 kV.

2.7 Compressive Strength

The diameter (d) and the height (h) of non-purified and purified hydrogels cylinders were determined using a caliper (BORT GmbH, Weinstadt-Benzach, Germany). Then, compressive testing was carried out in an Instron 5542 load frame equipped with two cylindrical plates. The hydrogels were compressed until failure at 0.5 mm·min^{-1}, and the maximum load (F_{max}) and compressive strain were measured. The compressive stress (σ_c) was calculated according to Equation (2).

$$\sigma_c = \frac{F_{max}}{h \cdot d} \qquad (2)$$

The elastic modulus (E_c) was calculated from the slope of the stress-strain curve between 0.05 and 0.15 strain. Data are presented as mean ± SD, based on the test results of n = 4 specimens.

2.8 Swelling Capacity

Untreated hydrogel cylinders were incubated in 10 mL of PBS and stored in a shaking water bath at 37 °C. Every 24 h, the PBS was decanted; the gels were blotted dry and weighed. According to Equation (3), where m_t is the mass of the gel cylinder at time point t and m_0 is the initial mass of the gel, the swelling capacity (Q_t) was calculated.

$$Q_t = \frac{m_t - m_0}{m_0} \cdot 100\% \qquad (3)$$

2.9 Static pH and Equivalence Point Titration

Hydrogel cylinders were placed in 15 mL of a sodium chloride solution (c = 0.1 M). To determine the acid neutralizing capacity (ANC), the pH was kept at 7.0 over 24 h by using a BlueLine glass electrode connected to a TitroLine 7000 dosage system (SI Analytics GmbH, Mainz, Germany) filled with 0.1 M HCl. The ANC was calculated from the amount of neutralized hydrochloride, n(HCl), and the initial mass of the gel cylinder, m_0, according to Equation (4).

$$ANC = \frac{n(\mathrm{HCl})}{m_0} \qquad (4)$$

For equivalence point (EP) titration, 0.7 mL of the precursor mixture was pipetted to 15 mL of a 0.1 M NaCl solution. The mixture was brought to pH 11.0 with sodium hydroxide solution and titrated with 0.1 M hydrochloride solution until pH 3.0 was reached. The EPs were calculated from the slope of the V(HCl)-pH curve, where V(HCl) is the volume of neutralized standard solution.[23]

3. Results

Different alkaline interpenetrating polymer network hydrogels were analyzed for their suitability as bioactive wound dressing materials. In a bottom up approach, promising formulations were identified in wound healing assays and then further characterized for their relevant material properties.

3.1 Cell Viability and Wound Healing Capacity

First, IPN hydrogels consisting of PEGDA, alginate, and 1.0 - 3.5% VI were tested for their cell compatibility in MTT assays. It was abstained from testing higher VI concentrations as the resulting hydrogels showed little mechanical stability and a high sol content. Independent of the hydrogel composition, all tested formulations were non-cytotoxic (93.9 – 125.1% cell viability; Figure 1A). As a maximal pH activity was desired and VI containing hydrogels do not bear the risk of pH overmodulation,[10] PEGDA/3.5% VI/alginate (subsequently named $VI_{3.5}$) was the most interesting hydrogel composition.

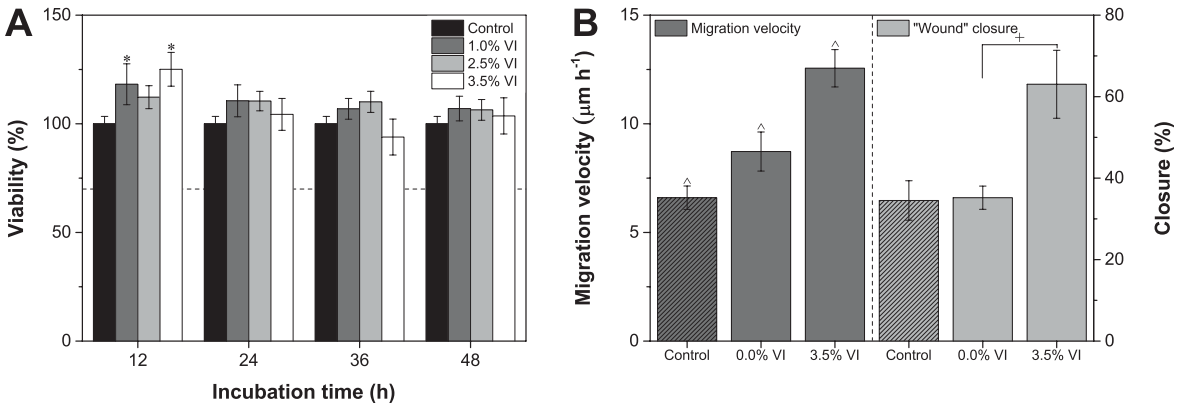

Figure 1. Cell viability in MTT assays (A). The broken line (---) marks the critical value of 70% cell viability.[21] Wound healing capacity in 2D migration experiments (B) for different PEGDA/VI/alginate hydrogels. Data are expressed as mean ± SD (A: n = 6; B: n = 3); * indicates statistically significant differences versus the untreated control ($p < 0.05$); ^ indicates statistically significant differences to all samples ($p < 0.05$); + indicates statistically significant differences between the groups ($p < 0.05$).

$VI_{3.5}$ hydrogels were further analyzed for their wound healing capacity in 2D cell migration assays. This experimental setup can be regarded as simplified wound model with easily adaptable wound healing conditions; in our study, the "wounds" suffered from an acidic pH. The application of non pH-modifying PEGDA/alginate hydrogels already enhanced the cell migration velocity (Figure 1B). With VI incorporation, however, the migration velocity as well as the gap closure further increased, by 44.0 and 79.1%, respectively.

In contrast, the application of PEGDA/0.5 – 2.0% DMAEMA/0.5% CEC IPN hydrogels caused a significantly enhanced cell migration velocity (around 11.7 $\mu m \cdot h^{-1}$; Figure 2A), combined with an almost complete gap closure (78.7 - 97.0%; Figure 2B) in acidic 2D migration experiments. The application of highly alkaline IPNs with 2.5% DMAEMA content enabled a comparable cell migration velocity, but suppressed the amount of gap closure. Furthermore, the cytocompatibility of the most promising hydrogel formulation PEGDA/2.0% DMAEMA/CEC (subsequently named $DMAEMA_{2.0}$) was verified in MTT assays. The detected cell viability ranged between 119.4 and 132.9%, dependent on the incubation time (see supporting information, Section 6.3, Figure S1).

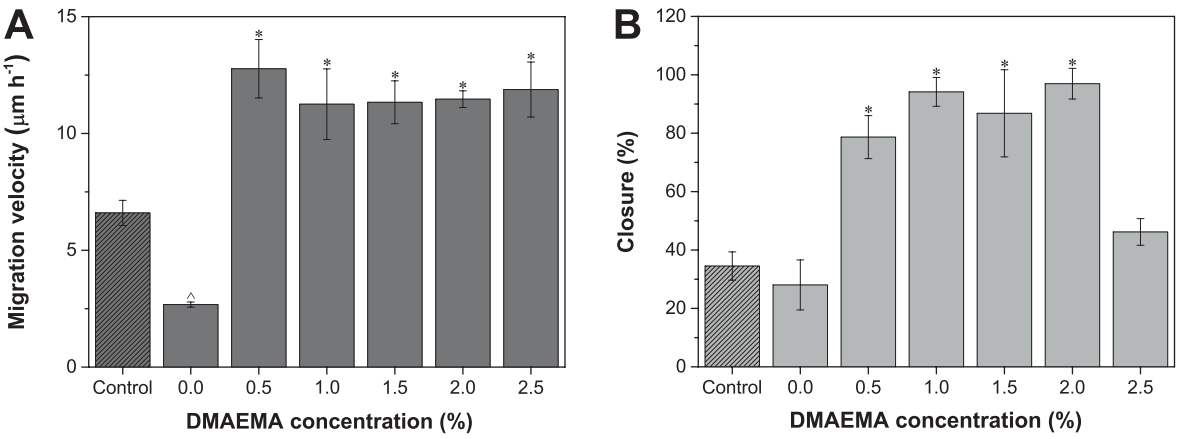

Figure 2. Cell migration velocity (A) and percentage of gap closure (B) in 2D migration experiments with different PEGDA/DMAEMA/CEC hydrogels applied. Data are expressed as mean ± SD (n = 3); * indicates statistically significant differences versus the untreated control ($p < 0.05$); ^ indicates statistically significant differences to all samples ($p < 0.05$).

The wound healing capacity of the two most promising hydrogel formulations $VI_{3.5}$ and $DMAEMA_{2.0}$ was more precisely assessed by wounded human skin constructs, which can be seen as an alternative to animal testing.[18] Since the skin constructs suffered from an acidic environment, the cell ingrowth in the untreated control was very poor (Figure 3B). Wound closure could be enhanced by the treatment with PEGDA/alginate and PEGDA/CEC hydrogels (Figure 3A). Due to the addition of pH-modifying components, cell ingrowth further increased by 46.2% with $VI_{3.5}$ and by 89.1% with $DMAEMA_{2.0}$ gels (Figure 3C and D).

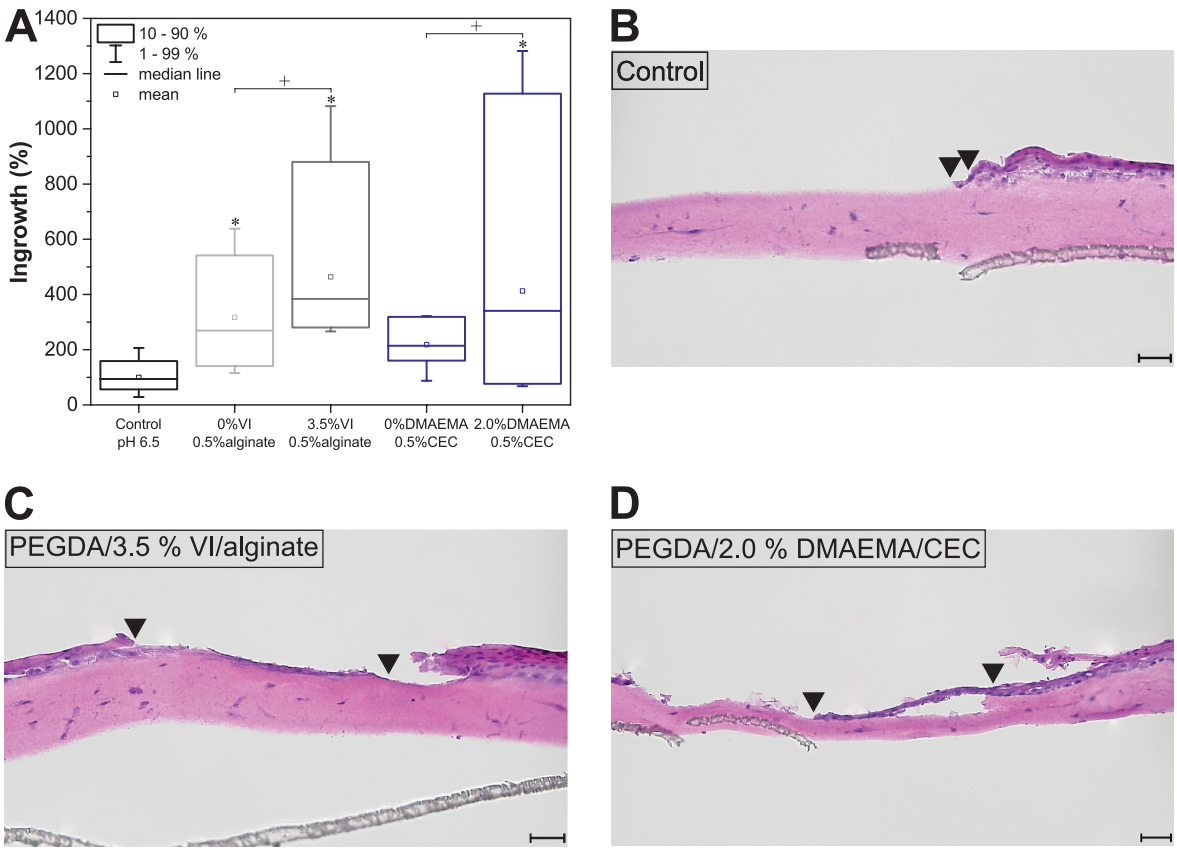

Figure 3. Percentage cell ingrowth in differently treated skin constructs (A). * indicates statistically significant difference versus the untreated control, set as 100% ($p < 0.05$); + indicates statistically significant differences between the groups ($p < 0.05$). H&E stained histological images of injured skin constructs after a healing period of 4 days (B – D); treatment as indicated in the upper left corner. The length of cell ingrowth is indicated by triangles. The length of the scale bars is 50 µm.

3.2 Microstructure and Cell Adhesion

The hydrogel microstructure is related to numerous material properties. Therefore, lyophilized hydrogel samples were examined by scanning electron microscopy (Figure 4A and B). Since $VI_{3.5}$ and $DMAEMA_{2.0}$ hydrogels showed major structural differences, their performance as cell scaffold in cell adhesion tests was complementary as well (Figure 4C and D). Primary human dermal fibroblasts were able to adhere and spread at the rough and porous VI containing IPN hydrogel surface, whereas no adhesion was detected at the smoother and less porous DMAEMA containing IPN hydrogel surface.

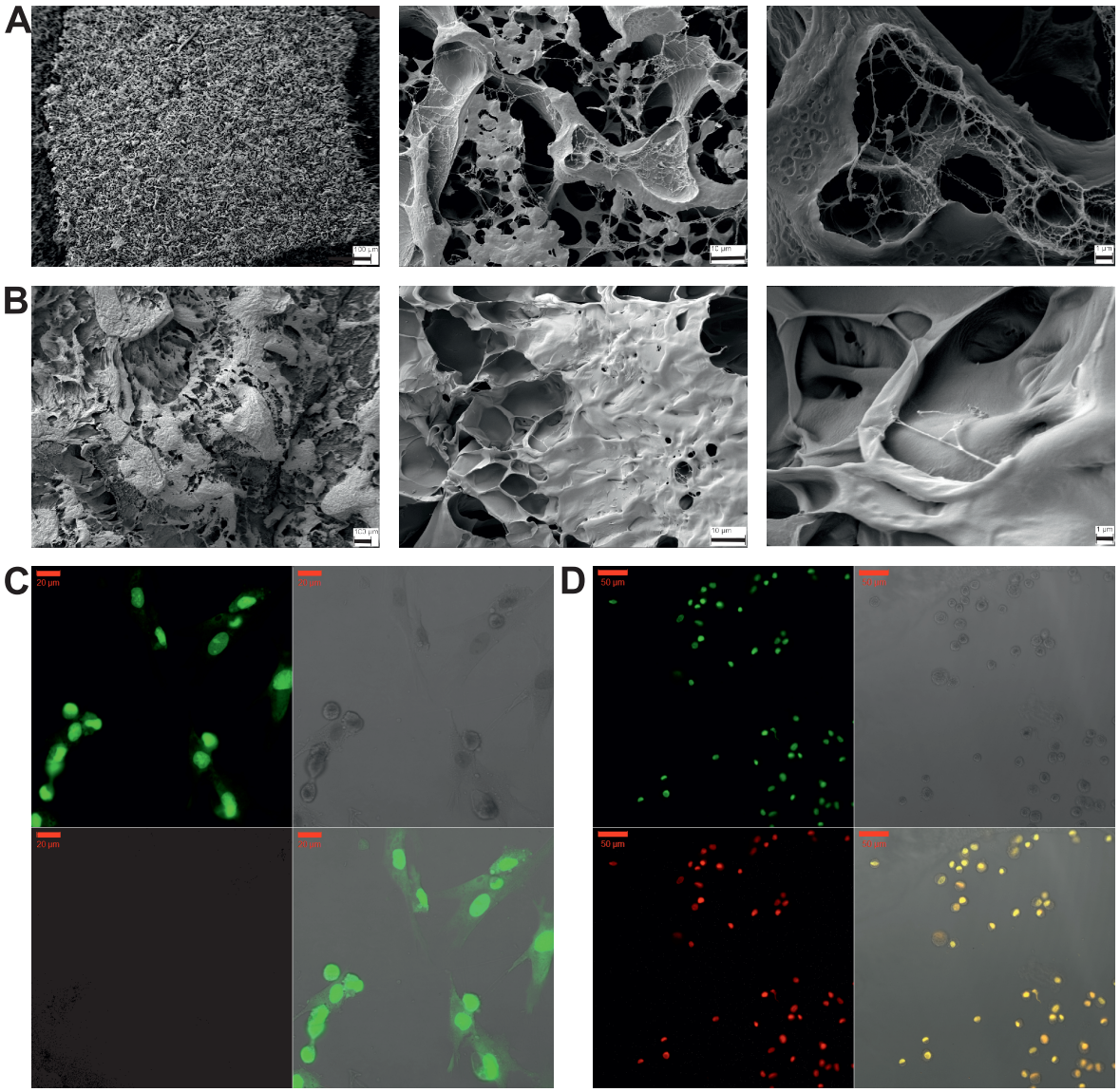

Figure 4. SEM images of lyophilized $VI_{3.5}$ (A) and $DMAEMA_{2.0}$ (B) hydrogels. The length of the scale bars is 100/10/1 µm. HDFa cells seeded on the $VI_{3.5}$ (C) and $DMAEMA_{2.0}$ (D) hydrogels. In clockwise direction: HDFa stained green, bright field, merged images, dead cells stained red.

3.3 Mechanical Properties

Wound dressing materials must withstand the applied forces during application and wearing. Furthermore, they should be flexible enough to follow the patients' movements and to fit even irregular wound shapes. Hence, the hydrogel performance under compressive load was evaluated for the most promising alkaline hydrogels $VI_{3.5}$ and $DMAEMA_{2.0}$. Insights into the mechanism of hydrogel stabilization were expected from the comparison to their neutral analogues, carrying 3.5% and 2.0% 2-hydroxyethyl methacrylate ($HEMA_{3.5}$ and $HEMA_{2.0}$) instead.

The maximum compressive stress, σ_c, of the $VI_{3.5}$ hydrogels was 0.371 ± 0.185 MPa with a corresponding elastic modulus, E_c, of 39.7 ± 3.6 kPa (Figure 5A and B). The substitution of VI by HEMA caused a significant reduction of the σ_c and E_c values, whereas purification in water had no impact on the mechanical properties of these hydrogels.

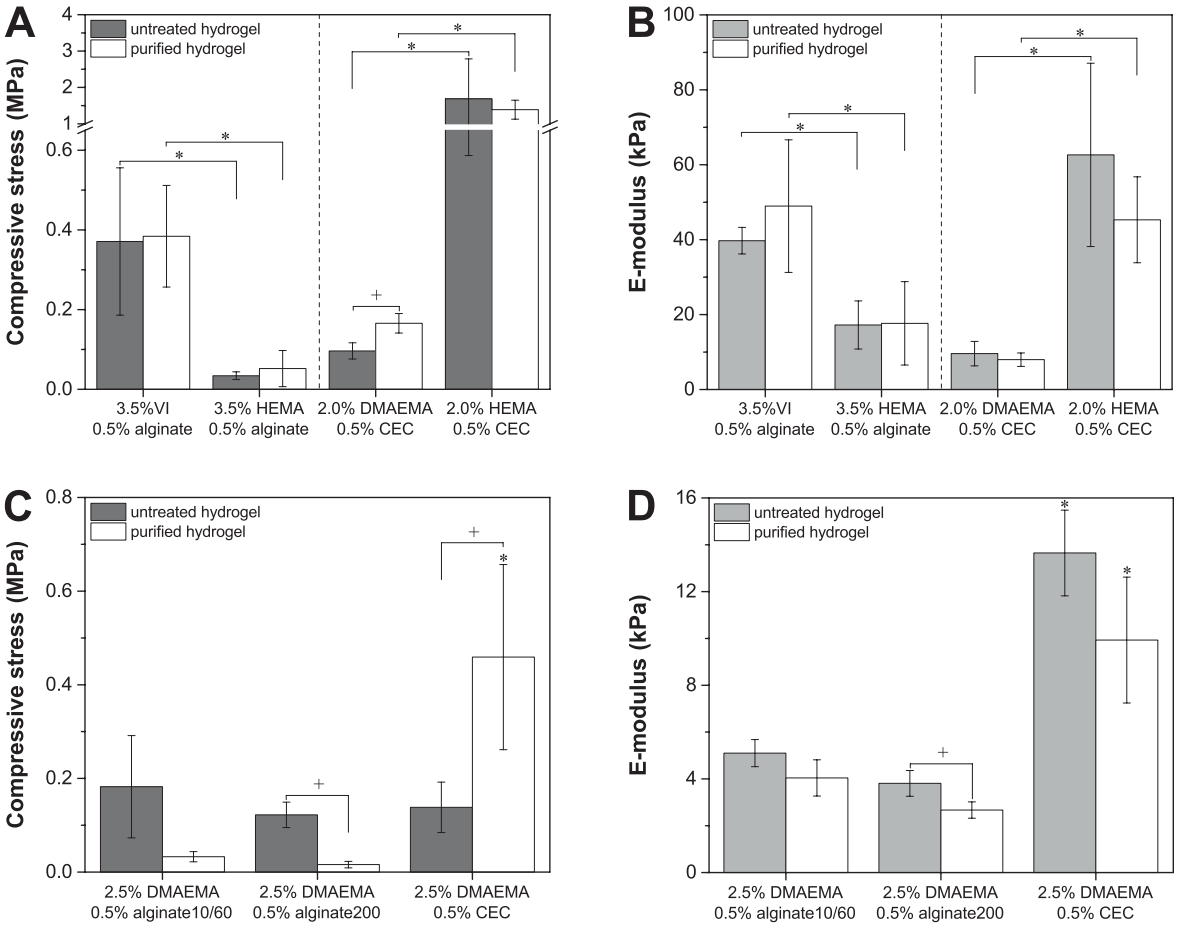

Figure 5. Compressive stress σ_c at maximum load (A, C) and calculated E-modulus E_c (B, D) of different alkaline hydrogels with and without prior purification in water. Data are expressed as mean ± SD (n = 4); + indicates statistically significant differences between untreated and purified samples ($p < 0.05$); * indicates statistically significant differences between the groups ($p < 0.05$).

The $DMAEMA_{2.0}$ gels were less stable (σ_c = 0.096 ± 0.020 MPa) and less stiff (E_c = 9.6 ± 3.3 kPa) than the $VI_{3.5}$ and the respective $HEMA_{2.0}$ hydrogels (Figure 5A and B). Yet, in contrast to all other formulations, purification in water led to an improved maximum compressive stress of the $DMAEMA_{2.0}$ hydrogels (σ_c = 0.166 ± 0.024 MPa; Figure 4A). These findings could be further emphasized when the DMAEMA content was increased to 2.5% (Figure 5C and D). Hydrogels with varying secondary network (alginate 10/60, alginate 200, or CEC) were affected differently by the purification step and in a higher

extent than the *DMAEMA$_{2.0}$* gels. Both purified alginate containing formulations showed decreased values for σ_c and E_c, whereas a strengthening effect of 232% was detectable for the purified PEGDA/2.5% DMAEMA/CEC formulation.

3.4 Swelling and Buffer Capacity

The fluid handling properties of dressing materials are of special interest when chronic wounds are targeted. All examined IPN hydrogels showed a significantly higher swelling capacity than the pure 10% PEGDA hydrogels (Figure 6). Addition of VI (*VI$_{3.5}$*) or HEMA (*HEMA$_{3.5}$*) did not have any further impact on the amount of liquid uptake (around 35%). In contrast, *DMAEMA$_{2.0}$* hydrogels could absorb up to 189% PBS.

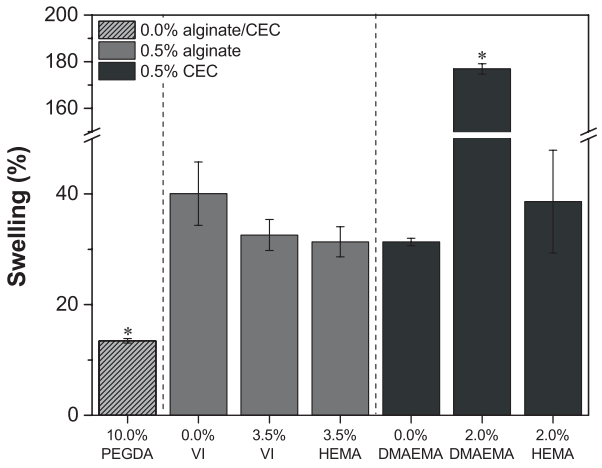

Figure 6. Swelling capacity of different alkaline hydrogels and control samples. Data are expressed as mean ± SD (n = 3). * indicates statistically significant differences to all samples ($p < 0.05$).

Static pH titration, which can be seen as an indicator for the ability of pH-modification, underlined, that PEGDA/alginate hydrogels are not pH active, whereas PEGDA/CEC hydrogels were able to neutralize 0.004 mmol hydrochloride per gram of hydrogel (Figure 7). Furthermore, the ANC measurements emphasized the differing buffer strength of the two alkaline substances; *DMAEMA$_{2.0}$* gels were able to neutralize three times more hydrochloride, even though *VI$_{3.5}$* gels carried approximately three times more amino groups.

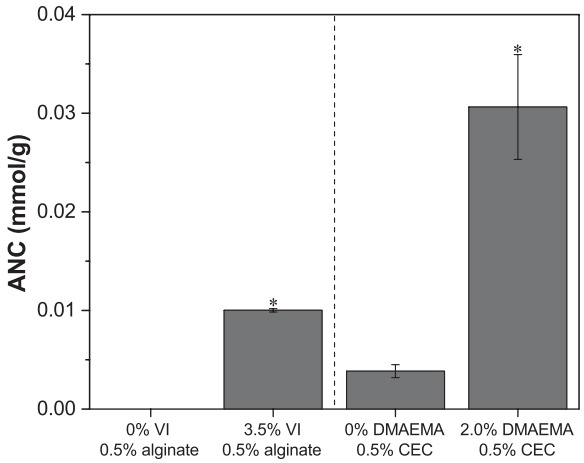

Figure 7. Acid neutralizing capacity of different alkaline hydrogels and control samples. Data are expressed as mean ± SD (n = 3); * indicates statistically significant differences versus the respective control ($p < 0.05$).

Furthermore, the equivalence points of the *VI*$_{3.5}$ and *DMAEMA*$_{2.0}$ formulation were assessed, indicating pH 2.67 (-COOH, alginate), 4.18 (-COOH, alginate), and 8.44 (-NR_2, VI); and pH 4.02 (-COOH, CEC), 5.79 (-NH_2, CEC), 7.23 (-NHR', CEC), 8.97 (-NR'$_2$, CEC), and 10.43 (-NR^*_2, DMAEMA), respectively. The pH of the *VI*$_{3.5}$ precursor mixture was 8.5, which implies -COO^-/-NR_2 > -NHR_2^+ as main ionic structure, and 10.0 for the *DMAEMA*$_{2.0}$ precursor mixture, which implies -COO^-/-NH_2/-NR'H/-NR'$_2$/-$NHR^*_2{}^+$ as main ionic structure of the IPN systems (see Figure 8 for illustration).

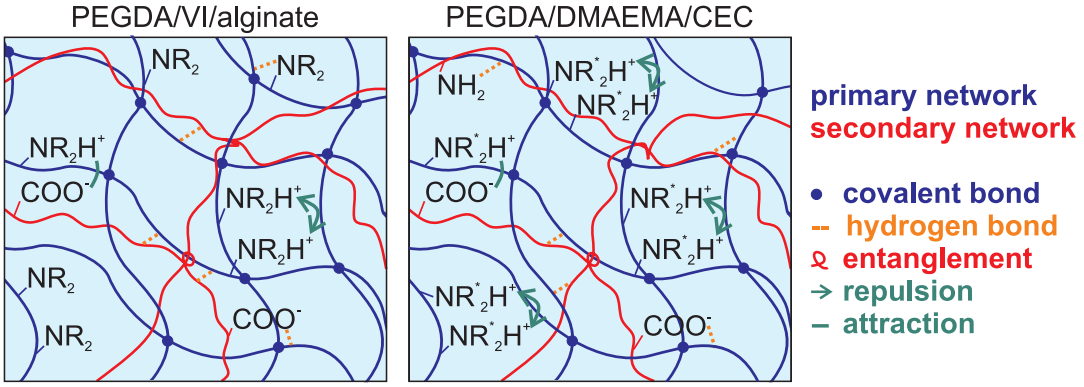

Figure 8. Schematic structure of the alkaline IPN hydrogels PEGDA/VI/alginate and PEGDA/DMAEMA/CEC.

4. Discussion

Based on our bottom-up approach by initially analyzing different hydrogel formulations in cell-based assays, we identified two different hydrogel formulations as potential pH-modulating wound dressings. The first one consisted of 3.5% VI, 0.5% alginate, and

6.0% PEGDA, an IPN hydrogel with slightly buffering pH-modulating precursor (VI) and a non pH-active secondary network (alginate). The second formulation consisted of 2.0% DMAEMA, a strong base and buffering substance, 0.5% CEC, a derivate of chitosan which is water soluble at neutral pH and can also take part in pH-regulation, combined with 7.5% PEGDA. The well-known wound healing ability of alginate was confirmed for PEGDA/alginate hydrogel samples in 2D wound healing assays.[16] Since the "wounds" suffered from an acidosis, a treatment with pH-modulating $VI_{3.5}$ hydrogels enhanced the cell migration even further. In contrast to alginate, chitosan has lost its supportive healing ability, probably related to the conducted structural modifications. As DMAEMA is a stronger base than VI, the optimal DMAEMA ratio (2.0%) was lower than the optimal VI ratio (3.5%). Hydrogels carrying 0.5 – 2.0% DMAEMA were able to rise the in vitro "wound" pH toward physiological values in 2D healing assays (pH = 7.1 – 7.3, data not shown), which was reflected in a significantly enhanced cell migration velocity and gap closure. A pH over-regulation (pH 7.8 for 2.5% DMAEMA containing hydrogels) resulted in a gap closure comparable to that of the untreated, acidic control. However, one should keep in mind that an alkaline pH value is favorable for the aimed application as skin graft dressing and the detected medium pH is lower than the actual pH in immediate surroundings to the hydrogel dressing. More application-orientated healing experiments were therefore conducted on wounded human skin constructs, used as an alternative to the only limited reliable animal model.[19] The detected findings underlined the hydrogels' promising performance in 2D migration assays. The ability of alginate to enhance the cell migration was confirmed once more. The slightly enhanced cell ingrowth after PEGDA/ CEC treatment might be related to the small pH-modulating effect of CEC containing hydrogels (see Figure 6 for comparison). On the other hand, the strongly pH-modulating $VI_{3.5}$ and $DMAEMA_{2.0}$ hydrogels significantly enhanced the wound healing in the treated skin constructs.

Further enhancement of the healing process in chronic wounds might be achieved by wound dressings with incorporated cells.[24] Therefore, the developed hydrogels were additionally examined for their ability to serve as HDFa scaffolds. The successful cell adhesion on $VI_{3.5}$ hydrogels can be explained by their favorable porous and fibrous structure, which enables the exchange of metabolites, gas, and nutrients.[25,26] Microfiber formation might occur due to intermolecular hydrogen bond interactions between amino and carboxyl groups.[25] The smooth and far less porous surface of the $DMAEMA_{2.0}$ network might be owed to DMAEMA and CEC as film formers.[27,28] A comparable structure was

already described by Liu et al.[29] In contrast to porous surfaces, these materials inhibit cellular attachment. Further, enhanced amounts of positive charges at the material surface might be responsible for the damage of cell membranes.[25]

In a second step, the developed hydrogels were evaluated for their suitability as wound dressings concerning their physiochemical properties. Specific mechanical requirements of wound dressings are difficult to define. Dependent on the formulation and the water content, fragile materials, bearing only 1 to 6 N, as well as very tough dressing materials, bearing up to 3.7 MPa, were described in literature.[30,31] In any case, the dressings have to withstand the applied load during application, wearing, and removal. As radical initiator and unreacted monomer need to be removed prior to a medical application, a potential impact of purification on the mechanical properties should be examined as well.[31] *VI$_{3.5}$* hydrogels showed sufficient stability and high elasticity, regardless of the incubation process (Figure 5A and B). The mechanism of hydrogel stabilization in VI containing gels was clarified by compressive tests of hydrogels carrying HEMA instead. Like the VI molecules, HEMA influences the network formation of PEGDA by only contributing to linear chain growth. Both molecules can engage in stabilizing hydrogen bonds (via -NR$_2$ or -OH/-C(O)O-) with the PEG backbone and the alginate network, yet only VI molecules can form additional ionic interactions. Their partially ionized amino groups might bind to the deprotonated carboxylic acid groups of alginate (see Figure 8 for comparison).[32,33]

DMAEMA containing hydrogels, on the other hand, showed a significantly weakened and more flexible texture in comparison to the HEMA containing control gels. This might be due to the fact that the DMAEMA amino groups in *DMAEMA$_{2.0}$* hydrogels are mainly present in their protonated form (EP = 10.43, pH = 10.0, see Figure 8 for comparison). Apparently, resulting repulsive forces between DMAEMA ammonium groups soften the hydrogel material. The data in Figure 5A indicate that incubation in water has nevertheless a strengthening effect on *DMAEMA$_{2.0}$* hydrogels. We hypothesize that facilitated ionic interactions between DMAEMA ammonium groups and CEC carboxylic acid groups play a role in this process. The reduction of the counter ion concentration and a possible geometrical reorganization during incubation in water might cause readily accessible ionic groups.[34] With an enhanced amount of positive charges in the hydrogel (2.5% DMEMA content; Figure 5C and D), the strengthening effect by incubation is even more pronounced, which pleads for this theory. Additionally, the compressive stress is dependent on the character of the secondary network. With rising accessibility of the

carboxyl groups (alginate 200, low α-L-guluronate (G) content < alginate 10/60, high G content < CEC), the compressive stress increased many times over.[35]

An appropriate liquid uptake by the applied dressing is inevitable as many chronic wounds and skin grafted injuries secrete a high amount of wound exudate. Otherwise, remaining exudate harms the surrounding tissue or included inflammation factors inhibit the healing process.[36,37] For instance Neoheal® hydrogel (Kikgel), a commercially available PEG-based dressing, has a swelling capacity of around 70% in 24 h, which is proven to be suitable for strongly exuding burns.[38] Therefore, $VI_{3.5}$ hydrogels (33% in 24 h) might be used for low or medium exuding wounds, whilst $DMAEMA_{2.0}$ hydrogels (177% in 24 h) might also be applied on strongly exuding wounds. The swelling capacity of the examined hydrogels is, like the mechanical properties, dependent on the amount and the strength of the ionizable groups incorporated into the polymer network. The driving force of the osmotic pressure is the aimed reduction of electrostatic repulsions between positively charged amino groups.[39] The incorporated amount of ammonium groups (CEC < VI < DMAEMA) also drives the acid neutralizing capacity, which was the far largest for $DMAEMA_{2.0}$ hydrogels. Again, no desired value might be given. The ANC requirements differ for varying wound types and patients.[3,6] In clinics, the individual needs of each wound might be determined by the use of pH-responsive wound sensors prior to dressing application.[6]

5. Conclusion

PEGDA/3.5% VI/alginate hydrogels are promising pH-modulating materials, which should be considered for the treatment of acidic chronic wounds. The hydrogels were able to bring the pH value of in vitro wounds back to neutral, thereby enhancing cell migration and proliferation. Furthermore, their material properties like liquid uptake and mechanical stability corresponded with the requirements of wound dressings, and the supplementary addition of cells might be a promising strategy to create a bioactive dressing that further stimulates the healing process. Therefore, future research should focus on the impact of these cell-laden $VI_{3.5}$ hydrogels in vitro and in vivo. PEGDA/2.0% DMAEMA/CEC hydrogels likewise showed convincing results in wound healing assays. Owing to the elevated pH-modulating ability, their application field might more likely be seen in the treatment of skin grafted wounds, where an alkaline environment is aimed. Since these

wounds are commonly covered by an additional backing dressing, reduced mechanical resistance might not be seen as a drawback.

6. Supporting Information

6.1 Materials

Toluene was purchased from Acros Organics (Geel, Belgium). Bovine collagen I (PureCol®) was obtained from Advanced BioMatrix (San Diego, USA). Fetal bovine serum for skin constructs was obtained from Biochrom (Berlin, Germany). Formaldehyde solution (4%) and reagents for hematoxylin and eosin staining were purchased from Carl Roth (Karlsruhe, Germany). Deuterated chloroform ($CDCl_3$) and water (D_2O) were purchased from Deutero GmbH (Kastellaun, Germany). Alginate (Protanal® LF 10/60FT and LF200 FTS) was kindly provided by FMC BioPolymer (Wallingstown, Ireland). Dichloromethane (DCM), diethyl ether, and ethanol were obtained from CSC Jäcklechemie (Nürnberg, Germany). Hydroxyethyl cellulose was obtained from Fagron (Barsbüttel, Germany). Dulbecco's modified eagle medium/nutrient mixture F-12 (DMEM/F12), Hank's balanced salt solution, high glucose DMEM, nutrient mixture F-12, penicillin–streptomycin, and phosphate buffered saline were purchased from Life Technologies (Carlsbad, CA, USA). Keratinocyte basal medium and keratinocyte growth medium supplements were obtained from Lonza (Basel, Switzerland). Dimethyl sulfoxide (DMSO), glacial acetic acid, hydrochloric acid, sodium hydroxide, and triethylamine were purchased from Merck KGaA (Darmstadt, Germany). Deionized water was obtained using a Milli-Q water purification system (Millipore, Schwabach, Germany). All other chemicals were obtained from Sigma Aldrich (Taufkirchen, Germany). If not stated otherwise, chemicals were used as received.

6.2 Precursor Synthesis

For the synthesis of N-carboxyethylchitosan (CEC), 2.00 g medium molecular weight chitosan (75 - 85% acetylation degree) was dissolved in 100 mL of an aqueous acrylic acid solution (0.10 $mol \cdot L^{-1}$) and stirred at 50 °C. After 65 h, 11.0 mL of a 1 M sodium hydroxide solution were added dropwise, the product was precipitated in ice-cool acetone, vacuum-dried, and redissolved in water. The product solution was purified in a 50 h dialysis against water (molecular weight cut-off 12000), dried under vacuum, and lyophilized to yield 2.01 g (85.0%).

^{1}H-NMR (300 MHz, D_2O, δ): 2.03 ppm (s, 0.27 H, -NHC(O)C*H*$_3$), 2.37 ppm (m, 0.32 H, -NHCH$_2$C*H*$_2$-), 2.70 ppm (m, 0.41 H, -NH(CH$_2$C*H*$_2$-)$_2$), 3.02 - 4.10 ppm (m, H polysaccharide), 4.35 - 4.70 (m, 1 H, H-1 polysaccharide). A ratio of 63.8% -NH_2, 9.3% -NHC(O)CH_3, 16.2% -NHR, and 10.7% -NR_2 with R = -NHCH$_2$CH$_2$- was calculated from the respective peak areas in relation to the peak area of H-1.

Poly(ethylene glycol) diacrylate was synthesized as previously reported.[40] In brief, poly(ethylene glycol) with a molecular mass of 6 kDa (PEG6k) was dried by azeotropic distillation in toluene. A solution of dry PEG6k in anhydrous DCM (100 mL, 42 mM) was cooled to 0 °C, and 1400 µL of triethylamine (10.0 mmol) and 1625 µL of acryloyl chloride (20.0 mmol) were added drop-wise. The solution was stirred overnight under argon atmosphere, filtered, washed with 2 M potassium carbonate solution, and dried over anhydrous magnesium sulfate. The product was precipitated in ice-cold diethyl ether and dried under vacuum to yield 17.02 g (66.3%).

^{1}H-NMR (300 MHz, $CDCl_3$, δ): 3.62 ppm (m, 310 H, -C*H*$_2$C*H*$_2$O-), 4.30 ppm (t, 2 H, -C*H*$_2$OC(O)-), 5.82 and 6.41 ppm (dd, 1 H, C*H*$_2$=CHC(O)O-), 6.13 ppm (dd, 1 H, CH_2=C*H*C(O)O-).

6.3 Cell Viability

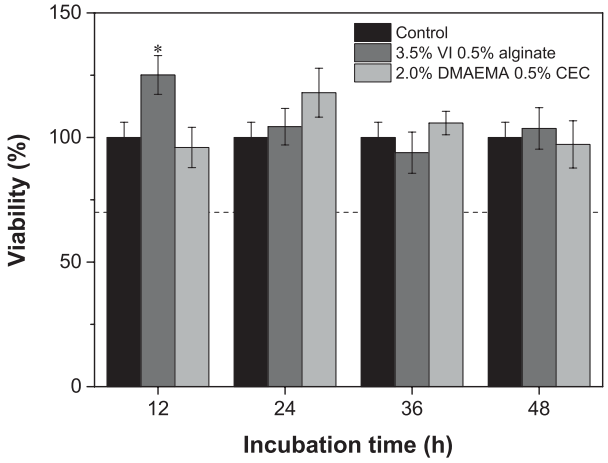

Figure S1. Cell viability in MTT assays referred to *VI*$_{3.5}$ and *DMAEMA*$_{2.0}$ hydrogels. The broken line (---) marks the critical value of 70% cell viability.[21] Data are expressed as mean ± SD (n = 6); * indicates statistically significant differences versus the untreated control ($p < 0.05$).

6.4 Statistical Analysis

If not stated otherwise, data are presented as mean ± standard deviation. For statistical analysis, Brown-Forsythe test was run followed by one-way ANOVA/Tukey' test or Kruskal-Wallis-ANOVA. Differences were considered statistically significant at $p < 0.05$.

References

1. Fife CE, Carter MJ. Wound care outcomes and associated cost among patients treated in US outpatient wound centers: Data from the US wound registry. Wounds 2012; 24: 10–17.
2. Schreml S, Szeimies R-M, Prantl L, Landthaler M, Babilas P. Wound healing in the 21st century. J. Am. Acad. Dermatol. 2010; 63: 866–881.
3. Schneider LA, Korber A, Grabbe S, Dissemond J. Influence of pH on wound-healing: A new perspective for wound-therapy? Arch. Dermatol. Res. 2007; 298: 413–420.
4. Schreml S, Szeimies R-M, Karrer S, Heinlin J, Landthaler M, Babilas P. The impact of the pH value on skin integrity and cutaneous wound healing. J. Eur. Acad. Dermatol. Venereol. 2010; 24: 373–378.
5. Sheybani R, Shukla A. Highly sensitive label-free dual sensor array for rapid detection of wound bacteria. Biosens. Bioelectron. 2017; 92: 425–433.
6. Schreml S, Meier RJ, Kirschbaum M, Kong SC, Gehmert S, Felthaus O, Küchler S, Sharpe JR, Wöltje K, Weiß KT, Albert M, Seidl U, Schröder J, Morsczeck C, Prantl L, Duschl C, Pedersen SF, Gosau M, Berneburg M, Wolfbeis OS, Landthaler M, Babilas P. Luminescent dual sensors reveal extracellular pH-gradients and hypoxia on chronic wounds that disrupt epidermal repair. Theranostics 2014; 4: 721–735.
7. Harrison BS, Hodges SJ. Topical wound treatment method and composition (US2015/0024053A1); 2013.
8. Boateng J, Catanzano O. Advanced therapeutic dressings for effective wound healing--A review. J. Pharm. Sci. 2015; 104: 3653–3680.
9. Li G, Zhang H, Fortin D, Xia H, Zhao Y. Poly(vinyl alcohol)-poly(ethylene glycol) double-network hydrogel: A general approach to shape memory and self-healing functionalities. Langmuir 2015; 31: 11709–11716.
10. Horta A, Piérola IF. Poly(N-vinylimidazole) gels as insoluble buffers that neutralize acid solutions without dissolving. J. Phys. Chem. B 2009; 113: 4226–4231.
11. Sharpe JR, Booth S, Jubin K, Jordan NR, Lawrence-Watt DJ, Dheansa BS. Progression of wound pH during the course of healing in burns. J. Burn Care Res. 2013; 34: e201-e208.
12. Karahaliloglu Z, Ercan B, Chung S, Taylor E, Denkbas EB, Webster TJ. Nanostructured anti-bacterial poly-lactic-co-glycolic acid films for skin tissue engineering applications. J. Biomed. Mater. Res. A 2014; 102: 4598–4608.

13. Sharpe JR, Harris KL, Jubin K, Bainbridge NJ, Jordan NR. The effect of pH in modulating skin cell behaviour. Br. J. Dermatol. 2009; 161: 671–673.
14. Zheng C, Liu X, Zhu J, Zhao Y. Preparation of cationic biodegradable dextran microspheres loaded with BSA and study on the mechanism of protein loading. Drug Dev. Ind. Pharm. 2012; 38: 653–658.
15. Jayakumar R, Prabaharan M, Sudheesh Kumar PT, Nair SV, Tamura H. Biomaterials based on chitin and chitosan in wound dressing applications. Biotechnol. Adv. 2011; 29: 322–337.
16. Lee W-R, Park J-H, Kim K-H, Kim S-J, Park D-H, Chae M-H, Suh S-H, Jeong S-W, Park K-K. The biological effects of topical alginate treatment in an animal model of skin wound healing. Wound Rep. Regen. 2009; 17: 505–510.
17. Patrulea V, Ostafe V, Borchard G, Jordan O. Chitosan as a starting material for wound healing applications. Eur. J. Pharm. Biopharm. 2015; 97: 417–426.
18. Hayden PJ, Bachelor M, Ayehunie S, Letasiova S, Kaluzhny Y, Klausner M, Kandárová H. Application of MatTek in vitro reconstructed human skin models for safety, efficacy screening, and basic preclinical research. Appl. In Vitro Toxicol. 2015; 1: 226–233.
19. Nunan R, Harding KG, Martin P. Clinical challenges of chronic wounds: Searching for an optimal animal model to recapitulate their complexity. Dis. Model. Mech. 2014; 7: 1205–1213.
20. Monsuur HN, Boink MA, Weijers EM, Roffel S, Breetveld M, Gefen A, van den Broek LJ, Gibbs S. Methods to study differences in cell mobility during skin wound healing in vitro. J. Biomech. 2016; 49: 1381–1387.
21. 10993-5:2009, Biological evaluation of medical devices - Part 5: Tests for in vitro cytotoxicity. Geneva, Switzerland: International Organization for Standardization; 2009.
22. Wallmeyer L, Lehnen D, Eger N, Sochorova M, Opalka L, Kovacik A, Vavrova K, Hedtrich S. Stimulation of PPARalpha normalizes the skin lipid ratio and improves the skin barrier of normal and filaggrin deficient reconstructed skin. J. Dermatol. Sci. 2015; 80: 102–110.
23. Moreira HR, Munarin F, Gentilini R, Visai L, Granja PL, Tanzi MC, Petrini P. Injectable pectin hydrogels produced by internal gelation: pH dependence of gelling and rheological properties. Carbohydr. Polym. 2014; 103: 339–347.

24. Mithieux SM, Weiss AS. Design of an elastin-layered dermal regeneration template. Acta Biomater. 2017; 52, 33-40.
25. Zheng Z, Zhang L, Kong L, Wang A, Gong Y, Zhang X. The behavior of MC3T3-E1 cells on chitosan/poly-L-lysine composite films: Effect of nanotopography, surface chemistry, and wettability. J. Biomed. Mater. Res. A 2009; 89: 453–465.
26. Nune KC, Misra RDK, Gaytan SM, Murr LE. Interplay between cellular activity and three-dimensional scaffold-cell constructs with different foam structure processed by electron beam melting. J. Biomed. Mater. Res. A 2015; 103: 1677–1692.
27. Fänger S, Heuer BD, Hiddemann S, Kröpke R, Kummer A. Hautpflege-Formulierungen mit einem sofort spürbaren Straffungseffekt (DE102009009758 A1); 2010.
28. Mourya V, Inamdar NN, Tiwari A. Carboxymethyl chitosan and its applications. Adv. Mat. Lett. 2010; 1: 11–33.
29. Liu Y, Wang C-F, Chen S. Facile access to poly(DMAEMA-co-AA) hydrogels via infrared laser-ignited frontal polymerization and their polymerization in the horizontal direction. RSC Adv. 2015; 5: 30514–30521.
30. Lai HL, Abu'Khalil A, Craig DQ. The preparation and characterisation of drug-loaded alginate and chitosan sponges. Int. J. Pharm. 2003; 251: 175–181.
31. Chang C-W, van Spreeuwel A, Zhang C, Varghese S. PEG/clay nanocomposite hydrogel: A mechanically robust tissue engineering scaffold. Soft Matter 2010; 6: 5157–5164.
32. Gursel YH, Senkal BF, Kandaz M, Yakuphanoglu F. Poly(N-vinylimidazole) based hydrogen bonded side chain liquid crystalline polymer. Polym. Adv. Technol. 2011; 22: 90–93.
33. Lemon MT, Jones MS, Stansbury JW. Hydrogen bonding interactions in methacrylate monomers and polymers. J. Biomed. Mater. Res. A 2007; 83: 734–746.
34. Rao KM, Rao, K S V Krishna, Ramanjaneyulu G, Rao KC, Subha MCS, Ha C-S. Biodegradable sodium alginate-based semi-interpenetrating polymer network hydrogels for antibacterial application. J. Biomed. Mater. Res. A 2014; 102: 3196–3206.
35. Lee KY, Mooney DJ. Alginate: Properties and biomedical applications. Prog. Polym. Sci. 2012; 37: 106–126.
36. Harding KG, Morris HI, Patel GK. Healing chronic wounds. Brit. Med. J. Int. ed. 2002; 324: 160–163.

37. Bianchi J. The effective management of exudate in chronic wounds. Wounds Int. 2012; 3: 14–16.
38. Burd A. Evaluating the use of hydrogel sheet dressings in comprehensive burn wound care. Ostomy Wound Manage. 2007; 53: 52–62.
39. You J-O, Rafat M, Almeda D, Maldonado N, Guo P, Nabzdyk CS, Chun M, LoGerfo FW, Hutchinson JW, Pradhan-Nabzdyk LK, Auguste DT. pH-responsive scaffolds generate a pro-healing response. Biomaterials 2015; 57: 22–32.
40. Koehler J, Wallmeyer L, Hedtrich S, Goepferich AM, Brandl FP. pH-modulating poly(ethylene glycol)/alginate hydrogel dressings for the treatment of chronic wounds. Macromol. Biosci. 2017; 17: 1600369.

Chapter 6

Buffering Hydrogel Wound Dressing Materials for a Universal Application onto Chronic Wounds

Abstract

A frequently neglected problem of chronic wounds is the associated shift of the wound pH. Yet, an excessively acidic or alkaline wound environment inhibits crucial healing processes such as cell migration, cell proliferation, and the proper activity of important enzymes. In this study, the development and characterization of buffering wound dressing materials is described. Poly(ethylene glycol) diacrylate (PEGDA) and alginate were combined with two different buffer systems, either modified 4-(2-hydroxyethyl)-1-piperazineethanesulfonic acid (HEPES) or acrylic acid (AA)/N,N-dimethylaminoethyl methacrylate (DMAEMA), to form pH-modulating hydrogels together. A variety of gels were analyzed in a bottom up approach, applying them in different wound healing assays. Thereby, the hydrogel composition 6.0% PEGDA/0.7% AA/2.8% DMAEMA/ 0.5% alginate was identified to be the most promising approach. The formulation was further examined for its material properties, showing an excellent fluid handling capacity in swelling (around 90% after 24 h) and water vapor transmission (304 $g \cdot h^{-1} \cdot m^{-2}$) experiments. An additional antimicrobial activity was achieved by the incorporation of poly(hexamethylene biguanide) hydrochloride (PHMB). The detected PHMB release was 3.8 – 7.0 mg per gram of hydrogel, dependent on the environmental pH. Considering all findings, the developed buffering hydrogel materials provide promising properties to serve as bioactive wound dressings for the treatment of chronic wounds.

1. Introduction

The pH value is an important parameter that characterizes the respective wound healing phase and might help predicting its success.[1] Normal wound healing is divided in three major phases: inflammation, proliferation, which includes granulation and epithelization, and remodeling of the original tissue.[2] The wound pH changes in accordance with the respective cellular processes over time (Figure 1), altered by different endogenous molecules like amino acids, fatty acids, lactic acid, and the sodium/hydrogen exchanger NHE1.[3,4]

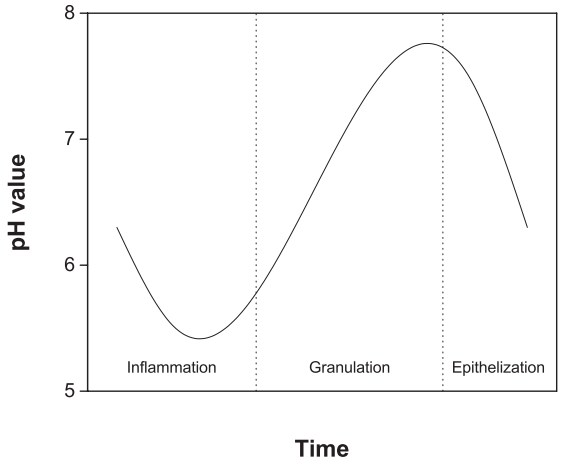

Figure 1. pH progression during normal wound healing.

The time course of the pH value in chronic wounds is different. Several clinical studies indicate that an alkaline pH is maintained permanently in the center of non-healing wounds (Figure 2).[3,5] A more recent study additionally identified a disadvantageous acidic environment (pH around 6.5) at the edges of chronic venous ulcers.[6] External factors which unbalance the wound pH are bacterial infections, necrosis, pus, and a disturbed skin barrier function.[3,7,8] In both cases (increased/decreased pH value), the interruption of the normal pH progression during wound healing causes numerous unfavorable effects. The migration and proliferation ability of dermal fibroblasts and keratinocytes are strongly dependent on the surrounding pH.[9] Furthermore, the optimal efficiency of human enzymes occurs at a very specific pH range. As a consequence, a pH shift might, amongst others, result in extracellular matrix degeneration by matrix metalloproteinases.[4] Biofilm production, an increased vulnerability to infections, and insufficient oxygen availability come along with it as well.[10]

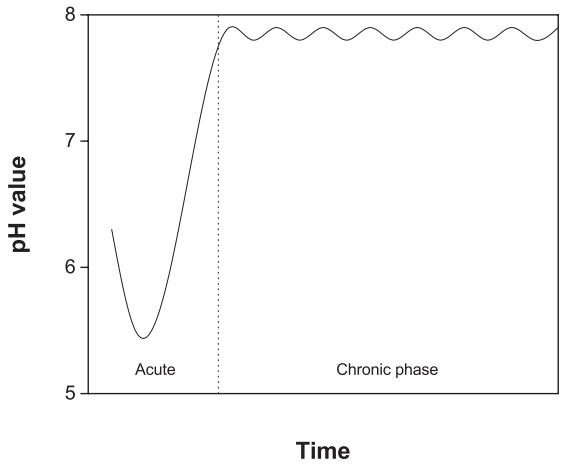

Figure 2. pH progression in chronic wounds suffering from an alkaline environment.

A precise pH-modifying treatment of chronic wounds might be a promising tool to finally enable wound healing. Some approaches were already described in literature. Chronic leg ulcers treated with an acidic rinsing solution (pH 6.0) showed an elevated epithelization and healing tendency in comparison to ulcers treated with a neutral emulsion (pH 7.3).[11] Furthermore, Leung et al. investigated the impact of acetic acid against bacterial load, finding an eradication rate of 97% after 5 weeks.[12] On the other hand, Sharpe et al. described a higher fibroblast and keratinocyte proliferation between pH 7.2 and 8.3.[9] Yet, a universal method for the successful treatment of pH-shifted chronic wounds is still missing.

Therefore, the aim of this study was the development of hydrogel wound dressing materials that are capable to act as interactive buffer in both, acidic and alkaline wound milieu. Hydrogels are particularly advantageous wound dressing materials, because they create a moist wound environment, which enhances for instance the re-epithelization.[13] Furthermore, their material properties are easily adaptable to the particular requirements by a precise modification of the polymer network. By this means, important wound dressing characteristics such as the exudate handling by evaporation/retention and uptake, and the mechanical stability and flexibility can be tuned.[14] Here, the recently described interpenetrating polymer network (IPN) hydrogel system poly(ethylene glycol) diacrylate (PEGDA)/alginate (see Chapter 2 for comparison) was supplemented with different buffer systems; modified 4-(2-hydroxyethyl)-1-piperazineethanesulfonic acid (HEPES) or a mixture of acrylic acid (AA) and N,N-dimethylaminoethyl methacrylate (DMAEMA) were incorporated in different concentrations. In a bottom-up approach, starting with cell-based assays, the developed hydrogels were analyzed for their ability to serve as buffering wound

dressing material. Based on the performance in contact with acidic and alkaline, two- and three-dimensional human skin wound models, a promising hydrogel formulation was identified. Further analysis was done concerning the important wound dressing material properties, such as the liquid uptake and the buffer capacity. To battle frequently occurring bacterial infections in chronic wounds, the buffering hydrogels were also examined for their suitability as antimicrobial drug release materials.[15]

2. Experimental Section

2.1 Materials

N,N-dimethylformamide extra dry (DMF) and toluene were obtained from Acros Organics (Geel, Belgium). Formaldehyde solution (4%) and reagents for hematoxylin and eosin (H&E) staining were obtained from Carl Roth (Karlsruhe, Germany). Diethyl ether and ethanol were purchased from CSC Jäcklechemie (Nürnberg, Germany). Deuterium oxide (D_2O) was purchased from Deutero GmbH (Kastellaun, Germany). Hydroxyethyl cellulose and poly(hexamethylene biguanide) hydrochloride (PHMB) solution were purchased from Fagron (Barsbüttel, Germany). HEPES was obtained from Fisher Scientific (Schwerte, Germany). Alginate (Protanal® LF 10/60FT) was kindly provided by FMC BioPolymer (Wallingstown, Ireland). Dulbecco's modified eagle medium/nutrient mixture F-12 (DMEM/F12), nutrient mixture F-12, and phosphate buffered saline (PBS) were obtained from Life Technologies (Carlsbad, CA, USA). Dimethyl sulfoxide (DMSO), glacial acetic acid, hydrochloric acid, sodium hydroxide, and triethylamine were purchased from Merck KGaA (Darmstadt, Germany). Deionized water was obtained using a Milli-Q water purification system (Millipore, Schwabach, Germany). All other chemicals were purchased from Sigma Aldrich (Taufkirchen, Germany).

2.2 Precursor Synthesis

HEPES acrylate (HEPESac) was synthesized under argon atmosphere (water and oxygen free conditions). For this purpose, 3.56 g HEPES (14.94 mmol) and 75 mL dry DMF were cooled down to 0 °C. 4.989 mL triethylamine (35.79 mmol) and 5.850 mL acryloyl chloride (58.02 mmol) were slowly pipetted to the solution. The reaction mixture was stirred overnight, filtered, and precipitated in 900 mL of ice-cold diethyl ether. The product was recrystallized from ethanol and dried under vacuum to yield 2.01 g (46.1%).

^{1}H NMR (300 MHz, D_2O, δ): 3.35 ppm (t, 4 H, -CH_2CH_2N-), 3.62 ppm (m, 10 H, -NCH_2CH_2N- and -CH_2CH_2S-), 4.53 ppm (t, 2 H, -OCH_2-), 6.00 ppm (d, 1 H, CH_2=CHC(O)O-), 6.20 (dd, 1 H, CH_2=C*H*C(O)O-), 6.46 ppm (d, 1 H, CH_2=CHC(O)O-). Poly(ethylene glycol) diacrylate (PEGDA) was synthesized as previously reported.[16]

2.3 Preparation of Hydrogels

The precursor mixtures were prepared as follows. PEGDA was dissolved in PBS and a suspension of the radical initiator 2-hydroxy-4′-(2-hydroxyethoxy)-2-methylpropiophenone (HHMP) in PBS was pipetted to the stirring solution. Then, a solution of alginate in PBS (c = 41.7 mg·mL^{-1}) and the required amount of AA, DMAEMA, or HEPESac solution were added drop-wise. The overall concentration of the polymer components was 10% in all groups. The assessed hydrogel formulations are listed in Table 1.

Table 1. Composition of the examined hydrogels. * The amount of radical initiator was related to the total monomer mass.

	Control gel	**HEPESac gel**	**AA DMAEMA gel**
PEGDA (%)	9.50	8.00 – 9.00	6.00
Alginate (%)	0.50	0.50	0.50
AA (%)	0	0	0.35 – 1.05
DMAEMA (%)	0	0	2.45 – 3.05
HEPESac (%)	0	0.50 – 1.50	0
HHMP (%)*	1.80	1.80	2.50

For skin construct healing assays, 1.4 mL of the precursor solution were cast into a 6 well-plate; for tensile testing and water vapor transmission studies, 8 mL of the precursor solution were cast into rectangular silicon molds. For all other experiments, cylindrical glass molds (1 cm diameter, 0.7 mL volume) were used. All samples were irradiated with UV light (366 nm, 6 W, 1 h 15). When indicated, the hydrogels (initial mass m_i) were purified for 24 h at 37 °C in 10 mL of PBS. Afterward, the induced weight gain was reversed by exposing the hydrogels to a stream of compressed air until m_i had been reached again.

2.4 Dynamic and Static pH Titration

For dynamic titrations, a mixture of the respective buffer (HEPES, HEPESac, or AA/DMAEMA with a mass ratio of 1:9, 1:4, or 3:7) and 15 mL of a 0.1 M sodium chloride solution was brought to pH 2.0 with 0.1 M HCl. The titration against 0.1 M NaOH was performed with a BlueLine glass electrode connected to a TitroLine 7000 dosage system (SI Analytics GmbH, Mainz, Germany). The buffer capacity range was identified based on the slope of the recorded titration curves.[17]

For static pH titrations, purified hydrogel cylinders were added to 15 mL of a 0.1 M sodium chloride solution. The pH was kept constant for 24 h by adding 0.1 M HCl (pH 7.0) or 0.1 M NaOH (pH 7.4). The acid (*ANC*) and base (*BNC*) neutralizing capacity were calculated according to Equation (1) and (2), respectively,

$$ANC = \frac{n(HCl)}{m_0} \qquad (1)$$

$$BNC = \frac{n(NaOH)}{m_0} \qquad (2)$$

where n is the amount of neutralized titrant and m_0 is the initial mass of the gel cylinder.

2.5 Cell Viability and Healing Assays

In vitro cell viability and healing assays were conducted as described previously.[16] In brief, the cell viability was evaluated in a common extract MTT assay.[18,19] For this purpose, hydrogel extracts (pH-modified extraction medium consisting of medium 199/F12 3:1, 10% fetal bovine serum (FBS), and 1.10 mM hydrocortisone, adjusted to pH 8.0 with 1 M NaOH or pH 6.0 with 1 M HCl) of different incubation intervals were pipetted to cultured adult human dermal fibroblasts (HDFa); pH-modified medium served as a control. After 24 h, the extract medium was exchanged by 130 µL of DMEM/F12, 50 µL of a MTT solution (c = 2.5 mg·mL^{-1} in PBS), and 20 µL of FBS. After further 4 h, the resulting blue dye was dissolved in 100 µL of a sodium dodecyl sulfate solution (c = 0.35 mmol·mL^{-1} in glacial acetic acid/DMSO 1:159) and the absorbance (A) at 570 and 690 nm was measured after 3 h of incubation at room temperature using a FluoStar Omega micro plate reader (BMG Labtech, Ortenberg, Germany). The cell viability (v) was calculated according to Equation (3). The data are presented as mean ± standard deviation (SD; n = 6).

$$v = \frac{A_{570,gel} - A_{690,gel}}{A_{570,ctrl} - A_{690,ctrl}} \cdot 100\% \qquad (3)$$

For two-dimensional (2D) cell migration assays, HDFa were seeded in cell culture inserts (Ibidi GmbH, Martinsried, Germany). After 24 h, the inserts were removed, and 8 mL of pH-modified medium (pH 6.0 or 8.0) and purified hydrogels in netwell inserts (Corning, Corning, NY, USA) were added; untreated cells served as a control. Every 12 h, the pH-modified medium was replaced. The cell migration was observed over 48 h using an Axiovert 200 microscope with a LSM 510 laser-scanning device (Zeiss, Jena, Germany). The area of cell migration was calculated using the LSM image browser (Zeiss, Jena, Germany); the cell migration velocity was calculated from the slope of the area closure/time curve.

Human skin constructs* were built according to the previously published method,[16] and wounds were induced by cutting the epidermal layer with a scalpel. The injured constructs were incubated with pH-adjusted medium (pH 6.5 or 8.0) containing 2.5% hydroxyethyl cellulose. The purified hydrogels were punched out in circular shape (1 cm diameter) and applied onto the wound. The medium was exchanged daily; the dressings were exchange after 2 days. After a healing period of 4 days, the constructs were embedded in tissue freezing medium, cut vertically into slices (7 µm) using a Leica CM1510 S cryotome (Leica Biosystems, Nussloch, Germany), and stained with conventional H&E according to standard protocols. The length of cell ingrowth was measured on microscope images (BZ-8000 microscope, Keyence, Neu-Isenburg, Germany) with ImageJ (National Institutes of Health, Bethesda, Maryland, USA).

2.6 Fluid Handling Capacity

Hydrogel cylinders were incubated in 10 mL of PBS at 37 °C in a shaking water bath. Every 24 h, the hydrogels were gently blotted dry and weighed. The swelling capacity (Q_t) was calculated according to Equation (4),

$$Q_t = \frac{m_t - m_0}{m_0} \cdot 100\% \qquad (4)$$

where m_t is the mass of the gel cylinder at time point t and m_0 is the initial mass of the gel.

The water vapor transmission rate (WVTR) was determined according to the ASTM E96/E96M-12 inverted water method.[20] Hydrogel sheets were fixed at a circular WVTR test dish (test area A = 10.18 cm^2) carrying 5 mL of deionized water. Water loss at 37 °C

* 3D human skin constructs were generated at the Institute of Pharmacy, Pharmacology and Toxicology, Freie Universität Berlin, with support and based on the method of S. Hedtrich and L. Wallmeyer.

and 21% relative humidity was measured every hour (0 – 10 h and ≥ 24 h) and the WVTR was calculated from the slope of the time/water loss curve (*G*) according to Equation (5).

$$WVTR = \frac{G}{A \cdot 1\text{h}} \qquad (5)$$

2.7 Mechanical Properties and Microstructure

The mechanical performance of the hydrogels was examined under tensile and compressive load with and without prior purification. The detailed procedure was described recently.[16] In brief, the hydrogel samples were loaded until failure, using an Instron 5542 load frame (Instron GmbH, Darmstadt, Germany). The detected maximum load under compression ($F_{max,c}$) and tension ($F_{max,t}$) was used to calculate the respective maximum stress (σ_c and σ_t) according to Equation (6) and Equation (7),

$$\sigma_c = \frac{F_{max,c}}{h \cdot d} \qquad (6)$$

$$\sigma_t = \frac{F_{max,t}}{h \cdot d} \qquad (7)$$

where h is the height and d is the diameter of the examined hydrogel sample. The elastic moduli (E_c and E_t) were calculated from the slope of the stress-strain curves between 0.05 and 0.15 strain.

Scanning electron microscopy (SEM) was conducted on lyophilized, gold-coated hydrogel cylinders. The samples were examined with a Crossbeam XB 340 scanning electron microscope (Zeiss, Jena, Germany) at a working voltage of 3.0 kV.

2.8 Drug Release

Hydrogel cylinders were loaded at 37 °C in 10 mL of a PHMB solution (c = 2 mg·mL^{-1} in saline) for 24 h. The antimicrobial drug release was detected in 10 mL of PBS (pH adjusted to 6.0/7.4/8.0) at 33 °C in a shaking water bath. Over a period of 7 days, 200 µL samples were taken and replaced by fresh buffer solution. The samples were stored at 4 °C until the experiment was completed. For the colorimetric concentration measurements, 10 µL of a sodium acetate solution (10 w% in deionized H_2O), 25 µL of an Eosin Y solution (0.025 w% in deionized H_2O), and 200 µL of diluted PHMB solution were mixed and stored in the dark for 15 min.[21] The altered Eosin Y absorbance at 545 nm was measured with a FluoStar Omega micro plate reader (BMG Labtech, Ortenberg, Germany). The PHMB release was calculated based on calibration measurements; the

amount of the initial PHMB load was calculated from the remaining volume of the incubation solution and its concentration.

2.9 Statistical Analysis

If not stated otherwise, the experiments were done in triplicate and the data are presented as mean ± SD. For statistical analysis, Brown Forsythe tests were run followed by one-way ANOVA/Tukey' test or Kruskal-Wallis-ANOVA. Differences were considered statistically significant at $p < 0.05$.

3. Results

3.1 Monomolecular Buffering System

Two different strategies for the development of buffering hydrogel materials were pursued. The first approach was an incorporation of the zwitterionic and biocompatible buffer molecule HEPES (pK_a = 7.5)[22] into the covalent network of the previously developed PEGDA/alginate IPN hydrogel system (see Chapter 2 for comparison). For this purpose, HEPES was chemically modified by introducing a reactive double bond, yielding HEPES acrylate (HEPESac) (Scheme 1).

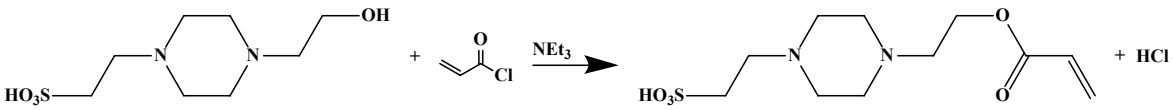

Scheme 1. Synthesis of HEPES acrylate.

The maximally possible HEPESac concentration in PEGDA/HEPESac/alginate hydrogels was 1.5%. At higher HEPESac ratios a great amount of white precipitation occurred in the precursor mixture. Therefore, further experiments were conducted with hydrogels carrying 0.5 - 1.5% HEPESac only.

3.1.1 Wound Healing Capacity

The time- and pH-dependent wound healing capacity of PEGDA/HEPESac/alginate IPN hydrogels was examined in 2D cell migration assays. 2D wound models suffering from non-physiological pH values (control pH 6/pH 8 in Figure 3) showed a slow cell migration into the "wound" area and a closure of only 29 and 51%, respectively. The application of PEGDA/alginate control hydrogels significantly enhanced the cell migration velocity in both groups and enabled a complete gap closure in spite of an alkaline environment.

Further improvement of the healing process by the addition of buffering HEPESac containing hydrogels could not be achieved.

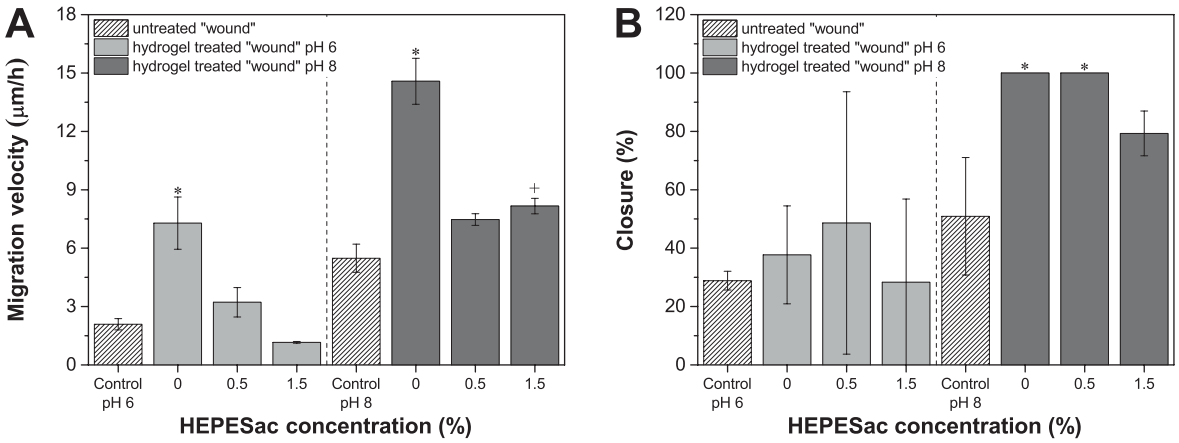

Figure 3. Cell migration velocity (A) and percentage of "wound" closure (B) in 2D migration assays with different IPN hydrogels applied. Data are expressed as mean ± SD (n = 3). + indicates statistically significant differences versus the untreated control ($p < 0.05$); * indicates statistically significant differences to all group members ($p < 0.05$).

The hydrogel cytotoxicity was determined via dye conversion in MTT assays. The results in Figure 4 indicate that none of the developed HEPESac gels were cytotoxic, as a cell viability of around 100% was maintained for all samples.

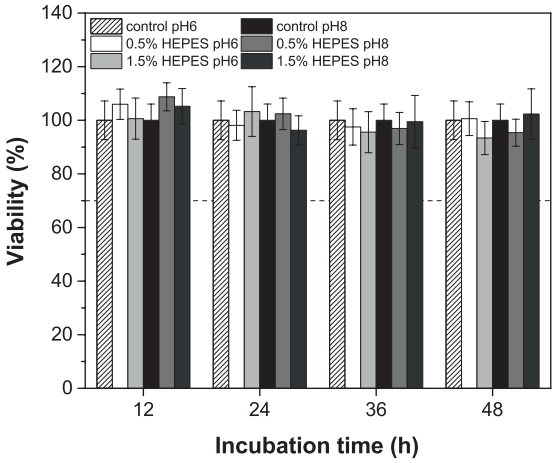

Figure 4. Viability of HDFa in contact with different PEGDA/HEPESac/alginate hydrogel extracts. The broken line (---) marks the critical value of 70% cell viability.[18] Data are expressed as mean ± SD (n = 6).

3.1.2 Buffer Capacity

The buffer capacity range of HEPES and HEPESac was verified in a titration against sodium hydroxide (Figure 5). Sections with a reduced slope, calculated by the first

derivation of the titration curve (data not shown), correspond to the buffer range.[17] In accordance to the literature, unmodified HEPES had a buffering effect between pH 6.8 and 8.2,[23] whereas a solution of modified HEPESac showed a flattened curve at a much more alkaline pH (pH > 8).

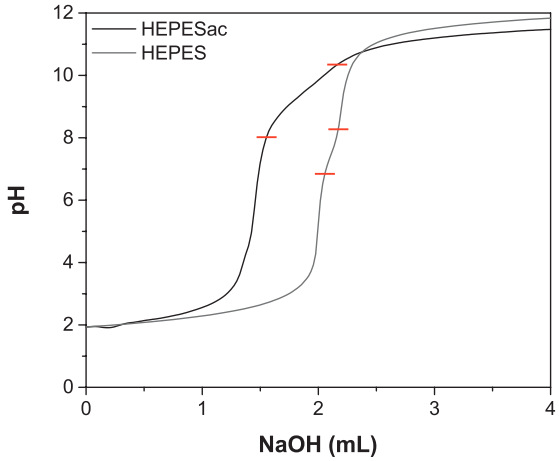

Figure 5. Titration of HEPES (grey curve) and HEPESac (black curve) solution against 0.1 M NaOH. Red horizontal lines mark the buffer capacity range.

As no satisfactory buffer and wound healing capacity could be detected for HEPESac and HEPESac containing hydrogels, further research focused on hydrogel formulations with a different, bimolecular buffering system.

3.2 Bimolecular Buffering System

A second approach to develop buffering hydrogel wound dressings was based on the previous work concerning acidic and alkaline hydrogels.[16,24] The IPN hydrogel formulation PEGDA/alginate (see Chapter 2 for comparison) was complemented with acrylic acid and 2-dimethylaminoethyl methacrylate as bimolecular buffering system (Scheme 2).

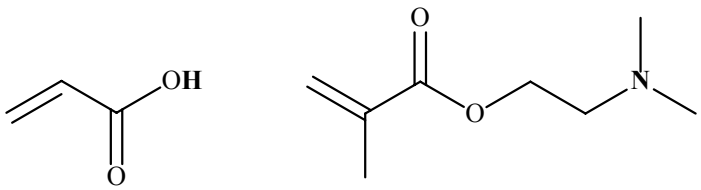

Scheme 2. Structural formula of AA (on the left) and DMAEMA (on the right).

3.2.1 Buffer Capacity

Potentially effective AA/DMAEMA ratios were determined in dynamic titrations against sodium hydroxide (Figure 6). As described above, the titration curve sections with a reduced slope correspond to the buffer capacity range. The results for the AA/DMAEMA buffer system are listed in Table 2. Based on these findings, three promising hydrogel formulations (0.35/0.70/1.05% AA content) were chosen for further investigations. The total buffer concentration in all hydrogel formulations was set to 3.5%, thus combining sufficient hydrogel mechanical stability with the greatest possible buffer content.

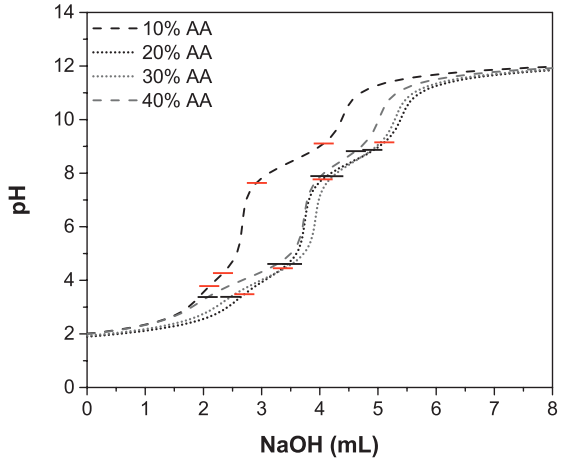

Figure 6. Titration of different AA/DMAEMA mixtures with 0.1 M NaOH. Red horizontal lines mark the buffer range of 10% and 20% AA mixtures; black horizontal lines mark the buffer range of 30% and 40% AA mixtures.

Table 2. pH-range of the buffer capacity of different AA/DMAEMA buffer systems, and the consequently examined hydrogel formulations.

Buffer system	pH (buffer capacity)	Hydrogel formulation
10% AA 90% DMAEMA	4.0 – 4.2, 7.8 – 9.2	0.35% AA 3.15% DMAEMA 6.00% PEGDA 0.50% alginate
20% AA 80% DMAEMA	3.5 – 4.6, 7.8 – 9.1	0.70% AA 2.80% DMAEMA 6.00% PEGDA 0.50% alginate
30% AA 70% DMAEMA	3.4 – 4.8, 7.9 – 9.0	1.05% AA 2.45% DMAEMA 6.00% PEGDA 0.50% alginate
40% AA 60% DMAEMA	3.3 – 4.9, 8.1 – 9.0	-

3.2.2 Wound Healing Capacity

Analogous to the experiments on HEPESac containing hydrogels, the ability of AA/ DMAEMA containing gels to promote wound healing in 2D migration assays was determined at first (Figure 7).

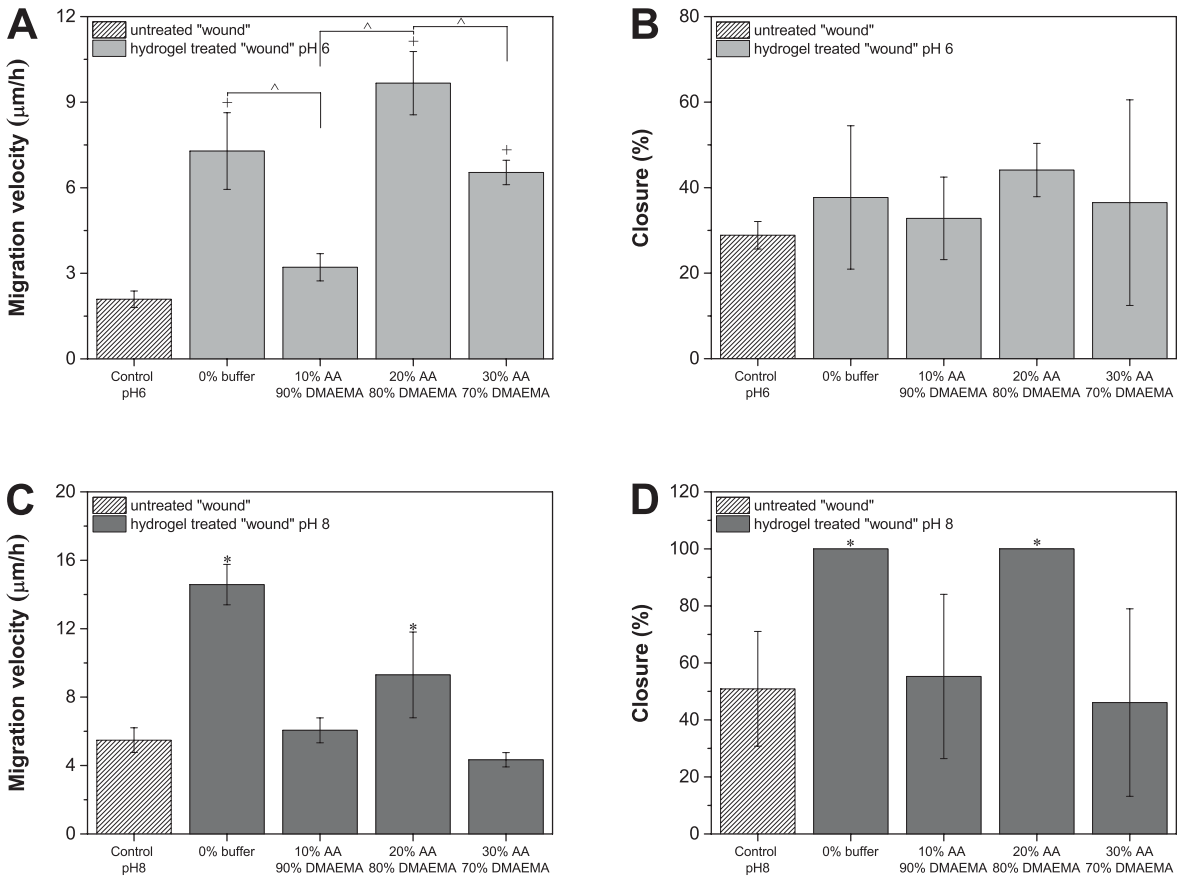

Figure 7. Cell migration velocity (A, C) and percentage of "wound" closure (B, D) in 2D migration assays with different AA/DMAEMA containing hydrogels applied at pH 6 (A, B) and pH 8 (C, D). Data are expressed as mean ± SD (n = 3); + indicates statistically significant differences versus the untreated control ($p < 0.05$); * indicates statistically significant differences to all group members ($p < 0.05$); ^ indicates statistically significant differences between the selected groups.

The most effective buffer system was the formulation with an AA/DMAEMA ratio of 20/80%; significantly enhanced cell migration velocities of 9.7 ± 1.1 μm (pH 6) and 9.3 ± 2.5 μm (pH 8) could be achieved in comparison to the respective controls (Figure 7A and C). The "wound" closure could not be improved significantly in acidic environment (around 44%); however, a complete gap closure occurred in alkaline environment (Figure 7B and D). Therefore, further tests were conducted with the PEGDA/ 0.7% AA/2.8% DMAEMA/alginate hydrogel formulation only. In comparison to the non pH-modifying hydrogel PEGDA/alginate (0% buffer), the cell migration velocity could be

enhanced by AA/DMAEMA (0.7/2.8%) containing hydrogel treatment at pH 6, but showed reduced values at pH 8; the amount of gap closure was slightly higher after the treatment with the buffering material.

The cytotoxicity of AA/DMAEMA (0.7/2.8%) containing hydrogels was determined in MTT assays. The cell viabilities were around 100% in all cases, indicating that the developed buffering hydrogel materials are non-cytotoxic (Figure 8).

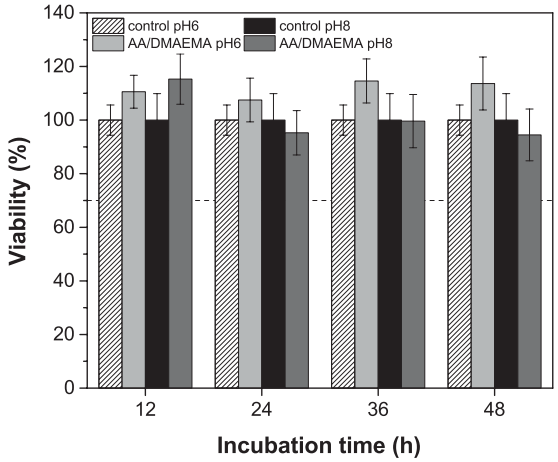

Figure 8. Cell viability of HDFa in contact with AA/DMAEMA containing (0.7/2.8%) IPN hydrogel extracts with different pH values. The broken line (---) marks the critical value of 70% cell viability.[18] Data are expressed as mean ± SD (n = 6).

A more detailed impression on the wound healing capacity of AA/DMAEMA (0.7/2.8%) containing IPN hydrogels was gained by applying them on three-dimensional (3D) wounded human skin constructs. Human skin models were chosen instead of animal models as the pH value of the in vitro wounds can easily be adapted by changes in the supplying cell culture medium. Representative images from the acidic and the alkaline control in comparison to the buffer hydrogel treated constructs are given in Figure 9. The natural structure of the skin, including the stratum corneum (S), the epidermis (E), and the dermis (D), was clearly visible (see Figure 9A for details). Wounds suffering from an acidic pH only showed a marginal tendency of keratinocyte migration. In contrast, complete wound closure with a thin layer of keratinocytes occurred already four days after AA/DMAEMA containing hydrogel treatment (Figure 9B). The significantly enhanced cell ingrowth amounted 402 ± 173% (Figure 10).

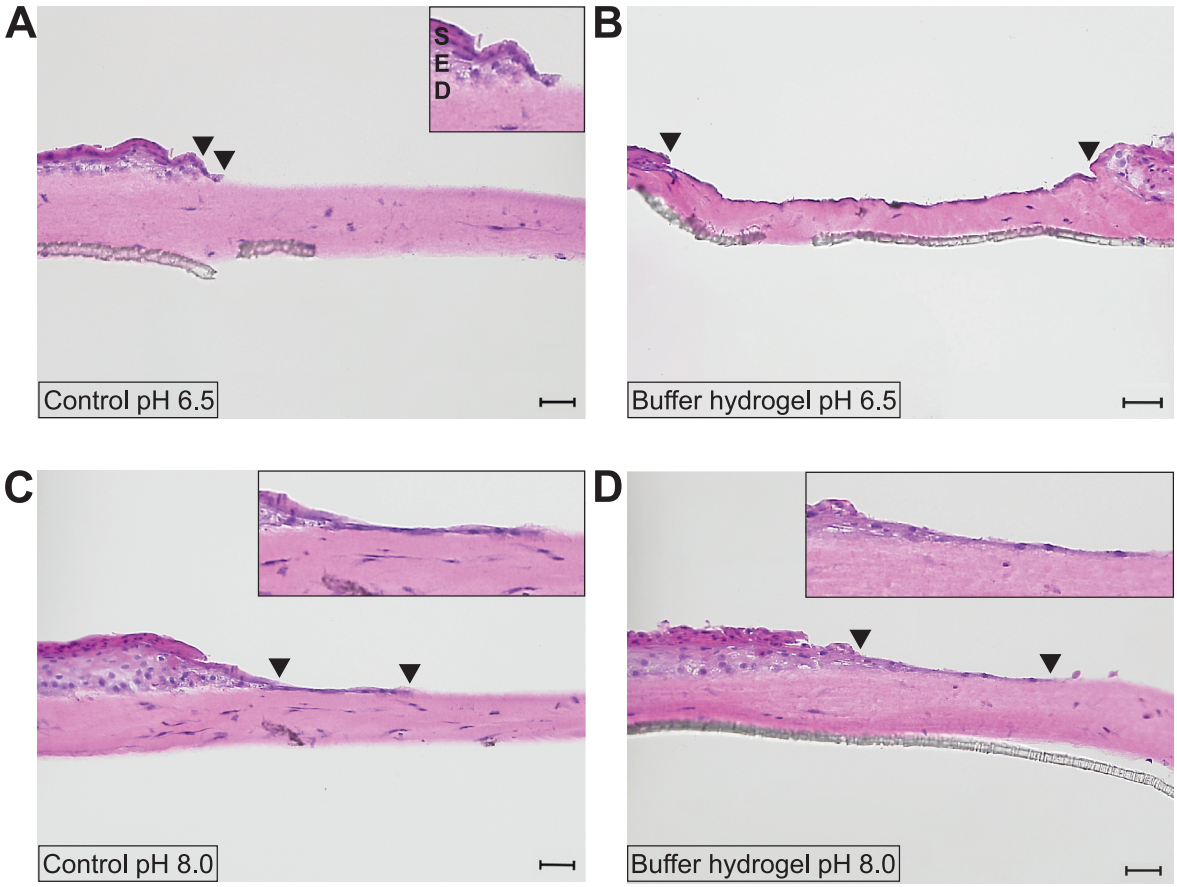

Figure 9. H&E stained histological images of injured skin constructs after a healing period of 4 days. The stratum corneum (S), epidermis (E), and dermis (D) equivalents are clearly visible. The untreated controls are shown on the left; skin constructs treated with AA/DMAEMA (0.7/2.8%) containing hydrogels are shown on the right. The length of cell ingrowth is indicated by triangles; the insets show a magnification of this area. The length of the scale bars is 50 μm.

The absolute amount of wound closure in alkaline wounds appeared to be higher than in acidic wounds (Figure 9C). As a result, the relative enhancement of wound closure caused by buffering hydrogel treatment at pH 8 was only around 68% (Figure 9D and Figure 10). Unlike 2D migration experiments indicated, applying non pH-modifying PEGDA/alginate hydrogels ("0% buffer" in Figure 10) had a smaller effect on wound closure than the treatment with buffering dressing materials.

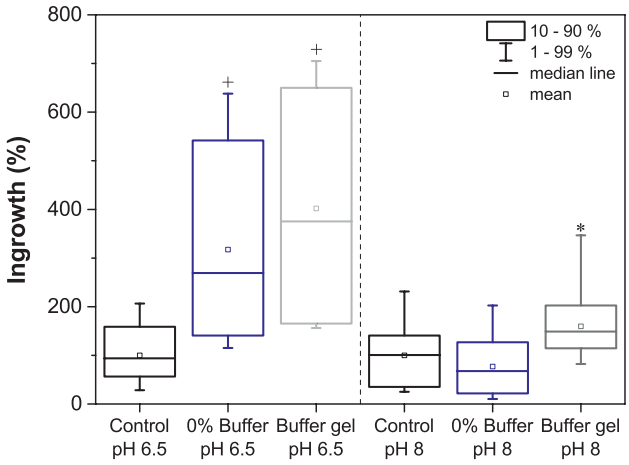

Figure 10. Ingrowth length in the untreated controls (mean set as 100%), and in skin constructs treated with 0% and 3.5% AA/DMAEMA containing hydrogels at pH 6.5 and pH 8. Data are expressed as boxplot (10 - 90%); + indicates statistically significant difference versus the untreated control ($p < 0.05$); * indicates statistically significant differences to all group members ($p < 0.05$).

3.2.3 Fluid Handling Capacity

Since the hydrogel formulation PEGDA/0.7% AA/2.8% DMAEMA/alginate was proven to be a promising treatment option for wounds suffering from non-physiological pH values, its material properties were subsequently examined. Indispensable properties of wound dressings are their liquid uptake (swelling), their water vapor transmission rate (WVTR) and, in the case of buffering dressings, their acid and base neutralizing capacity (ANC, BNC).[25,26] The partial replacement of PEGDA by AA/DMAEMA influenced all listed parameters (Table 3); the swelling capacity more than doubled after 24 hours and 7 days, the WVTR increased by 77%, and the buffer capacity rose from 0 to 0.025 (ANC) and 0.008 mmol·g^{-1} (BNC).

Table 3. Fluid handling characteristics and buffer capacity of different IPN hydrogels.

	9.5% PEGDA/ 0.5% alginate	**9.5% PEGDA/0.7% AA 2.8%DMAEMA/0.5% alginate**
Swelling 24 h (%)	40.05 ± 5.75	89.39 ± 4.72
Swelling 7 d (%)	41.19 ± 5.74	93.01 ± 5.98
WVTR (g·h^{-1}·m^{-2})	171.40 ± 0.30	304.14 ± 1.58
ANC (mmol·g^{-1})	0	0.025 ± 0.006
BNC (mmol·g^{-1})	0	0.008 ± 0.002

3.2.4 Mechanical Properties and Microstructure

In accordance with the highly porous and fibrous microstructure of the favorable AA/ DMAEMA (0.7/2.8%) containing IPN hydrogels (Figure 11A – C), the maximum tensile stress, σ_t, was rather low (29.1 ± 7.7 kPa; Figure 11D). The maximum compressive stress, σ_c, decreased from 199.1 ± 21.2 kPa to 118.5 ± 34.9 kPa due to an additional purification step in PBS. The calculated E-modulus was around 40 kPa for applied tensile and around 20 kPa for applied compressive load.

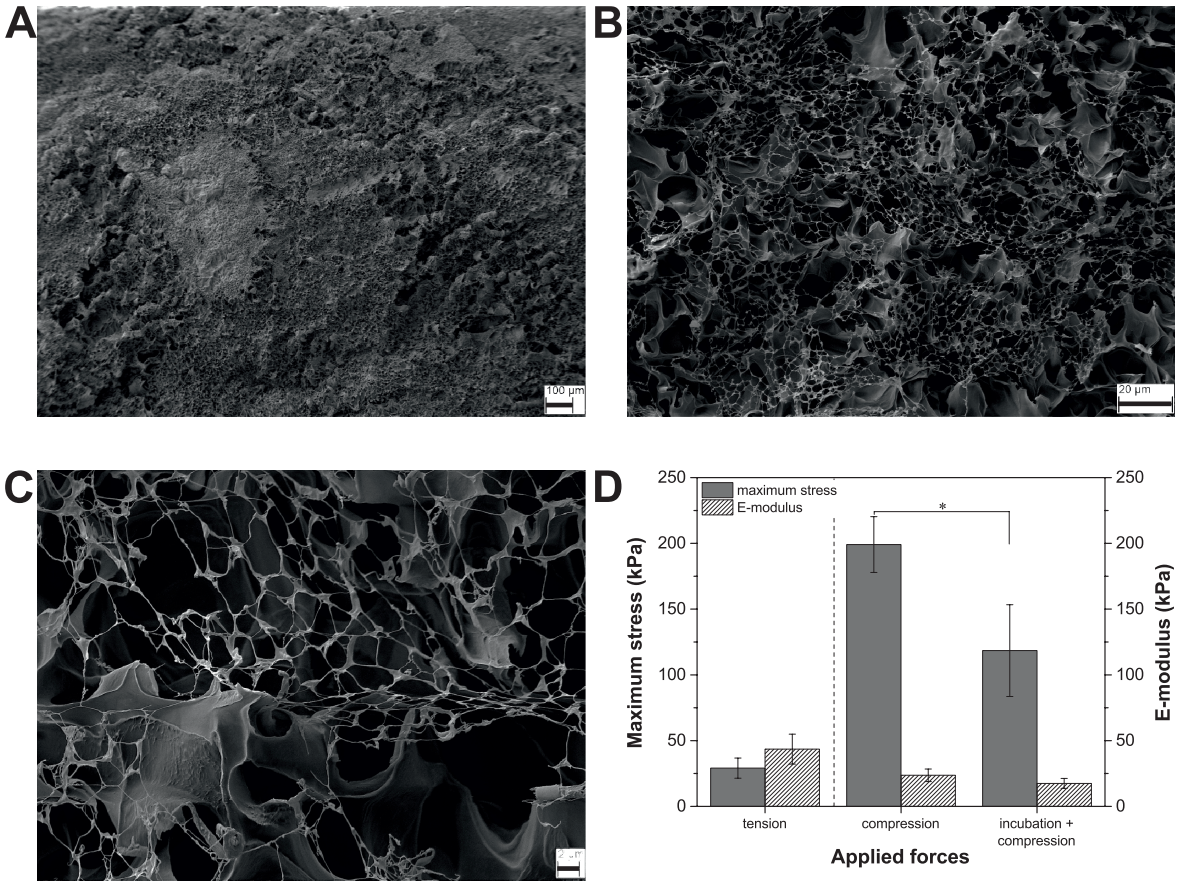

Figure 11. SEM images of lyophilized AA/DMAEMA (0.7/2.8%) containing IPN hydrogels with 50x (A), 500x (B), and 2000x (C) magnification. The length of the scale bars is 100/20/2 µm, respectively. Maximum stress σ_t/σ_c and calculated E-modulus E_t/E_c of AA/DMAEMA (0.7/2.8%) containing hydrogels under tensile and compressive load (D). Data are expressed as mean ± SD (n = 3). * indicates statistically significant differences between the selected groups ($p < 0.05$).

3.2.5 Drug Release

Apart from their pH-modulation capacity, the developed IPN hydrogels were also examined for their potential ability to release the antimicrobial drug PHMB to the wound site. The release rate of PHMB was strongly dependent on the surrounding pH (Figure 12).

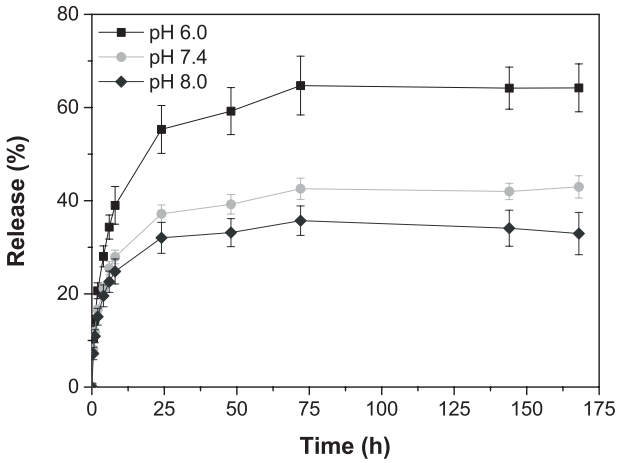

Figure 12. Percentage PHMB release from PEGDA/0.7% AA/2.8% DMAEMA/alginate IPN hydrogels at different pH values.

The highest maximal release of 64.2 ± 5.2% was detected in an acidic environment at pH 6.0. With rising pH, the PHMB release dropped to 43.0 ± 2.4% (pH 7.4) and 33.0 ± 0.7% (pH 8.0). Related to the initial load of approximately 11.2 mg PHMB per gram of hydrogel, a release of 7.0, 4.8, and 3.8 mg per gram of hydrogel could be achieved, respectively.

4. Discussion

4.1 Monomolecular Buffering System

The developed HEPES acrylate containing hydrogels did not show a convincing performance in wound healing assays. Since potential cell toxicity can be excluded (see Figure 4 for comparison), other factors must be responsible for these findings. One difficulty is displayed in the titration experiments. The buffer capacity of HEPES (pH 6.8 – 8.2) was shifted to higher pH values after the addition of the acrylate group. This might be due to steric hindrance, affecting the protonation of the preferred amino group (Scheme 3). After the polymerization of HEPESac, the spatial extent of the residue R is even more pronounced.

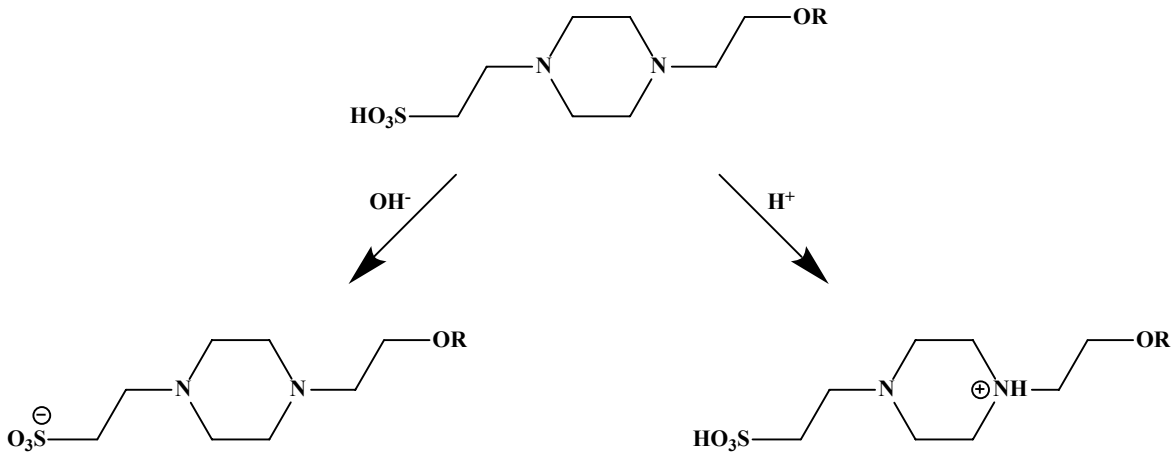

Scheme 3. (De-)Protonation of HEPES (R = H) and HEPESac (R = $C(O)C_2H_3$).[27]

Furthermore, complexation between HEPESac and alginate is an unwanted side effect during hydrogel formation.[28] Even though a white precipitation is only visible for high HEPESac concentrations (> 1.5%), precursor mixtures with lower HEPESac concentrations showed an elevated turbidity, pleading for the appearance of complexes as well. Occurring complexation is also in accordance with the findings in 2D wound healing assays. When alginate is taken out of the system by complexation with HEPESac, its ability to enhance the cell migration is suppressed. Considering all findings, the examined HEPESac containing hydrogels are not suitable for a buffering wound dressing application.

4.2 Bimolecular Buffering System

Alternatively, hydrogels with the bimolecular buffer AA/DMAEMA were analyzed. In 2D wound healing assays, the hydrogel formulation with a molar AA to DMAEMA ratio of 0.55 (0.70% AA/2.8% DMAEMA) appeared to be the most effective buffer system. Although, the amount of carboxylic acid groups is 45% lower than the amount of amino groups, the buffer capacity is balanced out for both, an acidic and an alkaline environment. This can be explained by the dominant AA acidity ($pK_a = 4.3$) which is significantly higher than the DMAEMA alkalinity ($pK_b = 5.6$).[29,30] In hydrogels with higher (1.05%) or lower (0.35%) AA concentrations, one part of the bimolecular buffer systems is predominant and therefore, an adequate pH regulation cannot take place. However, the supportive healing effect of the favorable pH-modulating hydrogel formulation is slightly reduced in alkaline medium, compared to the non pH-modifying PEGDA/alginate control gel. As already described for HEPESac containing gels, there might be a complexation between DMAEMA amino groups and alginate carboxylic acid groups. Yet, diffusing alginate

enhances the cell proliferation,[31] explaining the high wound healing capacity of PEGDA/ alginate gels. The findings on 3D wounded human skin constructs underline that the favorable PEGDA/0.7% AA/2.8% DMAEMA/alginate IPN hydrogels are non-cytotoxic. With the reduction of the liquid/hydrogel interface, the positive effect of diffusing alginate is reduced. In this more realistic chronic wound model, the supportive healing effects of alginate containing and pH-modulating wound dressings can clearly be separated.

Besides actively supporting the wound healing process, wound dressing materials must also fulfill several requirements concerning their material properties. The dressings should guarantee a moist wound bed environment, but at the same time, they should be capable to absorb excessive amounts of wound exudate.[2,26] Hydrogels enable both processes, liquid uptake and release, determinable via swelling and WVTR experiments. The WVTR of commercially available products ranges from 3.75 to 390 $g \cdot h^{-1} \cdot m^{-2}$, dependent on their composition.[32] The required liquid uptake for chronic wound dressings was recently calculated to be 57% or higher, related to the here examined sample size and shape.[16] Thus, the described buffering hydrogels perfectly meet both demands.

The ability of a material to intercept increased acid and base concentrations can be quantified by the acid and base neutralizing capacity.[25,33] Only little data can be found in literature describing ANCs or BNCs of wound dressings. Recently, comparable values were reported on promising acidic (BNC = 0.012 $mmol \cdot g^{-1}$) and alkaline (ANC = 0.010 - 0.031 $mmol \cdot g^{-1}$) hydrogel wound dressing materials.[16,24] The buffer capacity of the described AA/DMAEMA containing hydrogels was further evaluated in an indirect way, based on the conducted cell assays. Hence, the designed hydrogels are competitive buffering wound dressings.

The microstructure of the buffering hydrogels is related to the incorporation of AA and DMAEMA molecules. In comparison to non-buffering PEGDA/alginate gels (see Chapter 2 and 3 for comparison), great changes in the gel architecture are estimated. The buffer monomers AA and DMAEMA, which carry only one double bond per molecule in contrast to PEGDA, can contribute to chain growth, but cannot contribute to the three-dimensional network formation.[34] Additional superficial fiber formation (Figure 11C) might be caused by intermolecular interactions between DMAEMA amino groups, and AA and alginate carboxylic acid groups.[35,36] The resulting porous microstructure has, together with the incorporated charges, a positive impact on the osmotic pressure, driving the swelling capacity.[37,38]

The mechanical performance of the buffering gels is comparable to already described PEG-based hydrogels, which generally fail between 4 and 201 kPa with an E-modulus of 20 to 230 kPa.[39–43] Furthermore, the developed materials can maximally be deformed by 92% (data not shown), which is consistent with the elasticity of the human skin (70 – 100%).[44,45] Incubation in PBS, an essential step of purification from initiator and unreacted monomer prior to a biomedical application, effected significantly reduced σ_c values. These changes might be caused by ion exchange processes between PBS (K^+, Na^+, Cl^-, HPO_4^-) and the hydrogels, resulting in a break of stabilizing ionic interactions between carboxylic acid and amino groups.[46,47] Nevertheless, the mechanical properties still fit the described ranges of PEG-based hydrogels and fulfill the needs of wound dressing materials (elasticity $\geq$ 70%, sufficient mechanical stability for handling, application, and removal).[14,48]

The microbial infection of a wound has a wide range of consequences.[49] Bacterial waste products impair the healing process. Furthermore, the wound pH is shifted versus acidic or alkaline values, dependent on the sort and the amount of the present microbes. For not only treating the consequences, but also handling the initial cause of the pH-shift in infected, chronic wounds, the promising AA/DMAEMA (0.7/2.8%) containing IPN hydrogels were loaded with the antimicrobial drug PHMB. The detected drug release from the buffering hydrogels ranged between 33 and 64%. The incomplete PHMB release is related to hydrogen bonds and ionic interactions between the drug molecules, which carry positively charged imine groups, and the hydrogel, which carries negatively charged carboxylic acid groups (alginate, AA).[50] With increasing pH, the amount of protonated carboxyl groups is rising. Furthermore, the amount of positively charged amino groups of the hydrogel (DMAEMA) is rising as well. The resulting reduced attractive and increased repulsive forces enable an enhanced drug release at lowered pH values. The initial amount of PHMB in the hydrogels (approximately 1.12%) was higher than in commercially available dressings (0.10 – 0.65% PHMB, e.g., Suprasorb X + PHMB (Lohmann & Rauscher), Kendall (AMD), Prontosan (B. Braun Medical Ltd)). However, the effective PHMB concentration was 0.38 – 0.70%, which perfectly matches the aimed concentration range.

5. Conclusion

Due to the combination of acidic and alkaline monomers with PEGDA and alginate, buffering IPN hydrogel wound dressings could be developed. Their wound healing capacity was proven by 2D and 3D wound models, based on primary human dermal fibroblasts and keratinocytes. The performance of the buffering hydrogels was competitive with the recently examined performance of acidic wound dressings applied on alkaline wound models and alkaline dressings applied on acidic wound models.[16,24] Consequently, the described dressings might be applied in either case, representing a universal treatment option for wounds suffering from a non-physiological pH-shift. Moreover, the material properties were found to be sufficient for the desired application, allowing a high liquid uptake, mechanical flexibility, and antimicrobial drug release. Further research should focus on the variation of the incorporated pH-active monomers, targeting even higher buffer capacities for longer lasting wearing times.

References

1. Dargaville TR, Farrugia BL, Broadbent JA, Pace S, Upton Z, Voelcker NH. Sensors and imaging for wound healing: A review. Biosens. Bioelectron. 2013; 41: 30–42.
2. Moura LIF, Dias AMA, Carvalho E, Sousa HCd. Recent advances on the development of wound dressings for diabetic foot ulcer treatment-a review. Acta Biomater. 2013; 9: 7093–7114.
3. Schneider LA, Korber A, Grabbe S, Dissemond J. Influence of pH on wound-healing: A new perspective for wound-therapy? Arch. Dermatol. Res. 2007; 298: 413–420.
4. Schreml S, Szeimies R-M, Karrer S, Heinlin J, Landthaler M, Babilas P. The impact of the pH value on skin integrity and cutaneous wound healing. J. Eur. Acad. Dermatol. Venereol. 2010; 24: 373–378.
5. Sharpe JR, Booth S, Jubin K, Jordan NR, Lawrence-Watt DJ, Dheansa BS. Progression of wound pH during the course of healing in burns. J. Burn Care Res. 2013; 34: e201-e208.
6. Schreml S, Meier RJ, Kirschbaum M, Kong SC, Gehmert S, Felthaus O, Küchler S, Sharpe JR, Wöltje K, Weiß KT, Albert M, Seidl U, Schröder J, Morsczeck C, Prantl L, Duschl C, Pedersen SF, Gosau M, Berneburg M, Wolfbeis OS, Landthaler M, Babilas P. Luminescent dual sensors reveal extracellular pH-gradients and hypoxia on chronic wounds that disrupt epidermal repair. Theranostics 2014; 4: 721–735.
7. Dissemond J, Witthoff M, Brauns TC, Haberer D, Goos M. pH-Wert des Milieus chronischer Wunden. Der Hautarzt 2003; 54: 959–965.
8. Gethin G. The significance of surface pH in chronic wounds. Wounds UK 2007; 3: 52–56.
9. Sharpe JR, Harris KL, Jubin K, Bainbridge NJ, Jordan NR. The effect of pH in modulating skin cell behaviour. Br. J. Dermatol. 2009; 161: 671–673.
10. Percival SL, McCarty S, Hunt JA, Woods EJ. The effects of pH on wound healing, biofilms, and antimicrobial efficacy. Wound Repair Regen. 2014; 22: 174–186.
11. Wilson IA, Henry M, Quill RD, Byrne PJ. The pH of varicose ulcer surfaces and its relationship to healing. Vasa 1979; 8: 339–342.
12. Leung DK-C, Mok WF-M, Yu Dorothy Man-Wai, Au T-C. Use of distilled white vinegar dressing supplemental to oral antibiotics in the management of Pseudomonas Aeruginosa exit site infection in continuous ambulatory peritoneal dialysis patients. Hong Kong Journal of Nephrology 2001; 3: 38–40.

13. Junker JPE, Kamel RA, Caterson EJ, Eriksson E. Clinical impact upon wound healing and inflammation in moist, wet, and dry environments. Adv. Wound Care 2013; 2: 348–356.
14. Boateng JS, Matthews KH, Stevens HNE, Eccleston GM. Wound healing dressings and drug delivery systems: A review. J. Pharm. Sci. 2008; 97: 2892–2923.
15. Boateng J, Catanzano O. Advanced therapeutic dressings for effective wound healing--A review. J. Pharm. Sci. 2015; 104: 3653–3680.
16. Koehler J, Wallmeyer L, Hedtrich S, Goepferich AM, Brandl FP. pH-modulating poly(ethylene glycol)/alginate hydrogel dressings for the treatment of chronic wounds. Macromol. Biosci. 2017; 17: 1600369.
17. Curvale RA. Buffer capacity of bovine serum albumin (BSA). J. Argent. Chem. Soc. 2009; 97: 174–180.
18. 10993-5:2009, Biological evaluation of medical devices - Part 5: Tests for in vitro cytotoxicity. Geneva, Switzerland: International Organization for Standardization; 2009.
19. 10993-12:2009, Biological evaluation of medical devices - Part 12: Sample preparation and reference materials. Geneva, Switzerland: International Organization for Standardization; 2009.
20. E96/E96M-12, Standard test methods for water vapor transmission of materials. West Conshohocken, PA, USA: ASTM International; 2012.
21. Müller G, Kramer A, Schmitt J, Harden D, Koburger T. Reduced cytotoxicity of polyhexamethylene biguanide hydrochloride (PHMB) by egg phosphatidylcholine while maintaining antimicrobial efficacy. Chem. Biol. Interact. 2011; 190: 171–178.
22. Good NE, Winget GD, Winter W, Connolly TN, Izawa S, Singh RM. Hydrogen ion buffers for biological research. Biochemistry 1966; 5: 467–477.
23. Elder K, van den Bergh M, Woodward B. Troubleshooting and problem-solving in the IVF laboratory. Cambridge, United Kingdom: Cambridge University Press; 2015.
24. Koehler J, Wallmeyer L, Hedtrich S, Brandl FP, Goepferich AM. Alkaline poly(ethylene glycol)-based hydrogels for a potential use as bioactive wound dressings. J. Biomed. Mater. Res. Part A 2017; doi: 10.1002/jbm.a.36177.
25. Ibanez JG, Hernandez-Esparza M, Doria-Serrano C, Fregoso-Infante A, Singh MM. Environmental Chemistry: Fundamentals. New York, NY, USA: Springer Science & Business Media; 2010.

26. Romanelli M, Vowden K, Weir D. Exudate management made easy. Wounds Int. 2010; 1: S1–S5.
27. Martins AF, Prata MIM, Rodrigues SPJ, Geraldes, Carlos F G C, Riss PJ, Amor-Coarasa A, Burchardt C, Kroll C, Roesch F. Spectroscopic, radiochemical, and theoretical studies of the Ga^{3+}-N-2-hydroxyethyl piperazine-N'-2-ethanesulfonic acid (HEPES buffer) system: Evidence for the formation of Ga^{3+}-HEPES complexes in ^{68}Ga labeling reactions. Contrast Media Mol. Imaging 2013; 8: 265–273.
28. Kulig D, Zimoch-Korzycka A, Jarmoluk A, Marycz K. Study on alginate–chitosan complex formed with different polymers ratio. Polymers 2016; 8: 167.
29. Waters DJ, Engberg K, Parke-Houben R, Ta CN, Jackson AJ, Toney MF, Frank CW. Structure and mechanism of strength enhancement in interpenetrating polymer network hydrogels. Macromolecules 2011; 44: 5776–5787.
30. van de Wetering P, Zuidam NJ, van Steenbergen MJ, van der Houwen, O. A. G. J., Underberg WJM, Hennink WE. A mechanistic study of the hydrolytic stability of poly(2-(dimethylamino)ethyl methacrylate). Macromolecules 1998; 31: 8063–8068.
31. Lee W-R, Park J-H, Kim K-H, Kim S-J, Park D-H, Chae M-H, Suh S-H, Jeong S-W, Park K-K. The biological effects of topical alginate treatment in an animal model of skin wound healing. Wound Rep. Regen. 2009; 17: 505–510.
32. Sahraro M, Yeganeh H, Sorayya M. Guanidine hydrochloride embedded polyurethanes as antimicrobial and absorptive wound dressing membranes with promising cytocompatibility. Mater. Sci. Eng. C Mater. Biol. Appl. 2016; 59: 1025–1037.
33. Kerkhof NJ, Vanderlaan RK, White JL, Hem SL. pH-stat titration of aluminum hydroxide gel. J. Pharm. Sci. 1977; 66: 1528–1533.
34. Wu C-J, Wilker JJ, Schmidt G. Robust and adhesive hydrogels from cross-linked poly(ethylene glycol) and silicate for biomedical use. Macromol. Biosci. 2013; 13: 59–66.
35. Yang Z, Gu H, Zhang Y, Wang L, Xu B. Small molecule hydrogels based on a class of antiinflammatory agents. Chem. Commun. 2004: 208–209.
36. Zheng Z, Zhang L, Kong L, Wang A, Gong Y, Zhang X. The behavior of MC3T3-E1 cells on chitosan/poly-L-lysine composite films: Effect of nanotopography, surface chemistry, and wettability. J. Biomed. Mater. Res. A 2009; 89: 453–465.
37. Shou D, Ye L, Fan J, Fu K. Optimal design of porous structures for the fastest liquid absorption. Langmuir 2014; 30: 149–155.

38. Ebara M, Kotsuchibashi Y, Narain R, Idota N, Kim Y-J, Hoffman JM, Uto K, Aoyagi T. Smart Biomaterials. Tokyo, Japan: Springer Japan; 2014.
39. Lee SJ, Kim SS, Lee YM. Interpenetrating polymer network hydrogels based on poly(ethylene glycol) macromer and chitosan. Carbohydr. Polym. 2000; 41: 197–205.
40. Ajji Z, Othman I, Rosiak JM. Production of hydrogel wound dressings using gamma radiation. Nucl. Instrum. Meth. B 2005; 229: 375–380.
41. Hilmy N, Darwins D, Hardiningsih L. Poly(N-vinylpyrrolidone) hydrogels. Hydrogel composites as wound dressing for tropical environment. Radiat. Phys. Chem. 1993; 42: 911–914.
42. Parlato M, Reichert S, Barney N, Murphy WL. Poly(ethylene glycol) hydrogels with adaptable mechanical and degradation properties for use in biomedical applications. Macromol. Biosci. 2014; 14: 687–698.
43. Snyders R, Shingel KI, Zabeida O, Roberge C, Faure M-P, Martinu L, Klemberg-Sapieha JE. Mechanical and microstructural properties of hybrid poly(ethylene glycol)-soy protein hydrogels for wound dressing applications. J. Biomed. Mater. Res. A 2007; 83: 88–97.
44. Hansen B, Jemec GBE. The mechanical properties of skin in osteogenesis imperfecta. Arch. Dermatol. 2002; 138: 909–911.
45. Silver FH, Christiansen DL. Biomaterials Science and Biocompatability. New York, NY, USA: Springer; 1999.
46. Agrawal CM. Synthetic bioabsorbable polymers for implants. ASTM STP 1396. West Conshohocken, PA, USA: American Society for Testing and Materials; 2000.
47. Li J, Suo Z, Vlassak JJ. Stiff, strong, and tough hydrogels with good chemical stability. J. Mater. Chem. B Mater. Biol. Med. 2014; 2: 6708–6713.
48. Hrynyk M, Martins-Green M, Barron AE, Neufeld RJ. Alginate-PEG sponge architecture and role in the design of insulin release dressings. Biomacromolecules 2012; 13: 1478–1485.
49. Sheybani R, Shukla A. Highly sensitive label-free dual sensor array for rapid detection of wound bacteria. Biosens. Bioelectron. 2017; 92: 425–433.
50. Napavichayanun S, Amornsudthiwat P, Pienpinijtham P, Aramwit P. Interaction and effectiveness of antimicrobials along with healing-promoting agents in a novel biocellulose wound dressing. Mater. Sci. Eng. C Mater. Biol. Appl. 2015; 55: 95–104.

Chapter 7

Summary and Conclusion

1. Summary

Hydrogels are suitable base materials for various biomedical applications.[1] Because of their chemical versatility, good biocompatibility, and high water content (around 90%), hydrogels are particularly relevant to wound dressing applications. Thus, a high commercial and scientific interest in new hydrogel-based dressing materials has recently been observed. Special attention has been paid to the challenging treatment of complex acute wounds, e.g. suffering from deep tissue loss or heavy infection, and non-healing chronic wounds, e.g. induced by an underlying disease or bacterial colonization. As summarized in **Chapter 1**, bioactive hydrogel wound dressings are a particularly promising treatment option in this context.[2] Their supportive healing properties can be induced by bioactive hydrogel precursors, incorporated drugs, stem cells, and cell-derived proteins, such as growth factors. Despite the sustained research effort, a lot of these advanced approaches fail to be translated to a standard procedure in clinics. Impeding factors are inter alia the complexity of the manufacturing process, high costs, or a potential health hazard.[2–4] Moreover, hydrogel-based materials frequently suffer from rather low mechanical stability. Yet, mechanical resistance and flexibility is required for convenient application and wearability of wound dressings.

To overcome the described issues, new and applicable concepts of bioactive hydrogel wound dressings are urgently needed. One possible approach towards stable, yet flexible hydrogels is the use of interpenetrating polymer network (IPN) structures, typically showing enhanced material properties in comparison to single network hydrogels.[5] The concept of IPNs was therefore applied to hydrogel precursors which are suitable for wound dressing applications, namely synthetic, biocompatible poly(ethylene glycol) diacrylate (PEGDA) and naturally derived, bioactive alginate. By this means, the mechanical weakness of the single component PEGDA and alginate hydrogels was overcome, as the resulting IPN hydrogel dressings, assessed in **Chapter 2**, showed suitable maximal stress and strain values under compressive and tensile load. Additionally, the high swelling capacity of photopolymerized PEGDA (molecular weight $\geq$ 4 kDa)/alginate IPNs considerably exceeded the marginal liquid uptake of pure PEGDA hydrogels, which makes these IPN hydrogels suitable for wound dressing applications. The most promising PEGDA/alginate IPN hydrogel formulation was furthermore loaded with 0.34% poly(hexamethylene biguanide) hydrochloride (PHMB), allowing a medically relevant antimicrobial drug release for acute wound care.

In **Chapter 3**, the concept of PEGDA/alginate IPN hydrogel wound dressings was further developed to meet the special requirements for chronic wound dressings and particularly target the recently described non-physiological pH shift in chronic wounds.[6,7] In the case of an alkaline pH shift, acidic dressings could be beneficial for the healing process. Consequently, different acidic IPN hydrogel formulations consisting of PEGDA, alginate, and acrylic acid (AA) as the pH-modulating component, were developed and assessed, regarding their material and bioactive properties. The conducted experiments revealed that the swelling capacity, the mechanical performance, the microstructure, and the base neutralizing capacity were highly dependent on the exact hydrogel formulation, with 0.25% AA containing IPN hydrogels performing best. In addition to their excellent material properties, they were non-cytotoxic and could significantly enhance the wound healing in pH-shifted, in vitro wound models, which makes this formulation a promising approach to acidic chronic wound dressings.

A deeper understanding of crucial inter- and intra-network interactions helps to modify the IPN hydrogel material properties in such way that their active intervention in the healing process is optimized. Therefore, the influence of the two major effects in the investigated PEGDA/AA/alginate IPNs, namely ionic interactions via negatively charged carboxylic acid groups of AA and reduced network branching due to the incorporation of one-sided (AA) instead of two-sided (PEGDA) functionalized precursors, were distinguished by analyzing uncharged 2-hydroxyethyl methacrylate (HEMA) instead of AA containing IPN hydrogels. This comparison, drawn in **Chapter 4**, clearly illustrated that all material properties of the developed IPNs were almost exclusively dependent on the incorporated carboxylic acid groups. Further research focused on the impact of the primary network density, which was altered by changing the precursor molecular weight, comparing PEGDA with a molecular weight of 4 and 6 kDa, and the time frame of the radical polymerization, comparing thermally and UV-light activated reactions. The network density of the secondary network was additionally altered by changing the type of alginate polymerization, comparing physical entanglements with and without supplementing Ca^{2+} induced ionic interactions. These controlled adjustments of the hydrogel network structure permitted the adaption of important material properties such as the liquid uptake, the mechanical stability and flexibility, and the base neutralizing capacity to the wound dressing requirements. By this means, a new pH-modulating PEGDA4k/AA/Ca^{2+} alginate IPN hydrogel formulation with promising wound dressing properties was identified.

On the other hand, alkaline dressing materials should be beneficial to the healing process of acidic chronic wounds. Dependent on the pK_b value of the chosen pH-modifying precursor (N-vinylimidazole (VI), $pK_b = 7.0$; 2-dimethylaminoethyl methacrylate (DMAEMA), $pK_b = 5.6$), the alkaline PEGDA-based IPN hydrogels, discussed in **Chapter 5**, influenced the in vitro wound pH to a different extent. VI containing dressings had a less intensive effect, but in return, did not bear the risk of pH over-modulation. Furthermore, PEGDA/VI/alginate IPNs were used as human dermal fibroblast scaffolds, which is another strategy to actively improve the wound healing process. A stronger pH response was received by DMAEMA containing IPN hydrogels. Here, a precise choice of the right wound dressing buffer capacity is vital for avoiding an alkaline pH-shift in the treated lesion. However, this effect is aimed for skin grafted wounds, as an alkaline pH enables a successful growth and vascularization of skin grafts.[8,9] Based on the discussed approach, a promising alkaline PEGDA/DMAEMA/N-carboxyethylchitosan IPN hydrogel wound dressing formulation with proper material properties, no cytotoxicity, and a high supportive healing capacity could be developed.

Universal buffer hydrogel materials were developed in **Chapter 6**, aimed at achieving a pH-modulating chronic wound dressing which is independent from the direction of the pH shift. Following this strategy, less effort is needed for monitoring the patient's individual wound pH. To this end, the monomolecular buffer molecule 4-(2-hydroxyethyl)-1-piperazineethanesulfonic acid (HEPES) was chemically modified and thus covalently incorporated into the favorable PEGDA/alginate IPN hydrogel system. Yet, the HEPES buffer capacity was altered by this process, causing a loss of its beneficial impact on the wound pH. In contrast, the alternate bimolecular buffer system AA/DMAEMA retained its pH-modulating properties even after the polymerization process and the developed IPN hydrogels containing 0.7% AA and 2.8% DMAEMA showed convincing material and wound healing properties, as well as good suitability as antimicrobial PHMB delivery matrices.

The overall concept of the thesis is also summarized in Figure 1.

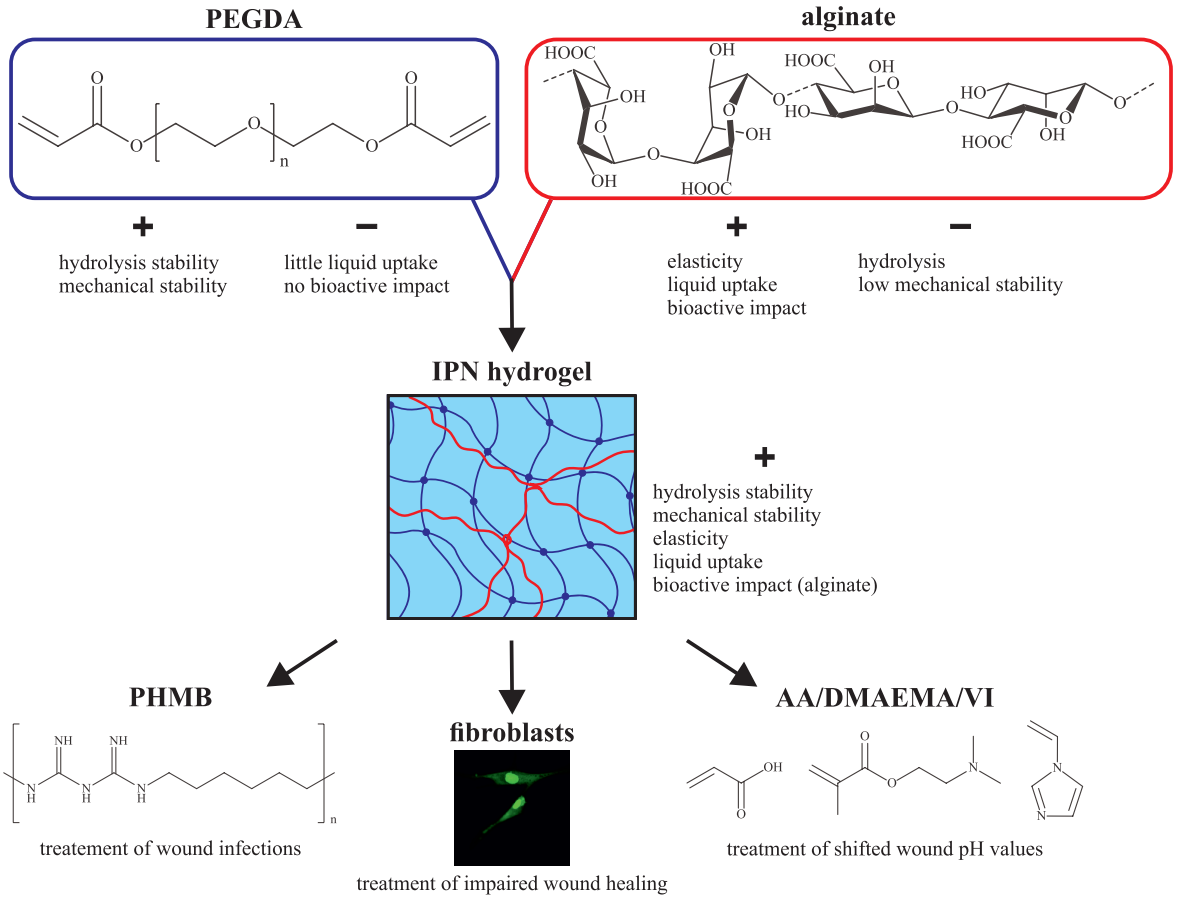

Figure 1. Applied concept of developing bioactive hydrogel dressings for acute and chronic wounds.

2. Conclusion

In conclusion, the formation of interpenetrating polymer network hydrogels from select biocompatible and bioactive precursors offers the possibility to develop new, highly potent treatment options for advanced wound care. Thereby, a proper understanding of the crucial material parameters and network interactions in the IPN structure is required to precisely adapt the material properties, synonymous with the hydrogel wound healing capacity. Specifically, by developing PEGDA/alginate IPN hydrogels with an adapted network structure, the advantageous properties from the single components were combined, whilst their former drawbacks were overcome, such as the common mechanical weakness of hydrogel materials. A supplementary incorporation of acidic and alkaline, pH-active monomers into the IPN hydrogel system furthermore enabled the creation of buffering hydrogel dressing materials for the treatment of pH-shifted non-healing wounds. Additional, bioactive healing properties were successfully accomplished concerning controlled drug release of antimicrobial PHMB and cell seeding.

Future research should focus on two main issues. First, the developed hydrogel wound dressing materials should be further optimized concerning the maximal possible wearing time, which is dependent inter alia on the duration of drug release, the buffer capacity strength, and the rate of cell survival when used as a cell scaffold. For this purpose, the existing formulations should be modified with regard to the decisive functional groups that are connected to the material's cell compatibility or can interact with drug molecules, influencing their release. Furthermore, alternative pH-modifying precursors might be screened. The second, more urgent target is a fast and effective progress of the described materials from a research level to reliable clinical treatment options. This includes experiments on significant animal models and, in a next step, the application in clinical studies.

Even though complementing research on the developed bioactive IPN hydrogel wound dressing materials is necessary, the significant potential of the here applied concept was clarified. Precisely modified IPN hydrogel structures provide a versatile, cost-effective, and promising approach to new and urgently needed treatment options for acute and chronic wounds.

References

1. Kirschner CM, Anseth KS. Hydrogels in healthcare: From static to dynamic material microenvironments. Acta Mater. 2013; 61: 931–944.
2. Boateng J, Catanzano O. Advanced therapeutic dressings for effective wound healing--A review. J. Pharm. Sci. 2015; 104: 3653–3680.
3. Spano R, Muraglia A, Todeschi MR, Nardini M, Strada P, Cancedda R, Mastrogiacomo M. Platelet rich plasma-based bioactive membrane as a new advanced wound care tool. J. Tissue Eng. Regen. Med. 2016; doi: 10.1002/term.2357.
4. Borena BM, Martens A, Broeckx SY, Meyer E, Chiers K, Duchateau L, Spaas JH. Regenerative skin wound healing in mammals: State-of-the-art on growth factor and stem cell based treatments. Cell. Physiol. Biochem. 2015; 36: 1–23.
5. Haque MA, Kurokawa T, Gong JP. Super tough double network hydrogels and their application as biomaterials. Polymer 2012; 53: 1805–1822.
6. Schreml S, Meier RJ, Kirschbaum M, Kong SC, Gehmert S, Felthaus O, Küchler S, Sharpe JR, Wöltje K, Weiß KT, Albert M, Seidl U, Schröder J, Morsczeck C, Prantl L, Duschl C, Pedersen SF, Gosau M, Berneburg M, Wolfbeis OS, Landthaler M, Babilas P. Luminescent dual sensors reveal extracellular pH-gradients and hypoxia on chronic wounds that disrupt epidermal repair. Theranostics 2014; 4: 721–735.
7. Sharpe JR, Booth S, Jubin K, Jordan NR, Lawrence-Watt DJ, Dheansa BS. Progression of wound pH during the course of healing in burns. J. Burn Care Res. 2013; 34: e201-e208.
8. Sharpe JR, Harris KL, Jubin K, Bainbridge NJ, Jordan NR. The effect of pH in modulating skin cell behaviour. Br. J. Dermatol. 2009; 161: 671–673.
9. Schneider LA, Korber A, Grabbe S, Dissemond J. Influence of pH on wound-healing: A new perspective for wound-therapy? Arch. Dermatol. Res. 2007; 298: 413–420.

Appendix

Abbreviations

2D	two-dimensional
3D	three-dimensional
AA	acrylic acid
AMA	alginate methacrylate
ANC	acid neutralizing capacity
ANOVA	analysis of variance
APS	ammonium persulfate
ASCs	adipose-derived stem cells
ASTM	American society for testing and materials
BNC	base neutralizing capacity
CEC	N-carboxyethylchitosan
D	dermis
DCM	dichloromethane
DMAEMA	2-dimethylaminoethyl methacrylate
DMEM	Dulbecco's modified eagle medium
DMF	N,N-dimethylformamide
DMSO	dimethyl sulfoxide
DN	double network
DPZ	dense polymer zone
E	epidermis
ECM	extracellular matrix
EGF	epidermal growth factor
E-modulus	elastic modulus
EP	equivalence point
F12	nutrient mixture F-12
FBS	fetal bovine serum
FGF	fibroblast growth factor

G	α-L-guluronate
GF	growth factor
GL	gluconolactone
HA	hyaluronic acid
HDFa	adult human dermal fibroblast
H&E	hematoxylin and eosin
HEMA	2-hydroxyethyl methacrylate
HEPES	4-(2-hydroxyethyl)-1-piperazineethanesulfonic acid
HEPESac	4-(2-ethyl acrylate)-1-piperazineethanesulfonic acid
HHMP	2-hydroxy-4′-(2-hydroxyethoxy)-2-methylpropiophenone
^{1}H NMR	proton nuclear magnetic resonance
IGF-1	insulin-like growth factor-1
IL-1	interleukin-1
IPN	interpenetrating polymer network
ISO	international organization for standardization
KBM	keratinocyte basal medium
KGF	keratinocyte growth factor
KGM	keratinocyte growth medium
MMP	matrix metalloproteinase
MRSA	methicillin-resistant *Staphylococcus Aureus*
MSC	mesenchymal stem cells
MTT	3-(4,5-dimethylthiazol-2-yl)-2,5-diphenyltetrazolium bromide
NHE1	sodium/hydrogen exchanger
NIPAAm	N-isopropylacrylamide
NPs	nanoparticles
PAA	poly(acrylic acid)
PAAm	polyacrylamide
PAMPS	poly(2-acrylamido-2-methylpropanesulfonic acid)
PBS	phosphate buffered saline
PDGF	platelet-derived growth factor
PEG	poly(ethylene glycol)
PEG2k	poly(ethylene glycol) with a molecular weight of 2 kDa
PEG4k	poly(ethylene glycol) with a molecular weight of 4 kDa
PEG6k	poly(ethylene glycol) with a molecular weight of 6 kDa

PEGDA	poly(ethylene glycol) diacrylate
PEGDA2k	poly(ethylene glycol) diacrylate with a molecular weight of 2 kDa
PEGDA4k	poly(ethylene glycol) diacrylate with a molecular weight of 4 kDa
PEGDA6k	poly(ethylene glycol) diacrylate with a molecular weight of 6 kDa
PEO	poly(ethylene oxide)
PHMB	poly(hexamethylene biguanide) hydrochloride
PLA	poly(lactic acid)
PRP	platelet-rich plasma
PU	polyurethane
PVA	poly(vinyl alcohol)
PVP	poly(vinyl pyrrolidone)
S	stratum corneum
SD	standard deviation
SEM	scanning electron microscopy
TEMED	N,N,N',N'-tetramethylethane-1,2-diamine
TGF-β	transforming growth factor-β
TIMPs	tissue inhibitors of metalloproteinases
TN	triple network
TNF-α	tumor necrosis factor-α
UV	ultraviolet
VEGF	vascular endothelial growth factor
VI	N-vinylimidazole
WVTR	water vapor transmission rate

List of Publications

Peer-reviewed publications

Koehler J, Brandl FP, and Goepferich AM. *Hydrogel wound dressings for a bioactive treatment of acute and chronic wounds*. Submitted to: European Polymer Journal 2017; Manuscript number: EUROPOL_2017_1345 **(Chapter 1)**.

Koehler J, Wallmeyer L, Hedtrich S, Brandl FP, and Goepferich AM. *Alkaline poly(ethylene glycol)-based hydrogels for a potential use as bioactive wound dressings*. In: Journal of Biomedical Material Research: Part A 2017; doi: 10.1002/jbm.a.36177 **(Chapter 5)**.

Koehler J, Wallmeyer L, Hedtrich S, Goepferich AM, and Brandl FP. *pH-modulating poly(ethylene glycol)/alginate hydrogel dressings for the treatment of chronic wounds*. In: Macromolecular Bioscience 2017; 17: 1600369. doi: 10.1002/mabi.201600369 **(Chapter 3)**.

Oral presentations

Koehler J, Goepferich AM, and Brandl FP. *pH-regulating hydrogel dressings for the treatment of chronic wounds*. Conference of the European Wound Management Association. Bremen, Germany, 2016.

Conference abstracts

Koehler J, Goepferich AM, and Brandl FP. *pH-regulating hydrogels for wound dressing applications*. World Biomaterials Conference. Montreal, Canada, 2016.

Koehler J, Goepferich AM, and Brandl FP. *pH-regulating hydrogel dressings for the treatment of chronic wounds*. Conference of the European Wound Management Association. Bremen, Germany, 2016.

Koehler J, Goepferich AM, and Brandl FP. *Interpenetrating polymer networks for wound dressing applications*. American Chemical Society National Meeting. San Francisco, CA, USA, 2014.

Acknowledgements

An dieser Stelle möchte ich mich ganz herzlich bei allen bedanken, die mich in den letzten Jahren unterstützt und damit maßgeblich zum erfolgreichen Abschluss dieser Arbeit beigetragen haben.

Mein besonderer Dank gilt Herrn Prof. Dr. Achim Göpferich, der diese Arbeit erst ermöglicht hat und mich bei deren Umsetzung stets durch interessante Diskussionen und kompetenten Rat unterstützte. Besonders bedanken möchte ich mich auch für die gewährten Freiheiten bezüglich der Weiterentwicklung des Forschungsprojektes und für die vielfältigen Gelegenheiten, meine wissenschaftlichen Ergebnisse auf nationalen und internationalen Konferenzen präsentieren zu dürfen. Ebenso danke ich herzlich für die Unterstützung des interessanten und erfolgreichen Forschungsaufenthaltes bei Frau Prof. Dr. Sarah Hedtrich an der Freien Universität Berlin.

Herrn Dr. Ferdinand Brandl danke ich herzlich für die Betreuung der Arbeit, die interessanten Anregungen und Diskussionen, und das hilfreiche Feedback.

Herrn PD Dr. Stephan Schreml danke ich für die interessanten Gespräche, die vielfältigen Anregungen und Ratschläge und die uneingeschränkte Hilfsbereitschaft. In diesem Zusammenhang möchte ich weiterhin Frau Judith Heider für ihre Großzügigkeit und ihre vielen hilfreichen Tipps in Bezug auf die Zellkulturarbeit danken.

Besonderer Dank gilt auch Frau Prof. Dr. Sarah Hedtrich und Frau Leonie Wallmeyer, die mir den spannenden Forschungsaufenthalt an der Freien Universität Berlin mit ermöglichten und die mit ihrer großen praktischen wie theoretischen Unterstützung bei der Arbeit an 3D in vitro Wundmodellen wesentlich zum Gelingen des Forschungsprojekts und des Aufenthalts in Berlin beitrugen.

Herrn Dr. Robert Meier danke ich für die Durchführung der pH-Sensor Messungen und die nette Hilfe bei der Auswertung.

Frau Viktoria Meßmann danke ich für die äußerst hilfreiche, nette und engagierte Unterstützung im Labor.

Für die unermüdliche und professionelle Einführung in das zellkultur-basierte Arbeiten, sowie die uneingeschränkte Unterstützung dabei, danke ich Frau Renate Liebl ganz herzlich.

Frau Andrea Blaimer und Frau Eva Wrobel danke ich herzlich für ihren unermüdlichen Einsatz hinter den Kulissen, der immer dazu beitrugen "den Laden am Laufen zu halten".

Weiterhin danke ich meinen Praktikanten, und insbesondere Frau Sabrina Russ, dass sie mit ihrem motivierten Einsatz interessante Impulse zum weiteren Verlauf der Forschungsarbeit gaben.

Nicht zuletzt gilt mein Dank allen aktuellen und ehemaligen Kollegen für die unkomplizierte Zusammenarbeit und die angenehme gemeinsame Zeit. Insbesondere danke ich:

Silvia Babl, Angelika Berié, Stefan Kolb und Edith Schindler für die Unterstützung in technischen und praktischen Fragen,

Luise Tomasetti, Vanessa Haas und Johanna Lempp, die meine schöne Zeit in Regensburg maßgeblich geprägt haben,

und Nadine Hammer für die schöne Zeit im gemeinsamen Labor.

Besonders danke ich noch meiner gesamten Familie und meinen Freuden für jedwede Unterstützung, ihren großen Beistand, ihre Geduld und alle angenehme Ablenkungen vom Laboralltag. Durch euren Rückhalt wurde ich immer wieder motiviert und bestärkt. Von Herzen vielen Dank dafür!

Statement in Lieu of an Oath

I hereby confirm that I have written this thesis on my own and that I have not used any other media or materials than the ones referred to in this thesis.

Regensburg, ...

(Julia Köhler)